Universidade de Aveiro Departamento de Química
2014

Maria João Valente Quental

Aplicação de líquidos iónicos na concentração de marcadores tumorais

Application of ionic liquids in the concentration of cancer biomarkers

Dissertação apresentada à Universidade de Aveiro para cumprimento dos requisitos necessários à obtenção do grau de Mestre em Bioquímica, ramo de Bioquímica Clínica, realizada sob a orientação científica da Doutora Mara Guadalupe Freire Martins, Investigadora Coordenadora do Departamento de Química, CICECO, da Universidade de Aveiro e coorientação do Professor Doutor João Manuel da Costa Araújo Pereira Coutinho, Professor Catedrático do Departamento de Química da Universidade de Aveiro.

Aos dois homens da minha vida.....

o júri

presidente

Dr[a]. Rita Maria Pinho Ferreira
Professora auxiliar do Departamento de Química, da Universidade de Aveiro

Dr[a]. Mara Guadalupe Freire Martins
Investigadora Coordenadora do Departamento de Química, CICECO, da Universidade de Aveiro

Dr. Ricardo Simão Vieira Pires
Investigador Auxiliar do Centro de Neurociências e Biologia Celular da Universidade de Coimbra

Agradecimentos

Parece que finalmente chegou altura de parar, olhar para trás e reflectir sobre tudo e todos que marcaram esta jornada. Em primeiro lugar gostava de agradecer à Drª Mara Freire, pelo o apoio incondicional, disponibilidade, assim como todas as oportunidades proporcionadas que me permitiram não só crescer a nivel profissional mas também pessoal. Um muito obrigada ao Professor João Coutinho, pelo apoio proporcinado e principalmente pela oportunidade concedida ao realizar este trabalho.

Um gigante obrigada a todos os membros do Path e mini Path, por serem um grupo sensacional e que de uma maneira ou de outra, todos marcaram esta etapa da minha vida. Ao Matheus, o co-oritentador de sonho, um obrigada de coração por tudo o que me ensinaste, todas as gargalhadas proporcinadas mas principalmente toda a paciência e carinho para aguentar as minhas neuras. Obrigada Ana Maria, nem todos os agradecimentos do mundo são suficientes, foste incansável, uma verdadeira amiga que agradeço todos os dias ter conhecido. Um obrigada igualmente especial à Mafalda, mais uma grande amiga nascida desta jornada, que pertendo manter por muito tempo. Sem esquecer a minha querida companheira Tati, porque sem ela nada disto tinha a mesma graça. Não posso deixar de agradecer à Helena por tudo o que me ensinou, assim como à Ana Filipa, que sempre estiverem presentes nos momentos em que a resposta não parecia surgir. Agradeço ainda à Francisca pelos belos momentos passados em frente ao HPLC na tentativa de perceber qual a razão pelo o qual tudo corria mal, sabendo nós que nunca iamos chegar á reposta. Agradeço à princesa do laboratório, Tani do meu coração, por tudo o que me ensinaste e aconselhaste, e ainda por nunca me deixares ficar sem um sorriso na cara.

Finalmente agradeço às duas pessoas mais importantes da minha vida, Tozé e Bernardo, obrigado por estarem sempre comigo, e permitirem que o final do dia fosse sempre a altura onde podia partilhar as alegrias assim como as angústias. Tozé sem ti é que realmente nada disto teria sido possivel. Obrigada amor, amo-vos daqui ao bali...

palavras-chave

Cancro da próstata, antigénio específico da próstata, biomarcadores, sistemas aquosos bifásicos, líquidos iónicos, albumina de soro bovino, capacidade tampão.

resumo

O cancro da próstata representa, nos dias de hoje, a terceira causa de morte mais comum entre os homens, sendo que, atualmente, não existe nenhum tratamento eficaz quando o tumor é diagnosticado já num estado avançado. Face a esta incapacidade, um diagnóstico precoce é essencial no sentido de aumentar a taxa de sucesso do tratamento. A quantificação do biomarcador Antigénio Prostático Específico (PSA) em soro continua a ser o tipo de rastreio mais utilizado uma vez que se trata de um método simples. No entanto, a maioria dos métodos de quantificação de PSA disponíveis no mercado apresentam diversas desvantagens, entre elas, o processamento extensivo da amostra, a necessidade de identificação e caracterização de anticorpos específicos e pessoal técnico altamente especializado. Neste sentido, com o objetivo de desenvolver um método eficiente para a extração e concentração de PSA a partir de fluidos humanos, e que permita ultrapassar os limites de deteção de equipamentos analíticos tradicionais, estudaram-se sistemas aquosos bifásicos (SAB) constituídos por líquidos iónicos (LIs) como uma técnica de extração e concentração do tipo líquido-líquido. Uma vez que os biomarcadores associados a tumores comercialmente disponíveis são produtos de elevado custo, foi selecionada uma proteína modelo (albumina do soro bovino, BSA) para o estudo de otimização de SAB e posterior aplicação na extração/concentração de PSA. Neste trabalho, foram estudados dois tipos de SAB: LIs + sais orgânicos e LIs + polímeros. Primeiramente foram avaliados SAB constituídos por um sal orgânico e biodegradável ($K_3C_6H_5O_7$) e uma nova classe de LIs com aniões com capacidade tampão (***Good's buffers***) combinados com os catiões tetrabutilamónio ($[N_{4444}^+]$) e tetrabutilfosfónio ($[P_{4444}]^+$). De seguida, foram avaliados SAB formados pelo polímero polipropileno glicol com massa molecular de 400 $g \cdot mol^{-1}$ (PPG 400) e líquidos iónicos constituídos pelo catião colínio ($[Ch]^+$) e uma vasta panóplia de aniões, incluindo os ***Good's buffers***. Os LIs selecionados permitiram estudar o efeito do anião e do catião sobre os diagramas de fase, ou seja a sua capacidade para formar um sistema de duas fases aquosas, assim como avaliar a sua potencialidade para extração e concentração de BSA (e posteriormente PSA) a partir de soluções aquosas. De acordo com os resultados obtidos foi possível, num único passo, alcançar a extração completa da BSA. Entre os vários SAB avaliados, os constituídos por $K_3C_6H_5O_7$ + $[N_{4444}]$[Tricina] e PPG 400 + [Ch][Tricina] foram considerados os sistemas mais eficazes para a etapa de extração (atingindo extrações completas). No entanto, os SAB compostos por polímeros não permitem atingir os níveis de concentração esperados, pelo que os sistemas constituídos por LIs e $K_3C_6H_5O_7$ são os SAB de eleição e provaram ser uma técnica promissora de extração e concentração que poderá no futuro ser implementada previamente às análises clínicas de PSA. Por fim, com o intuito de suportar esta afirmação, utilizou-se um SAB constituído por $K_3C_6H_5O_7$ e $[N_{4444}]$[Tricine] para extrair PSA onde foi possível confirmar a extração completa para a fase rica em LI.

keywords

Prostate cancer, prostate specific antigen, cancer biomarkers, aqueous biphasic systems, ionic liquids, bovine serum albumin, Good's buffers.

Abstract

Prostate cancer (CaP) is the third most common cancer-related cause of death in men. Currently, there are no effective therapeutic options for the treatment of advanced prostate cancer and its early detection is pivotal and can increase the curative successful rate. The quantification of prostate specific antigen (PSA) levels in serum remains the most commonly used screening approach. Nevertheless, most of the PSA assays currently applied present several drawbacks, namely a time-consuming sample processing, the identification and characterization of specific antibodies and the need of highly trained technical operators. Therefore, in order to develop an efficient method to extract and concentrate PSA from human fluids and also to overcome the limitations of traditional analytical equipment, in this work, aqueous biphasic systems (ABS) composed of ionic liquids (ILs) were employed as an extraction and concentration liquid-liquid technique. Since the commercially available cancer biomarkers are highly cost products, bovine serum albumin (BSA) was selected as a model protein to infer on the best ABS and their further application on the extraction/concentration of PSA. In this work, two types of ABS were studied: ILs + organic salts and ILs + polymers. First, ABS constituted by a biodegradable organic salt ($K_3C_6H_5O_7$) and a new type of ILs composed of anions with buffer capacity (Good's buffers) combined with the tetrabutylammonium ($[N_{4444}]^+$) and tetrabutylphosphonium ($[P_{4444}]^+$) cations were studied. ABS formed by polypropylene glycol with a molecular weight of 400 $g \cdot mol^{-1}$ (PPG4 00) and several cholinium-based ILs, including the Good's buffers anions, were also evaluated The selected ILs allowed the study of the effect of the anion and cation nature on the phase diagrams behaviour, and thus on their ability to form two-phase systems, as well as the investigation on their potential to extract and concentrate BSA (and thus PSA) from aqueous solutions. According to the obtained results, the complete extraction of BSA was achieved in a single step in various systems. Amongst the several ABS evaluated, those composed of $K_3C_6H_5O_7$ + $[N_{4444}]$[Tricine] and PPG 400 + [Ch][Tricine] were considered the most effective for the extraction (allowing complete extractions). However, ABS composed of polymers did not allow to achieve the concentrations factors initially expected and, therefore, ABS constituted by ILs and $K_3C_6H_5O_7$ are the best alternative and proved to be a promising concentration and extraction technique that may, in the near future, be implemented previously to the clinical analysis of PSA. Finally, in order to support this statement, the ABS formed by $K_3C_6H_5O_7$ and $[N_{4444}]$[Tricine] was used in the extraction of PSA and where it was confirmed the complete extraction of the cancer biomarker for the IL-rich phase.

Contents

List of Tables

List of Figures

List of Symbols

wt% – weight fraction percentage;

σ – standard deviation;

Abs – absorbance (dimensionless);

Abs^{IL}_{PSA} – absorbance PSA at the maximum wavelength in the IL-rich and in the salt-rich

Abs^{Salt}_{PSA} – absorbance PSA at the maximum wavelength in the salt-rich

M_w – molecular weight ($g \cdot mol^{-1}$);

R^2 – correlation coefficient (dimensionless);

α – ratio between the top weight and the total weight of the mixture (dimensionless);

$[IL]$ – concentration of ionic liquid (wt% or $mol \cdot kg^{-1}$);

$[IL]_{\mathrm{IL}}$ – concentration of ionic liquid in the ionic-liquid-rich phase (wt%);

$[IL]_{\mathrm{Salt}}$ – concentration of ionic liquid in the salt-rich phase (wt%);

$[IL]_{\mathrm{M}}$ – concentration of ionic liquid in the initial mixture (wt%);

$[Salt]$ – concentration of salt (wt% or $mol \cdot kg^{-1}$);

$[Salt]_{\mathrm{IL}}$ – concentration of salt in the ionic-liquid-rich phase (wt%);

$[Salt]_{\mathrm{Salt}}$ – concentration of salt in the salt-rich phase (wt%);

$[Salt]_{\mathrm{M}}$ – concentration of salt in the initial mixture (wt%);

$[Salt]$ – concentration of salt (wt% or $mol \cdot kg^{-1}$);

$[PPG]$ – concentration of PPG (wt% or $mol \cdot kg^{-1}$);

$[PPG]_{\mathrm{IL}}$ – concentration of PPG in the ionic-liquid-rich phase (wt%);

$[Salt]_{\mathrm{PPG}}$ – concentration of salt in the PPG-rich phase (wt%);

$[PPG]_{\mathrm{M}}$ – concentration of PPG in the initial mixture (wt%);

$EE_{\mathrm{BSA}}\%$ – percentage extraction efficiency of BSA (%);

$EE_{\mathrm{PSA}}\%$ – percentage extraction efficiency of PSA (%);

F_{CBSA} – BSA concentration factor;

w_{IL} – weight of the IL-rich phase;

w_{salt} – weight of the salt-rich phase;

Acronyms

ACT – alpha-1-antichymotrypsin;

A2M – alpha-2-macroglobulin;

API – alpha-1-protease inhibitor

ABS – aqueous biphasic systems;

B – bottom phase;

BPH – benign prostate hyperplasia;

BPSA – benign PSA;

BSA – bovine serum albumin

C – critical point;

CaP – prostate cancer;

ELISA – enzyme-linked immunosorbent assay;

DRE – digital rectal examination;

ER – endoplasmic reticulum;

ERSPC – european randomized study of screening for prostate cancer;

FDA – Food and Drug Administration;

fPSA – free PSA;

GB – Good's buffers;

HEPES – N-cyclohexyl-2-aminoethanesulfonic acid;

HPLC – High-performance liquid chromatography;

iPSA – intact PSA;

K_2CO_3 – potassium carbonate;

$K_3C_6H_5O_7$ – potassium citrate;

K_3PO_4 – potassium phosphate;

LLE – liquid-liquid extraction;

MALDI-TOF MS – matrix-assisted laser desorption/ionization - time of flight mass spectrometry;

NNS – number needed to screen;

NNT – number needed to treat;

PEG – polyethylene glycol;

PI –prediction interval;

pI– isoelectric point;

PPG – polypropylene glycol;

PPG 400 – polypropylene glycol with a molecular weight of 400 $g \cdot mol^{-1}$;

PSA – prostate specific antigen;

proPSA – precursor isoforms of PSA;

ROS – reactive oxygen species;

T – top phase;

tPSA – total PSA;

TL – tie-line;

TRIFA – immunochemiluminescent;

TRUS – transrectal ultrasound;

RNA – ribonucleic acid;

SDS-PAGE – sodium dodecyl sulfate-polyacrylamide gel electrophoresis;

SPE – solid-phase extraction;

SPR – surface plasmon resonance technology;

[Ch][Ac] – (2-hydroxyethyl)trimethylammonium (cholinium) acetate;

[Ch][But] – (2-hydroxyethyl)trimethylammonium (cholinium) butanoate;

[Ch]Cl – (2-hydroxyethyl)trimethylammonium (cholinium) chloride;

[Ch][DHPhs] – (2-hydroxyethyl)trimethylammonium (cholinium) dihydrogen phosphate

[Ch] [DHCit] – (2-hydroxyethyl)trimethylammonium (cholinium) dihydrogen citrate

[Ch][Gly] – (2-hydroxyethyl)trimethylammonium (cholinium) glycolate;

[Ch][HEPES] – (2-hydroxyethyl)trimethylammonium (cholinium) 2-[4-(2-hydroxyethyl)piperazin-1-yl]ethanesulfonate;

[Ch][Lac] – (2-hydroxyethyl)trimethylammonium (cholinium) lactate;

[Ch][MES] – (2-hydroxyethyl)trimethylammonium (cholinium) 2-(N-morpholino)ethanesulfanate;

[Ch][Prop] – (2-hydroxyethyl)trimethylammonium (cholinium) propionate;

[Ch][Tricine] – (2-hydroxyethyl)trimethylammonium (cholinium) N-2(2-hydroxy-1,1-bis(hydroxymethyl)ethyl)glycinate;

$[C_8mim]Br$ –1-octyl-3-methylimidazolium bromide;

$[C_6mim]Cl$ – 1-hexyl-3-methylimidazolium chloride;

$[P_{4444}]Cl$ – tetrabutylphosphonium chloride;

$[N_{4444}]Cl$ – tetrabutylammonium chloride;

[N_{4444}][CHES] – tetrabutylammonium 2-(cyxlohexylamino)ethanesulfonate;

[P_{4444}][CHES] – tetrabutylphosphonium 2-(cyxlohexylamino)ethanesulfonate;

[N_{4444}][MES] – tetrabutylammonium 2-(N-morpholino)ethanesulfonate;

[P_{4444}][MES] – tetrabutylphosphonium 2-(N-morpholino)ethanesulfonate;

[N_{4444}][HEPES] – tetrabutylammonium 2-[4-(2-hydroxyethyl)piperazin-1-yl]ethanesulfonate;

[P_{4444}][HEPES] – tetrabutylphosphonium 2-[4-(2-hydroxyethyl)piperazin-1-yl]ethanesulfonate;

[N_{4444}][TES] – tetrabutylammonium 2-[[1,3-dihydroxy-2-(hydroxymethyl)propan-2-yl]amino] ethanesulfonate;

[P_{4444}][TES] – tetrabutylphosphonium 2-[[1,3-dihydroxy-2-(hydroxymethyl)propan-2-yl]amino] ethanesulfonate;

[N_{4444}][Tricine] – tetrabutylammonium N-2(2-Hydroxy-1,1-bis(hydroxymethyl)ethyl)glycinate;

[P_{4444}][Tricine] – tetrabutylphosphonium N-2(2-Hydroxy-1,1-bis(hydroxymethyl)ethyl)glycine;

1. General introduction

1.1 Scope and Objectives

Prostate cancer is a prevalent, worldwide concern among male adults [1]. At present, there is no curative therapy available for locally advanced or metastatic prostate disease, which makes its early detection a powerful way to increase the curative success rate [2]. A desired goal in the development and identification of prostate cancer is based on finding biomarkers by noninvasive assays to replace the currently used diagnostic techniques, like biopsy that it is still known as the diagnostic "gold standard". However, this procedure has a high risk of adverse events, such as bleeding and sepsis, and it is associated with 15% to 20% of false-negative results [3]. On the other hand, the identification and quantification of biomarkers in human serum and urine can be seen as an alternative approach to the standard tissue biopsy procedure. For instance, prostate specific antigen (PSA) has been identified as the most reliable tumor marker for an early diagnostics of prostate cancer [4].

Commercial kits for the PSA quantification are now offered by several companies, but some of them require the identification and characterization of immunoassay-qualified antibodies and highly qualified technical operators [5]. Also, the investment on time and resources required to generate such immunoassays are considerable, what often obstruct it's development on clinically specific chemistry laboratories [6]. Therefore, the main objective of this work consists on the development of an alternative platform for the extraction and concentration of PSA from human urine samples using a liquid-liquid extraction procedure. To this end, aqueous biphasic systems (ABS) formed by ionic liquids (ILs), an inorganic salt and water, as well as the combination of ILs and polymers will be investigated. Since commercially available cancer biomarkers are highly cost products and are distributed in small concentrations, it is necessary to carry out previous optimizations tests with cheaper and model compounds in order to achieve an improved ABS. Thus, bovine serum albumin (BSA), the most abundant protein in blood plasma of many species, was chosen as a model protein.

As a first approach, several experimental studies were attempted aiming at developing an optimized size-exclusion high-performance liquid chromatography (HPLC) quantification method for the model protein that can be applied further, only with small adjustments, on the PSA quantification. After defining the conditions for the quantification method, a large array of novel systems were investigated by combining potassium citrate ($K_3C_6HPO_4$) with Good's buffers ionic liquids (GB-ILs), *i.e.*, ILs that can maintain the pH

of the aqueous solution, being this an important property when dealing with proteins. All the new ABS were characterized by their ternary phase diagrams, tie-lines (TLs) and tie-line lengths (TLLs) at 25 ºC, followed by studies on their application in the extraction/concentration of BSA. All the GB-ILs were synthesized in this work and their synthesis and characterization are also described.

In a second stage, ABS formed by polypropylene glycol 400 (PPG 400) and cholinium-based ILs were further explored. In addition to the ternary phase diagrams, TLs and tie-line lengths (TLLs) initially ascertained, their extraction and concentration abilities were also evaluated. The stability of BSA in the ILs solutions was also evaluated.

Finally, it was addressed the real and prospective application of IL-based ABS for the possible concentration of cancer biomarkers from biological fluids, maintaining BSA as the model protein. In this context, two of the best systems, namely $K_3C_6H_5O_7$ + $[N_{4444}]$[Tricine] and PPG 400 + [Ch][Tricine] were selected. The results revealed that the system formed by $K_3C_6H_5O_7$ + $[N_{4444}]$[Tricine] is promising for the extraction process (100% of extraction achieved in a single-step procedure) and further concentration that could be used in PSA clinical analysis in the near future. Aiming at supporting this statement the ABS formed by $K_3C_6H_5O_7$ and $[N_{4444}]$[Tricine] was used in an isolated experiment with PSA and where it is confirmed the complete extraction of the cancer biomarker for the IL-rich phase by UV-spectroscopy.

1.2 Prostate Cancer Overview

1.2.1 Epidemiology and Risk Factors

Prostate cancer (CaP) is the third most common cancer-related cause of death in men, and resulted in more than 29,720 estimated deaths by the end of 2013 [1], a value that exceeds the expected number (28,170) of the year before [7]. In Europe, CaP is one of the most frequent solid neoplasms, with a predicted death rate of 10.52 cases *per* 100 000 men for 2013 (Figure 1.1) [8]. The vast majority (approximately 95%) of prostatic tumors are adenocarcinomas, whereas "adeno" refers to the glandular structure while carcinoma relates to the origin of cancer from the prostatic epithelium [9].

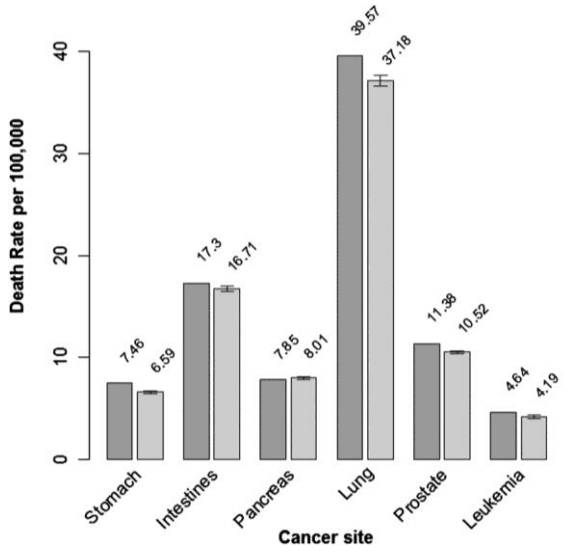

Figure 1.1. Bar-plots of standardized death rates per 100,000 individuals (men) for the year of 2009 (dark grey) and the predicted rates for 2013 with a 95% prediction interval (light grey) for in men in the EU [11].

With the increasing interest from the medical community, several risk factors for prostate cancer have been identified, of which the most common include old age, race, inherent susceptibility and environmental factors [10]. More specifically, those at higher risk for developing prostate cancer include men over the age of 65, African-American individuals, and those who first-line relatives have/had CaP (the risk is at least doubled). In addition, factors such diet, sexual behaviour, alcohol consumption, exposure to ultraviolet radiation and occupational exposure have all been discussed as being of etiological importance [10].

Despite prostate cancer is a multifactorial disease, a lot of scientists affirm that the most significant risk factor is advanced age [11]. About 60% of all prostate cancer cases

are diagnosed in men with 65 years old or older, and 97% occur in men with 50 years old or older [12]. In addition, the incidence of prostate cancer increases more with age than any other type of cancer [10]. The relationship between CaP and advanced age likely reflects the interplay of environmental, physiological, and molecular influences with normal consequences of aging that presumably exacerbate the related effects. During aging, the progressive accumulation of DNA adducts and an increase in the DNA strand-break frequency in most tissues tend to occur [10]. It is believed that these age-related changes are caused by oxidative stress, which arises as a result of an imbalance in cellular prooxidant-antioxidant status [11]. Cellular oxidants, such as free radicals and reactive oxygen species (ROS), are produced during natural metabolic processes. ROS are highly reactive and potentially damaging to cells, because they directly damage macromolecules and organelle functions [10]. Damage to DNA by ROS results in single-strand and double-strand breaks, apurinic and apyrimidinic sites, ring-saturation of thymine derivatives, and adduct formation. Moreover, ROS can catalyze the oxidative modification of proteins, including enzymes involved in DNA repair. Together, these direct and indirect influences of ROS on DNA create an ideal environment for mutagenesis and tumor initiation [10].While the precise molecular consequences of aging involved in the development of prostate cancer have not been totally elucidated, several studies described gene expression changes associated with aging, particularly in prostatic stroma, and including genes involved in inflammation, cellular senescence and oxidative stress as the most possible causes [11].

At present, there is no curative therapy available once the disease spreads the limits of the organ. Since there are no effective therapeutic options for advanced prostate cancer, early detection of the tumor is pivotal and can increase the curative successful rate [2].

1.2.2 Diagnosis

Most cancer patients have a low-risk, clinically localized disease at diagnosis and can be treated effectively with surgery and radiation. Like most types of cancer, if cancer prostate is diagnosed in its early stages, there is a higher probability of an efficient treatment (Table 1.1). However, CaP survival is related to many factors, especially the extent of the tumor at the time of diagnosis. Approximately 10% to 20% of patients are diagnosed with locally advanced (affecting nearby tissues, such as the bladder or rectum)

or metastatic disease (affecting other areas in the body, usually the lymph nodes or bone). In general, the outcomes for such cases are less likely to be improved by therapy than those with lower volume or grade tumors [13]. The most common clinical symptoms are haematuria (presence of erythrocytes in the urine) and urinary obstruction, although they usually do not appear until the tumor has already invaded the nearby tissue or the lymph nodes. Cancer that spreads outside the gland may also result in lower extremity oedema from regional lymphatic obstruction or pain from bone metastasis [14]. Nevertheless, for most men, prostate cancer is of slow growing and does not result in clinical signs or symptoms during their lifetime. Consequently, the screening for CaP if of outmost importance, and requires that diagnostic tests must be performed in the absence of any symptoms or indications of disease, and which is often a major challenge [15].

Table 11. Year relative survival rate corresponding to the stage that prostate cancer was diagnosed [16].

Stage	5-year relative survival rate
Local	100%
Regional	100%
Distant	28%

Currently, prostate cancer diagnostic tests include digital rectal examination (DRE), prostate-specific antigen (PSA) blood test and transrectal ultrasound (TRUS) guided biopsy [15]. PSA test and DRE are used as primary screening tools in early detection of prostate cancer and TRUS-guided needle biopsies are techniques more directed to confirm diagnosis already proposed by PSA or DRE testing, or both [2]. Histopathological interpretation by Gleason score, a score based on the histological pattern of the tumor, is also applied in the diagnosis of CaP, being very useful, especially in stratifying patients into different risk groups [17]. This score represents a strong measure of how aggressive the prostate cancer is and can be used to determine the prognosis and type of therapy [17].

Although DRE and TRUS guided biopsies are widely employed by diagnosticians, they present some disadvantages. DRE has poor reliability, particularly in small tumors that have not reached the prostatic capsule [18]. TRUS guided biopsy is known for being a very invasive technique that carries out significant risks, such as subsequent infections. Two recent large cohort studies [3, 19] demonstrated that there is a significant

hospitalization rate due to infections following biopsy, with a 3–4 fold increase above normal levels. In addition, these techniques exhibit limits on the ability to diagnose CaP because they do not permit the clinic to distinguish between benign prostate hyperplasia (BPH) and CaP [2]. Histopathological studies of prostate tissue can identify CaP in most cases, however, these methods also present some limitations. First of all, it is an invasive technique since it is necessary to perform a biopsy. Secondly, the Gleason's grading scale used by pathologists is at least semi-quantitative since it may be difficult to search every cell of every tissue slice. At last, there is a lack of concordance between the threshold of scoring between different pathologists [20]. In contrast, the quantification of PSA levels in biological fluids, especially in serum from a simple blood sample, is a less invasive screening tool, is easily performed, acceptable by the general population, accurate, and significantly affects the outcome of the disease. Consequently, PSA tests remain the most commonly used screening approach for prostate cancer [21].

1.3. Tumour Biomarkers

The introduction of biomarkers for disease diagnosis and management has revolutionized the practice of oncology. The National Cancer Institute defines a biomarker as "a biological molecule found in blood, other body fluids, or tissues that is a sign of a normal or abnormal process or of a condition or disease" [22]. Biomarkers are molecules whose detection or evaluation provides information about a disease beyond the standard clinical parameters that are gathered by the clinician. These can be proteins, metabolites, RNA transcripts, DNA, or epigenetic modifications of DNA, among other alterations. They can be detected in patient tissue samples, obtained either by biopsy or surgical resection, or noninvasively through the isolation of cells and/or molecules from bodily fluids, such as blood or urine. It's now established that biomarkers can be valuable in the identification of the disease and its progression, identify high-risk individuals, and allow to monitor the individuals' response to treatments. Furthermore, the identification of biomarkers can be carried out by non-invasive techniques and low-cost techniques [23] Therefore, the detection of tumour markers plays an important role in screening, diagnosis and to evaluate the prognosis of the diseases. Unlike most cancers, prostate cancer management has long used biomarkers. PSA has been identified as the most reliable tumor marker for the early diagnostics of prostate cancer [24].

1.4. Prostate Specific Antigen as a Cancer Prostate Biomarker

Prior to the 30s, there were no biochemical markers for the screening of prostate adenocarcinoma, and the diagnosis was only achieved by clinical history and physical examination. In 1938, Gutman observed, for the first time, that serum acid phosphatase (PAP), one of the major proteins secreted by prostate columnar epithelium secretory cells, appeared in high levels in patients with metastatic adenocarcinoma of the prostate [25]. However, since PAP is present in many normal blood components and organs and is highly concentrated in several non-prostatic malignancies, it exhibits lack in specificity for prostatic tissue and which makes it useless as a tumor marker [26]. In 1979, Wang et al. [27] reported on the purification of the PSA from prostate tissue. The authors showed that the antigen was present in normal and benign hyperplastic, as well as in malignant prostatic tissue and that it could not be detected in any other human tissue [27]. Since this discovery, PSA emerged as a potential prostate cancer biomarker. The first utility of PSA as a biomarker was in the monitoring of the disease status in patients with prostate cancer. After these findings, and because the PSA test is an inexpensive blood test that can be easily obtained, its application led to its increasing role as a screening modality. In 1994, the FDA approved PSA as a screening tool based on the seminal work of Catalona and colleagues [28] where they reported that the combination of the serum PSA measurement with levels ≥ 4.0 ng/mL, combined with other clinical findings, such as the results of DRE, improved the detection of prostate cancer.

1.4.1. Prostatic Cancer Screening

Prostate cancer diagnosis can be achieved by studying the prostate specific antigen levels in blood, where a high level could indicate the presence of cancer. In general, a PSA value of > 4.0 µg/L (and more recently > 2.5 µg/L) has been defined in the literature [29] as abnormal and it is frequently used as a cut-off, although for younger men a cut-off level of < 2.5 ng/mL is often used. For values between 4.0 and 10.0 µg/L, the grey zone, there exists a 22% to 27% likelihood of cancer, whereas values above 10 µg/L yield up to a 67% chance of prostate cancer [30]. Nevertheless, the PSA levels increase steadily with aging, and some urologists advocate the use of age-related “normal” PSA cut-points [31], rather than using the limit of > 4 µg/L as universal. Oesterling et al. [32] and Anderson et al. [33] noted that the upper limit of the PSA cutoff, achieving 95% of specificity, would increase

with age. Therefore, to maintain the equitable 95% specificity or an equivalent 5% false-positive rate across different ages, the PSA cutoff for recommending biopsy must necessarily increase with age. Based on cohorts of 537 patients with cancer-free status and benign prostatic hyperplasia, and 1,716 cancer-free, symptom-free, healthy volunteers who were between 40 and 79 years old, more general reference ranges were proposed as described in Table 1.2 [31].

Table 12. Values of reference range of PSA levels in serum for men with 40-79 years old [32, 33].

References	Age Group PSA Cutoff (ng/ml)			
	40–49	50–59	60–69	70–79
Oesterling et al. [32]	2.5	3.5	4.5	6.5
Anderson et al. [33]	1.5	2.5	4.5	7.5

In addition, it is already known that PSA levels in black men are higher compared to those in white men regardless of age, which also implies a careful interpretation of PSA levels [31]. Another fact that is important to have in mind is that the PSA level is a continuous parameter, so the higher the value, the more likely is the existence of CaP (Table 1.3) [29].

Table 13. Risk of prostate cancer in relation to PSA values in serum [29].

PSA level (ng/mL)	Risk of CaP (%)
0–0.5	6.6
0.6–1	10.1
1.1–2	17.0
2.1–3	23.9
3.1–4	26.9

1.4.2. Prostate Cancer Stage and Grade

PSA levels strongly discriminate different cancer stages: they are higher in men with localized disease, and even higher in patients with metastatic [30]. Numerous subsequent studies have confirmed the original data from Stamey et al. [34], where they affirmed that a higher PSA level is associated with a large tumor volume [35], higher clinical stage [34],

pathological stage [20] and Gleason grade [20, 35]. Usually, the PSA levels in biological fluids are combined with the Gleason sum score. This score ranges from 2 to 10 and consists of 2 summed grade patterns that can vary from 1 (well differentiated) to 5 (poorly differentiated) [20]. The combination of these two techniques allows the risk stratification and clinical stage of men with localized CaP, and which include low risk men (PSA < 10 ng/mL and Gleason grade ≤ 6), intermediate risk men (PSA 10-20 ng/mL or Gleason grade = 7) and high risk men (PSA > 20ng/mL or Gleason grade 8-10). These risk stratifications then guide the treatment decisions and enable to predict disease characteristics and treatment outcomes.

1.4.3. Monitoring Therapy and Disease Recurrence

After the diagnosis of prostate cancer, the question regarding the best treatment for each patient arises. If there is an indication that the cancer is localized within the prostate and that the patient has a life expectancy larger than ten years, radical prostatectomy is the treatment of choice [36]. Many patients are cured of prostate cancer by this treatment and the frequency of performing this procedure has increased significantly to ∼40% of all prostate cancers, partially owing it to the PSA screening. PSA testing in post-prostatectomy patients is of most importance in deciding who has residual disease, who has relapsed (and when) and who can be considered cured. This has been the most widely accepted application of PSA testing in clinical practice [36]. After radical prostatectomy, PSA should decrease to undetectable concentrations because all the source tissue has been removed. The serum half-life of PSA has been estimated as 2.2-3.2 days [37]. PSA reaches a new steady state after a given number of half-lives subsequent to surgery, depending on the amount of prostatic tissue that was present. Non-negligible PSA and increasing PSA concentrations indicate either that the entire prostate was not excised or that PSA is being produced by metastases of the original tumor. Lange et al. [38] reported that patients with a PSA level < 0.4 μg/L, 3-6 months after radical prostatectomy, lead to recurrence 6 to 49 months after surgery ($P < 0.0001$).

The widespread use of the PSA test led to the prostate cancer being diagnosed at earlier stages [4]. The patients proportion diagnosed at local stages increased significantly and diagnoses of disseminated disease were drastically reduced [4]. Consequently, a decline in mortality rate has been observed which is also attributed to the possibility of

making a prompt treatment of the localized disease [4]. The European Randomized Study of Screening for Prostate Cancer (ERSPC) detected an improvement in cancer mortality rate in a PSA screened group [21]. More recent data from the Gottenberg arm of the ERSPC trial have emerged [39]. With a longer term 14-year follow-up period, in comparison with the 9-year follow-up data of the ERSPC trial, this study demonstrated a reduction in the number needed to screen (NNS) and the number needed to treat (NNT) to prevent 1 death by 5- and 4-fold, respectively [39]. Of note, the Gottenberg arm study had a shorter screening interval and lower PSA threshold required for initiation of further investigations [39]. When the data from the ERSPC trial are extrapolated in a longer period of follow-up, a similar reduction in NNS and NNT is also seen in comparison with the original 9-year follow-up data [40]. This indicates that significant benefits from treating PSA screened diseases are likely to occur over a decade after treatment. Support for PSA screening may arise as the longer-term follow-up data of these trials. Moreover, additional studies [41, 42] proved that PSA levels indicate the risk of prostate cancer, years or even decades, before diagnosis. All these studies [41, 42] show that men who will eventually develop prostate cancer have increased PSA levels years or decades before the cancer is diagnosed.

Despite the great utility of PSA for CaP detection, as a single test, it also has several limitations. While essentially organ-specific, PSA is not cancer-specific since raised levels may also indicate benign prostatic hyperplasia, prostatitis (inflammation of the prostate), or small tumors that do not prove to be fatal. Another issue with the PSA test is that false positives are common, and many men with elevated PSA levels do not have prostate cancer at all [23]. Furthermore, treatment of these slow-growing tumors is costly and often involves life changing surgeries that may not be necessary. These facts put in cause the viability of the routine PSA screening for prostate cancer [23]. Despite these drawbacks, routine PSA screening has been advocated as a mean to reduce disease-specific mortality by detecting early CaP, amenable to radical treatment with curative intent. Influential groups, such as the American Urological Association, the National Comprehensive Cancer Network, and the European Association of Urology support the importance of PSA screening in CaP [43].

In the last years, several studies were conducted with the finality of refining the PSA test, increasing its diagnostic accuracy by improving the specificity of PSA in the early

detection of CaP. They include the measurement of the PSA density of the transition zone and the quantification of free to total PSA ratio and PSA molecular forms such as free PSA (fpsa), precursor isoforms of PSA (proPSA) and benign PSA (BPSA) [18]. However, the determination of the PSA density implies a biopsy. On the other hand, the measurement of molecular forms of PSA seems to be the most promising diagnostic tools so far [44].

1.5. PSA Molecular Characteristics

PSA is a serine protease that belongs to the family of glandular kallikrein related peptidases, clustered in a locus that spans approximately 280 kb of chromosome 19q133–4 [45]. This protein is encoded by the prostate-specific gene kallikrein 3 (KLK3). *PSA* gene expression in the prostate is regulated by androgens; two functional androgen-response elements are present in the proximal promoter of the *PSA* gene [45]. PSA in blood exists in multiple forms: free or in complexes with various protease inhibitors; as proprotein or mature protein; and as intact or nicked [45]. These forms, and their implications for prostate cancer, will be discussed further below.

1.5.1 Biosynthesis

Transcription and expression of PSA are basically restricted to prostate epithelial cells and periurethral glands, and are dependent upon androgen mediation. PSA is translated as a proenzyme, pre-pro-PSA (261 amino acids), with 24 additional residues in the pre-region (17 residues), and which are the signal peptide and the propeptide (seven residues). The signal peptide directs the protein to the membrane of the endoplasmic reticulum (ER) [46]. In the ER, the prepeptide is removed and the resulting pro-PSA is transported within vesicles to the plasma membrane, where it is secreted into the lumina of prostate ducts (Figure 1.2). The protease or proteases responsible for the clipping of PSA remained unidentified for a long time [46]. It was suggested that PSA can be autocatalytic, but the cleavage sites observed are highly suggestive of a trypsin like enzyme. Moreover, it was demonstrated that this enzymatic activity belongs to hK2, the protein most closely related to PSA (~80% amino acid sequence identity), being responsible for the cleavage of propeptide to form the extracellular mature PSA (237 amino acids) [47]. The cleavage of the *N*-terminal seven amino acids from proPSA generates the active enzyme, which has five intrachain disulfide bonds, a single asparagine-linked oligosaccharide, and a weight of

33 kDa. This proPSA cleavage normally occurs between the arginine at position 7 and isoleucine at position 8, with the isoleucine becoming the *N*-terminus of the mature active protein [45]. The sugar-chain structure of PSA is determined by a series of processing reactions catalyzed by Golgi glycosidases and glycosyl transferases. In its final form, PSA is secreted into semen, at concentrations of 0.5–5 mg/mL, becoming one of the major proteins in seminal plasma. In comparison, it is found at lower concentrations in the serum [47].

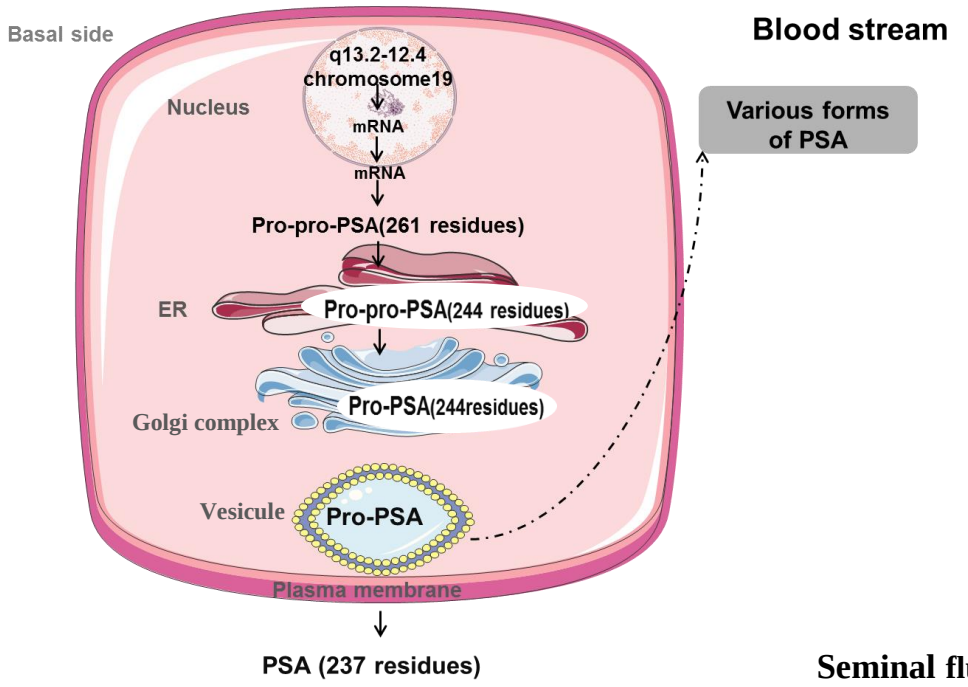

Figure 12. Schematic representation of PSA processing in epithelial cells of the prostate. ER, endoplasmic reticulum. Adapted from Reference [46].

Active PSA generated by hK2 can diffuse into the circulation, where it is rapidly bounded by protease inhibitors. This active PSA also undergoes proteolysis in the ER to generate inactive PSA which can enter the bloodstream (much smaller proportion than in semen) and circulates in an unbounded state (free PSA). In CaP, the loss of basal cells, the basement membrane and also the normal lumen architecture, results in a decrease in the ER processing of pro PSA to active PSA, and active PSA to inactive PSA, and with relative increases in bound PSA and proPSA in serum (Figure 1.3) [45]. While PSA is primarily produced by prostatic epithelial cells, PSA has also been detected in trace amounts in the paraurethral and perianal glands, endometrium, normal breast tissue, breast

tumors, breast milk, female serum, adrenal neoplasms and renal cell carcinomas [48] However, these sites do not normally contribute to measurable levels of PSA in the circulation [48, 49].

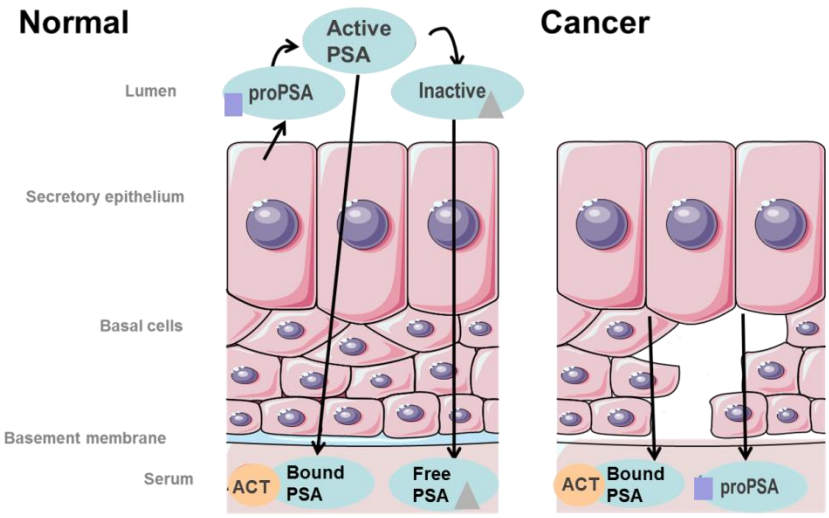

Figure 13. Model of PSA biosynthesis in normal prostate epithelium versus cancer. Adapted from Reference [48].

1.5.2. Structure

PSA is a glycoprotein with 28 kDa consisting of a single polypeptide chain of 237 amino acids and a single *N*-linked sugar-moiety [50]. This *N*-linked moiety comprises about 8% of the total mass of this protein. With regard to this moiety, a biantennary complex type with fucose linkages to the inner most *N*-acetylglucosamine (GlcNAc) was proposed, by NMR spectroscopy, as the major sugar-chain structure of PSA purified from seminal plasma [46]. It was also demonstrated that PSA is composed of 92% of peptides and 8% of carbohydrates, whereas the carbohydrate fraction is constituted by 4.84% of hexoses, 2.87% of hexosamines, and 0.25% of sialic acid [51]. The backbone contains a single carbohydrate unit attached at asparagine45 that increases the molecular weight by another 2-3 kDa and, in its mature form, exhibits five disulphide bonds [50].

In Figure 1.4, the 3D structure of PSA is displayed. The protein consists of two 6-strand antiparallel β-barrels and three α-helices. The catalytic site (Ser 195, His 57, and Asp 102) is conserved and localized in a cleft between two β-barrels [50]. The presence of

this characteristic His-Asp-Ser triad and a catalytic domain similar to those of other kallikrein-related peptidases is the reason for the categorization of PSA as a serine protease. The sequence also contains the GWG motif, which is a typical pattern present in many proteins with proteolytic activity. This motif contains Trp located in the β-barrel nearby the disulphide bond Cys 157-Cys [50]. Like for all serine proteases, the substrate and inhibitor recognition is mainly governed by the binding of the P1 residue to the S1 pocket of the enzyme [52].

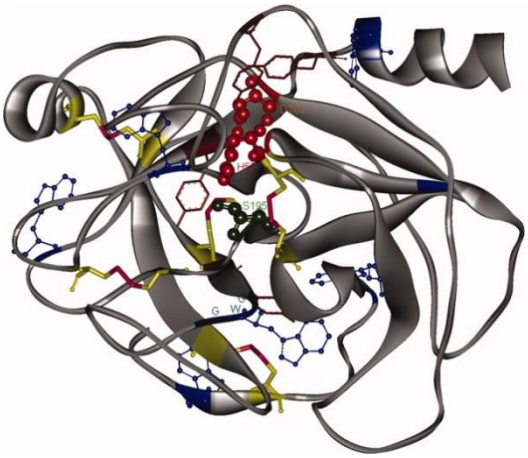

Figure 14. Cartoon representation of the crystal structure of the Prostate Specific Antigen (PDB ID: 1PFA). Catalytic Ser195, His57, Asp102 are highlighted in big ball and stick. Trp is highlighted in small ball and stick. Tyr is highlighted as sticks. Cys is highlighted as sticks [48].

1.5.3. Physiological Role

There is a great deal of interest and in determining the biochemical and physiological role of PSA. While most of the other kallikreins have trypsin-like proteolytic activity [52], PSA is considered a chymotrypsin-like protease. It shows similarities with chymotrypsin in the S1 specificity pocket of the catalytic site (presence of a serine at the bottom) and also preference for cleavage after the hydrophobic residues in the P1 position [52]. Despite these chymotrypsin similarities, PSA also displays enzymatic properties that differentiate it from chymotrypsin and other serine proteases. These differences suggest that there may be highly specific protein substrates for PSA that are not yet identified [53, 54]. Lilja et al. [55] revealed, in 1988, that the physiological function of PSA is the liquefying of seminal fluids, and this remains the most commonly accepted hypothesis until today. PSA liquefy

the seminal clot formed after ejaculation, in order to facilitate the transport of spermatozoa along the female reproductive tract. Gel structure dissolution occurs due to the PSA restricted chymotrypsinlike endoproteolytic activity, which allows the cleavage of semenogelin 1 and 2 (SEMG1, SEMG2), fibronectin, laminin and gelatin [55, 56]. Its activity is strongly inhibited by Zn^{2+}, that is 100 times more abundant in semen than in serum [57].

Outside its physiological role, PSA may participate in the process of neoplastic growth and metastasis. PSA may influence, in particular, the tumoral growth of prostate cells through the degradation of the insulin like growth factor [58]. Other authors suggest that PSA performs the proteolysis of extracellular matrix proteins, such as fibronectin and laminin, and could also mediate invasion and the metastasis of CaP cells [49]. Further, PSA has been shown to stimulate the mitogenic activity of osteoblasts, possibly due to the activation of latent transforming growth factor-β and proteolytic modification of cell adhesion receptors [49].

1.5.4. Physicochemical Properties

PSA is a glycoprotein that has several isoenzymes, two intact and nicked forms of PSA, in the isoelectric point (pI) range of 6.5–8 [59]. The intact isoenzymes display high enzyme activity and, on the other hand, nicked forms display very low or no enzymatic activity [60]. It seems that the differences in the sialic acid content are the origin on the existence of these multiple isoforms. Each PSA molecular form contains six immunoreactive, antibody binding sites (epitopes) [61]. Serum levels of substances are dependent on their production and distribution, but also on their rate of elimination. Free PSA is quickly eliminated from blood, with a terminal half-life of ~14 hours [49]. For total PSA (tPSA) measured in the conventional PSA tests, the terminal half-life is about 2.2-3.2 days [51]. In Table 1.4 some important biochemical characteristics of PSA are summarized.

Table 14. Biochemical characteristics of PSA [59, 60] [49, 51, 61].

Biochemical characteristics of PSA		
Molecular Mass (kDa)		28–33
Number of epitopes		6
Class		Glycoprotein
Subunit		Monomer
pI		6.5–8
Half-life	fPSA	~ 14 hours
	tPSA	2.2-3.2 days

1.5.5. Molecular Derivatives

It was initially assumed that the PSA measured in serum was the natural 28 kDa form of the protein containing 237 amino acids [51]. Only later it was discovered that PSA in serum appears in two different forms, either as complexed to other proteins (inhibitors) or as a free unbound form, "complexed PSA" and "free PSA", respectively [47]. Both complexed PSA and free PSA are combined to give a measure of tPSA conventionally used in the diagnostic of prostate cancer. While PSA isolated from seminal plasma is composed mainly of the catalytically active free form, in serum, the majority of PSA is complexed with endogenous inhibitors [45]. The most recognized inhibitors are alpha-1-antichymotrypsin (ACT), alpha-2-macroglobulin (A2M) and alpha-1-protease inhibitor (API). These protease inhibitors prevent the potential damage of the protease activity of PSA [62]. ACT covalently bound to PSA is the most common form and has a molecular weight of 80-90 kDa. The formation of this complex was described by the esterification of Ser-189 of PSA with Leu-358 of ACT. This leads to the cleavage of ACT between Leu-358 and Ser-359, as indicated by Sodium Dodecyl Sulfate -polyacrylamide gel electrophoresis (SDS-PAGE) and *N*-terminal sequence analysis [63]. Matrix-assisted laser desorption/ionization - time of flight mass spectrometry (MALDI-TOF MS) revealed molecular weights of 80.8 kDa for PSA-ACT, 28.3 kDa for PSA, and 56.9 kDa for ACT [64].

Several researchers have found that as the percentage of fPSA decreases, the probability of having cancer increases, suggesting that this form could possibly make an improved diagnostic [44]. The most convincing results came from a careful meta-analysis of 66 studies, which clearly verified a better diagnostic performance (that is, a higher

prostate cancer detection rate) for fPSA than for tPSA [65]. It was also established that the calculation of the percentage of free PSA in relation to tPSA (the free PSA ratio), allows a modest but significant improvement, in the discrimination of prostate cancer from benign disease such as benign prostatic hyperplasia. This combination seems to increase in patients with borderline or intermediate PSA values (4-10 ng/mL) and negative DREs [49].

1.5.5.1. Free PSA

Of the various modifications of serum PSA used to improve its specificity in detecting CaP, the concept of free to total PSA ratio (f/t PSA) is the most widely used approach [35]. It has been shown that the analysis of free PSA reduces the number of negative biopsies by 25% [66]. Free PSA is generally lower in prostate cancer, and ranges from 1% to 10%, when compared to the benign prostate enlargement [66]. This patterns is mostly due to the reduced exposure of PSA to abundant proteolytic enzymes in seminal fluid [66]. Since fPSA provides better cancer discrimination, several investigations have focused on further discriminating fPSA into different molecular forms [66, 67]. fPSA in serum is now known to be composed of at least three distinct forms of inactive PSA, and as shown in Figure 5. The first PSA form may contain a number of minor variants, but appears to be largely composed of intact PSA that is similar to native, active PSA, except for structural or conformational changes that have rendered it to be enzymatically inactive. A second form of PSA, called BPSA, is an internally cleaved or degraded form of PSA that is more highly associated with Benign prostatic hyperplasia (BPH) [68]. BPSA is identical to native mature PSA, and also contains 237 amino acids, but has 2 internal peptide bond cleavages at Lys182 and Lys145. The last has been identified as the proenzyme or precursor forms of PSA (proPSA), and is the form mostly associated to cancer[69]. ProPSA in serum and tissues was found to be comprised of several truncated proPSA forms (Figure 1.5), containing from 1 to 5 amino acids in the pro leader peptide instead of the native 7 amino acids. The native proPSA (otherwise known as [-7]proPSA) exists in a truncated form containing a seven amino acid *N*-terminal pro-leader peptide (APLILSR). Partial cleavage of [-7]proPSA results in the shortening of the seven amino acid pro-leader peptide to form [-5]proPSA (LILSR), [-4]proPSA (ILSR) and [-2]proPSA (SR) [62]. Immunohistochemical studies have shown that BPSA is expressed preferentially in the transitional zone of the prostate and is associated with pathological BPH, while proPSAs

are expressed almost exclusively in the peripheral zone of the prostate where most prostate cancers are known to emerge [62]. The truncated proPSA form contains pro leader peptides of 2 amino acids, and where [-2]proPSA is of particular interest [45]. One potential explanation for the enrichment of truncated proPSA forms is that these truncated forms are more resistant to activation than the intact proPSA. The truncated proPSA forms are therefore more stable. Subsequent studies on prostate tissues already proved that these PSA forms are highly enriched in prostate tumors and are a more specific prostate cancer marker [69]. Furthermore, amino acid sequencing showed that the proPSA is mainly comprised of a truncated form of [-2]proPSA rather than the usual seven amino acids ([-7]proPSA) [62].

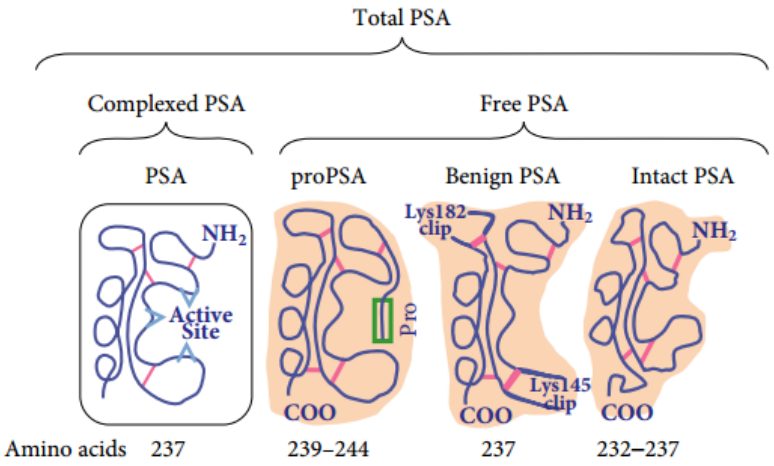

Figure 15. Schematic representation of the partitioning of free prostate-specific antigen (fPSA) into various precursor isoforms of PSA (proPSA), benign PSA and inactive PSA (iPSA) in serum, with the respective amino acid number. cPSA = complexed prostate-specific antigen [62].

The proPSA forms are especially useful in the 2.5–4 ng/mL PSA range, while the other PSA forms show little diagnostic utility [70]. A current systematic review and meta-analysis demonstrated that the percentage of [-2]proPSA in relation to fPSA ([-2]proPSA/fPSA × 100) has greater accuracy than tPSA or fPSA in detecting CaP, and also that [-2]proPSA might be helpful in preferentially identifying those patients who might harbor a more aggressive form of the disease [71]. Based on this, Beckman Coulter (Coulter ACCESS® immunoassay system) introduced a measure of prostate health index

(phi) (64). This value is calculated from a combination of tPSA, free PSA and a measure of a truncated PSA isoform, [-2]proPSA [62].

In healthy adult males aged ≤ 50 years-old, the concentrations are 10^6-fold higher in seminal fluid than in blood, in which the median PSA level is ~0.6 ng/mL [49]. In seminal fluid, PSA predominantly occurs in a free and active single-chain form, and only a minor proportion (≤5%) exists as inactive (due to internal cleavages) [56, 72]. The occurrence of this inactive form is due to a formation of covalent complexes with SERPINA5 (protein C inhibitor), which is abundantly released from the seminal vesicles [73]. In contrast, the majority of PSA that enters in blood is intact, non-catalytic and the predominant proportion is covalently linked to ACT [45]. PSA levels in blood span a ~10^5-fold range, from <0.1 to 10^4 ng/mL, with levels above 10^2 ng/mL found almost exclusively in men with advanced prostate cancer [49]. The increased blood levels of PSA in men with cancer cannot be explained by increased PSA expression; during the development and progression of prostate cancer, PSA expression may actually decrease slightly. The increased blood PSA levels must instead be caused by increased release of PSA into blood, consequently to the already mention rupture of prostate gland architecture, characteristic of CaP [49].

1.5.6. Stability of Sample Storage of Total and Free PSA

Clinical results for quantifying serum PSA are not usually urgently requested, and hence, samples are commonly stored and assayed in bundles or in batches for cost-efficiency [74]. PSA species are both pH- and temperature-labile, which implies a special care in sample handling and storage, since it might influence PSA stability in serum. Changes in immunoreactivity or alterations in the binding affinity with the specific antibody during the sample store are the major drawbacks [75]. Several investigators have reported the stability of tPSA in serum samples [65, 75]. It was already confirmed that tPSA is sufficiently stable at room temperature for 24h, after serum separation and storage in a refrigerator at 4°C for up to 1 week, or in a domestic freezer at -20°C for 1 month (76). In 2008, Reed et al. [75] have gone further when demonstrating that tPSA measured in serum exhibits a high correlation with the ones measured in the same serum after 7 years of storage at -80 ºC. However, this is not valid for fPSA since it is the most thermolabile isoform. In general, it is recommended to prepare samples for analysis within 8 h after venipuncture, with the storage of samples at 4 ºC when analyzed on the day of collection,

or to storage at temperatures of -70 ºC with additional adjustment of pH to 5.5 when not analyzed within 8 h after collection [76]. These procedures guarantee a sufficient stability of all PSA forms and eliminates pre-analytical factors as interfering variables [65, 76].

1.6. PSA Separation/Concentration Methods

Since the launch of the first test to measure serum tPSA by the Hybritech Corporation in 1986 [77], numerous others assays for fPSA, PSA-ACT and tPSA have become commercially available [5, 6]. In general, PSA is purified from either prostatic tissue or seminal plasma [46]. A typical purification scheme starts with ammonium sulfate fractionation, which is followed by separation methods including gel-filtration chromatography, isoelectric focusing, lectin-affinity chromatography, polyacrylamide gel electrophoresis and high-performance liquid chromatography [46]. These methods have mostly contributed to the discovery and identification of different molecular forms and biochemical properties of PSA. For a clinical application, immunoassays are the most common type of assays commercially available and that have the FDA approval [46]. Amongst the various kinds of identification and quantification for PSA, the fluorescence microscopy [78], surface plasmon resonance technology (SPR) [79], immunochromatography [80], lateral flow immunoassay [81], enzyme-linked immunosorbent assay (ELISA) [5], and immunochemiluminescency (TRIFA) [82] are widely employed. Usually, all commercial immunoassays consist on adding PSA monoclonal antibodies to serum (or plasma) and to incubate the biological fluid using standard methods and conditions [76]. Anti-PSA monoclonal antibodies bounded to PSA are detected and the probability that a carcinoma is present increases with increasing the PSA binding to antibodies [76]. For example, the Hybritech immunoassay, is a 2-site immunoenzymatic sandwich assay that utilizes alkaline phosphatase monoclonal antibody to capture the PSA and sandwich it with paramagnetic particles coated with another monoclonal antibody [6].

Even some of the tests and techniques mentioned above exhibit a high detection limit, most have significant drawbacks. Table 1.5 presents a summary of the techniques and methods commonly applied in the measurement of PSA levels and respective identification.

For instance, enzyme-linked immunosorbent assay (ELISA) is a powerful technique for antigen quantification; although, considerations such as laborious treatment steps, high cost of antibodies, low reproducibility, and the requirement of signal amplification using biochemical reaction have to be taken into account [6].

Fluorescence and electrochemistry-based methods require the labelling of the target analyte with dyes and conductors for signal generation and amplification. Sample loss during the modification steps may also affect the quantification results. Besides, prolonged exposure of fluorescence dye to excitation light source causes the photobleaching and quenching of signals that may lead to false negative and underestimated results [83].

Although SPR can provide a rapid, label-free and real time monitoring of the analyte by measuring the change in refractive indices, its high dependency on the physical refractive properties limits the types and size of analyte that can be detected by SPR and so restricts the choices of materials for biosensing [83].

Table 15. Comparison of literature methods for purification/concentration of PSA molecular forms from different human matrices.

Purification/Concentration Method	PSA molecular form	Matrix	PSA recovery (%)	Ref.
ELISA	tPSA	Serum	99.5	[5]
Sensitive rapid tandem bioluminescent enzyme immunoassay (BLIA)	PSA/ACT	Serum	85.6	[84]
Imunofluorometric assays (TRIFA)	fPSA	Serum	47.5	[82]
Indirect Immunosorption	fPSA PSA/ACT	Serum	60	[85]
Cibacron blue affinity-based depletion	fPSA; PSA/ACT	Serum	5	[86]
Mixed polyclonal antibody and protein G column	fPSA PSA/ACT	Serum	70	[86]
Column of immobilized monoclonal antibodies(commercial antibody fragment Vivapure anti-HSA kit)	free PSA PSA/ACT	Serum	95	[86]
Thiophilic gel	fPSA	seminal plasma	96	[87]
Thiophilic gel	TPSA	prostate tissue	87	[57]
Ultrogel ACA44 column	fPSA	Serum	96	[88]
Affinity chromatography size-exclusion and ion exchange chromatography, anion-exchange chromatography	isoforms of PSA	seminal plasma	55	[59]
Ammonium sulfate precipitation, hydrophobic interaction chromatography, gel filtration and anion-exchange chromatography	isoforms of PSA	seminal plasma	30	[60]
Chip EIA	tpsa	Serum	88.9	[6]

1.7. Concentration and Extraction of PSA Using Aqueous Biphasic Systems (ABS)

In 1896, Beijerinck [89] first reported the occurrence of aqueous biphasic systems (ABS), when discovering that agar and gelatin, dissolved at certain concentrations in aqueous media, formed two liquid aqueous-phases. However, only in 195, Albertson [90] introduced ABS as an extractive/separation technique for biomolecules by their partitioning between the coexisting phases. These two-phase systems are formed spontaneously upon mixing two aqueous solutions of structurally different components, such as two polymers, two salts or one polymer and one salt [91]. One of the aqueous phases will be enriched in one of the solutes while in the other phase there is prevalence for the second polymer or salt.

For the design of ABS as extraction and concentration processes, their phase diagrams and respective tie-lines are required. All ABS have a unique phase diagram under a particular set of conditions, such as pH and temperature [91]. These diagrams are useful to known in which conditions it is possible to form a biphasic mixture and at which ternary compositions the extraction can be performed. They reflect the concentration of the phase-forming components required to form a two-phase system, the concentration of the phase components in the top and bottom phases, and the ratio of phase volume or weight. Figure 1.6 depicts the common representation of an ABS composed of polypropylene glycol (PPG), a salt and water in an orthogonal representation where the amount of water is omitted. The binodal curve represents the border between the miscible and immiscible regions. In all phase diagrams, the biphasic region is localized above the solubility curve, and below it is the single phase region. The larger the biphasic region, the higher the ability of the phase-forming components to undergo liquid-liquid demixing [91, 92]. The critical point of the ternary system is Point C, where the two binodal nodes meet. In Figure 1.6 the binodal curve is represented by the black line, and three mixture compositions at the biphasic region and the critical point are identified as X, Y, Z and C, respectively. The mixtures X, Y and Z are along the same tie-line (TL) meaning that all the initial mixtures will present the same top ($[PPG]_{PPG}$, $[PPG]_{Salt}$) and bottom phase compositions ($[Salt]_{PPG}$, $[Salt]_{Salt}$) [92].

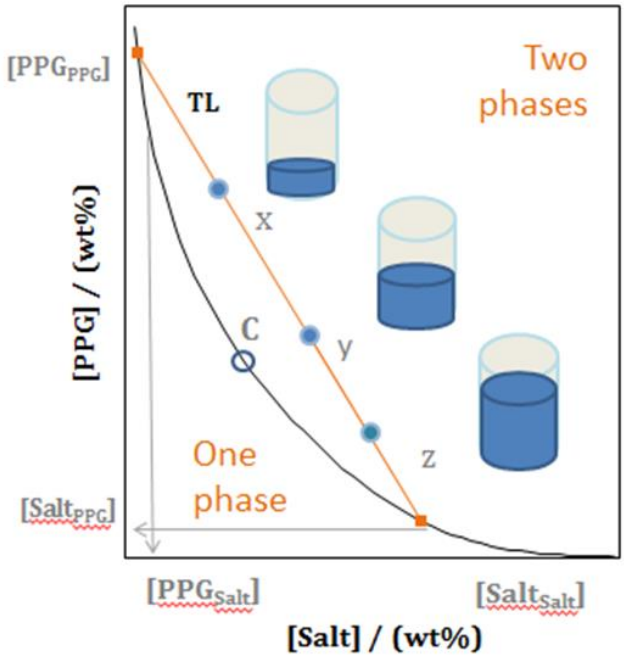

Figure 16. Representation of the phase diagram of an ABS. Binodal curve: (-); Critical point: C; tie-line (TL); Mixture compositions at the biphasic region (X, Y and Z). Adapted from Reference [92].

The tie-line length (TLL) is a numerical indicator of the composition difference between the two phases and is generally used to correlate trends in the partitioning of solutes between the phases. The length of each tie-line is related with the weight of the phases and defines the difference in compositions among the coexisting phases [92].

ABS have been thoroughly explored in the past years, and are currently seen as a powerful technique for the purification and extraction of biomolecules [93, 94]. ABS have already been successfully applied in the separation and purification of different biological materials, such as cells, virus, organelles, nucleic acids, lipids, amino acids, proteins, antibodies and enzymes, without significant denaturing effects [91]. Their biocompatible character is derived from a high water content in both phases, up to 70-90 wt%, which provides a mild environment to extract biomolecules/bioparticles [95].

In general, the partitioning of a molecule between the two phases in an ABS is a complex phenomenon, driven by several competing interactions and properties of the partitioned solute and phase components. Properties, such as the isoelectric point, surface hydrophobicity, molecular weight, ionic strength, electrochemical and conformational characteristics of the target biomolecule influence the partitioning behaviour between the coexisting phases [91]. Some of these characteristics can even be indirectly influenced by

other conditions, such as pH, and type and concentration of the phase-forming components. By controlling these factors, it is possible to foreseen a selective partitioning and to recover a target product [91]. The interactions involved in the partitioning of proteins in ABS are usually short-range (van der Waals) and long-range electrostatic molecular interactions between the biomolecule and the surrounding phases [96]. Other driving force in ABS partitioning is the excluded volume effect [91]. The complexity of chemical and physical interactions involved in the partitioning process in ABS are also responsible for making these systems very powerful in contrast to other established separation techniques [92].

ABS may represent an appealing alternative to the current request for fast, economic, and easy-to-implement processes. Integrating, clarification, concentration and purification in a single operation unit is possible, and, since it is a liquid system, it can be easily scaled-up only by increasing the components volume [97]. Other advantages include a comparatively low energy and time consumption, and low material cost. These methods have been replacing other extraction techniques which use volatile and hazardous organic solvents, two-step precipitation and ion exchange chromatography [98, 99]. For instance, Aguilar et al. [98] compared the performance of ion exchange chromatography and an ABS composed of PEG/phosphate-salt for the partial purification of penicillin acylase, and verified that not only the number of unit operation steps is decreased from 7 to 4, but it is also more cost effective with a high enzyme recovery (97%). A comparison between a purification process using ion-exchange chromatography, with a previous acetone fractionation, and an ABS extraction demonstrated superior overall recovery of the enzyme α-galactosidase in ABS (11.5 *vs.* 87.6%, respectively) [99].

Other widely used technique for the extraction/purification of proteins/enzymes consists on the precipitation of the target molecule. Usually, this technique is applied with the same purpose of the ABS, as a primary recovery step aiming at capturing the biomolecule and sometimes achieving a concentration and partial purification, and thus increasing the efficiency of the subsequent steps. A comparison between the two methods was already performed and ABS exceeded the precipitation method, leading to a greater recovery yield (88 % *vs.* 49 %) and purity (100 % *vs.* 89 %) of the target biomolecule [100]. From the described investigations, it is clear that ABS can serve as an alternative to other conventional separation processes, in particular for proteins and enzymes.

For long, the studied ABS were based in the coexistence of two immiscible aqueous-rich phases formed by polymer–polymer, polymer–salt and salt–salt mixtures [91]. Although, since the demonstration by Rogers and co-workers [101] on the possibility of creating ABS by mixing ionic liquids (ILs) and inorganic salts in aqueous solutions, novel ABS composed of ILs + water + organic/inorganic salts, amino acids, polymers or carbohydrates have become the focus of many other studies [94]. The main advantages of these new ABS, when compared to polymer–polymer systems, relay on their lower viscosities and on the possibility of tailoring the polarities of the coexisting phases [102]. Moreover, they usually display a quick phase separation [103], higher extraction efficiencies and allow their design [104]. IL-based ABS are also a potential alternative to polymer + salt ABS, since the latter presents a hydrophobic phase mostly composed of the polymer and a highly charged and hydrophilic aqueous phase [91].

1.7.1. Ionic-liquid-based (IL- based) ABS

Ionic liquids (ILs) were first reported at the beginning of the 20th century by Paul Walden [105], when testing new explosive compounds, for the substitution of nitroglycerin, while synthesizing ethylammonium nitrate. At the time, the discovery of a liquid salt at room temperature did not receive an extensive attention; only in 1934, Charles Graenacher [106] filled the first patent for an industrial application regarding ILs for the preparation of cellulose solutions. During the 2nd World War, new patents involving the use of ILs in mixtures of aluminium chloride (III) and 1-ethylpyridinium bromide for the electrodeposition of aluminium were filled [107, 108]. Nevertheless, only in the past few years, with the appearance of air and water stable ILs, the research and development of novel ILs and their possible applications increased significantly [93, 101, 104, 109-112].

ILs are salts formed entirely of ions, and consist of large asymmetric organic cations and usually an organic or inorganic anion. Due to the large size of their ions, their charges are frequently diffuse. As a result, they present reduced electrostatic forces which makes difficult to them to form a regular crystalline structure, and therefore, they can be liquid at or near room temperature. The most commonly studied ILs are nitrogen-based and their general cation chemical structures are presented in Figure 7.

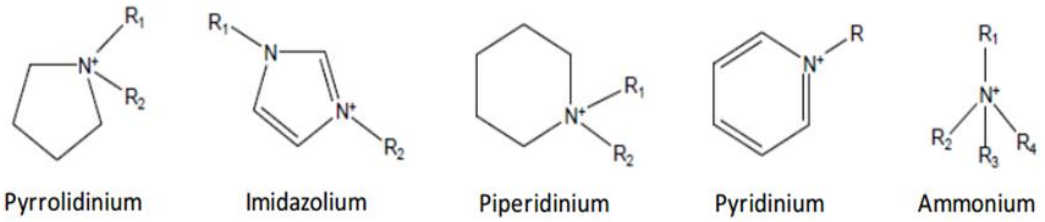

Figure 17. Chemical structures of the cations of nitrogen-based ILs.

The most interesting features of ILs can be attributed to their ionic character, such as a negligible vapor pressure, low flammability, high thermal and chemical stabilities and an enhanced solvation ability for organic, inorganic and organometallic compounds [91]. The ILs negligible volatility and non-flammability have contributed to their common designation of "green solvents" [113]. In addition, one of the main advantages of ILs is the fact that their physical and chemical properties can be tuned by changing the cation and the anion for a given application - "designer solvents". This feature promotes the possibility of tailoring their properties, such as hydrophobicity and solution behaviour, thermophysical properties, and variable biodegradation ability or toxicological characteristics [91].

The extraction of proteins using IL-based ABS was first achieved by Du et al. [111] on the extraction of proteins from human body fluids by employing a 1-butyl-3-methylimidazolium chloride ($[C_4mim]Cl$) + K_2HPO_4 system. After this proof of principle, other authors studied the extraction of proteins and enzymes, such as bovine serum albumin, lysozyme, trypsin, myoglobin, horseradish peroxidase, cytochrome c, γ-globulins, haemoglobin, peroxidase and ovalbumin using IL-based ABS, and revealed that their enzymatic activity or stability was not compromised [91]. The possibility of ILs to be tailored to exhibit specific properties combined with the optimization of the experimental conditions, makes possible that IL-based ABS could be used as a moderate environment for proteins without change on their chemical structure while preventing their denaturation [91].

1.7.2. Bovine Serum Albumin (BSA) as a Model Protein in Extraction/Concentration Procedures

Since the commercially available cancer biomarkers are highly cost products and are mostly offered in very small concentrations it is necessary to initiate the experimental investigations on extraction/purification/concentration procedures using model compounds aiming at defining the improved ABS. In this work, bovine serum albumin (BSA), the most abundant protein in blood plasma of many species (up to 40 mg/mL) [114], was chosen as a model protein before the experimental studies with PSA. Currently, several studies already reported on the ability of IL-based ABS for the extraction and purification of BSA [115-117].

BSA is a single-chain protein that belongs to the class of serum albumins and is constituted by the twenty essential amino acids within a structure that contains 583 units. The molecular weight for BSA, calculated from different techniques, ranges from 66411 to 66700 Da and "the best value" in solution is 66500 Da [114]. The structure of BSA at the physiological pH is predominantly α-helical (67%) with the remaining polypeptide chain occurring in turns and extended or flexible regions between subdomains with no β-sheets. The BSA molecule is made up of three homologous domains (I, II and III) which are divided into nine loops by 17 disulfide bounds [118, 119].

The charged groups are evenly distributed in BSA; the net negative charge is highest in the N-terminal domain and the lowest in the C-terminal domain. Furthermore, several isomers of BSA exist at various pH values [120]. Its main physicochemical properties are presented in Table 1.6.

Table 16. Physicochemical properties of BSA [114, 121].

Molecular weight ($g \cdot mol^{-1}$)	66.50
Solubility in water at 25 ºC	highly soluble in water
Number of amino acids	585
pI in water at 25 ºC	4.7

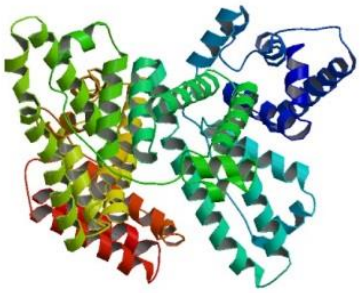

Figure 1.8. BSA structure [122]

2. Extraction of BSA using IL + Salt ABS

2.1. Introduction

Proteins exhibit admirable biological properties, being considered very important biomolecules [123]. The production and applications of proteins have rapidly grown up in different fields, such as biochemical research, and in the chemical, food and pharmaceutical industries [123]. Due to their wide application, it is necessary to maintain the three-dimensional structure of proteins through some weak interactions including hydrogen bonds, dispersive and ionic interactions [123]. Consequently, many efforts have been made in order to acquire knowledge on extraction procedures for proteins and pharmaceutical products. However, due to their poor stability, a change in the micro-environment of proteins disrupts these interactions, causing denaturation of proteins which leads to protein unfolding and inactivation [123]. Therefore, the demand to develop not only biocompatible but also cheaper and sustainable extraction and purification processes for proteins has led to an intense effort to develop clean manufacturing methods and easily scaled-up industrial techniques [124].

The traditional protein purification methods include ammonium sulphate precipitation, electrophoresis, ion-exchange chromatography, and affinity chromatography [98, 99]. These methods are not only time and cost consuming, but also are responsible for their loss of stability. In addition, some of these methods employ organic compounds, presenting therefore some drawbacks since they are volatile and hazardous to human health and to the environment [125].The use of aqueous biphasic systems (ABS) based on the application of ionic liquids (ILs) emerged in recent years [101] and are a clean alternative for traditional organic-water extraction systems.

Proteins' stability is strongly affected by the proton activity of the supporting solution and has an optimum pH that can be adjusted by the addition of a proper biological buffer. It is generally accepted that, at appropriate concentrations, hydrophilic ILs tend to dissociate in aqueous solutions, fully or partly, and into ions which form neutral or very weakly basic solutions [116]. Certainly, this pattern is not always true because there are some functionalized ILs that work as Lewis acidic or basic catalysts [126]. Adding a buffer into aqueous IL solutions, when dealing with protein stability, will not provide an adequate pH control since the ILs acidity or basicity could swamp the buffer effect [116]. Therefore, it is crucial to look for alternative pH control methods, and in particular in the design of ILs with buffering characteristics. Good and his research team [127] have designed

biological buffers (Good's buffers, GB) that fit these criteria and that can be used as ILs precursors.

Good's buffers are zwitterionic amino acid derivatives, and they are the most widely used biological buffers. It was suggested that these Good's buffers act as kosmotropic substances (strongly hydrated molecules) and protein structure stabilizers [127]. Since Good's buffers are zwitterionic compounds they can be used as anion or cation radicals of ILs [127]. This possibility creates new protein stabilizing ILs with self-buffering characteristics.

Novel GB-ILs were synthesized in this work while showing that they control the pH of the aqueous environment, and can thus stabilize proteins. The GB-ILs adopted in this work are based on N-(2-hydroxy-1,1-bis(hydroxymethyl)ethyl)glycine (Tricine), 2-[1,3-dihydroxy-2-(hydroxymethyl)propanyl]amino]ethanesulfonic acid (TES), N-cyclohexyl-2-aminoethanesulfonic acid (CHES), N-cyclohexyl-2-aminoethanesulfonic acid (HEPES), and 2-(N-morpholino)ethanesulfonic acid (MES). These buffers were converted into anions and coupled to the tetrabutylammonium ($[N_{4444}]^+$) and tetrabutylphosphonium ($[P_{4444}]^+$) as cations. These GB-ILs were then used as constituents of aqueous biphasic systems (ABS), combined with potassium citrate in aqueous media, as alternative extraction media for proteins. Initially, the ternary phase diagrams, tie-lines (TLs) and tie-line lengths (TLLs) were determined at 25 ºC. Then, these systems were investigated as liquid-liquid extraction systems for BSA, used here as a model protein.

Size-exclusion HPLC is a highly precise and sensitive tool for quality control of proteins and which allows to infer on the protein stability, as well as on other contaminant proteins in solution, and was employed here as a quantification technique.

2.2. Experimental Section

2.2.1. Chemicals

The salt potassium citrate tribasic monohydrate ($K_3C_6H_5O_7 \cdot H_2O$, purity ≥ 99 wt%) was obtained from Sigma–Aldrich Chemical Co. (USA). BSA/fraction V, pH = 7.0, was obtained from Acros Organics. Methanol (HPLC grade, purity > 99.9%) was obtained from Fisher Scientific. Acetonitrile (purity > 99.7%) was supplied from Lab-Scan. The buffers required for the ILs synthesis, namely CHES (purity > 99 wt%), HEPES (purity > 99.5 wt%), MES (purity > 99 wt%), Tricine (purity > 99 wt%), and TES (purity > 99 wt%)

were purchased from Sigma–Aldrich Chemical Co. The hydroxide-based compounds, as cation precursors, $[N_{4444}][OH]$ (40 wt% in H_2O) and $[P_{4444}][OH]$ (40 wt% in H_2O) , were also supplied by Sigma–Aldrich Chemical Co. Sodium hydroxide pellets were acquired from Eka Chemicals-. Dimethyl sulfoxide (DMSO, purity > 99.9 wt%) and deuterium oxide (D_2O purity > 99.9 wt%) were obtained from Sigma–Aldrich Chemical Co..

Purified water passed through a reverse osmosis and a Milli-Q plus 185 water purifying system was used in all experiments.

2.2.2. Experimental Procedure

2.2.2.1 Synthesis and Characterization of Good's buffer ionic liquids

The GB-ILs were synthesized *via* neutralization of the base with the appropriate acid. A slightly excess of an equimolar aqueous solution (1:1.1) of buffer was added drop-wised to a tetrabutylphosphonium or tetrabutylammonium hydroxide solution. By way of example, tricine buffer was added dropwise into an aqueous solution of tetrabutylphosphonium hydroxide. The mixture was stirred continuously for at least 12 h at room temperature (≈ 25 ºC). The anion source (1.1 equivalents of acid) was added to an aqueous solution of $[P_{4444}][OH]$ (1 equivalent, 40 wt.% in water) and the mixture was stirred at room temperature for at least 12 h to produce the ionic liquid and water as by-product.

The mixture was then evaporated at 50-60 °C under reduced pressure and which gives rise to a viscous liquid. A mixture of acetonitrile and methanol (1:1, v:v) was added to the viscous liquid and then vigorously stirred at room temperature for 1 h. The solution was then filtered to remove any excess buffer. The solvent mixture was evaporated and the GB-IL product was dried in vacuum (10 Pa) for 3 days at room temperature. The water content in each GB-IL was measured by Karl–Fischer (KF) titration, using a KF coulometer (Metrohm Ltd., model 831). The chemical structures of the GB-ILs were confirmed by ^{1}H and ^{13}C NMR spectroscopy (Bruker AMX 300) operating at 300.13 and 75.47 MHz, respectively. Chemical shifts are expressed in δ (ppm) using tetramethylsilane (TMS) as internal reference and D_2O as deuterated solvent. The synthesized ILs synthetized in this work showed high purity level without signs of decomposition.

2.2.2.2. Phase Diagrams and Tie-lines (TLs)

The binodal curve of each ABS was determined through the cloud point titration method at 25 (± 1) ºC and atmospheric pressure. The experimental procedure has been validated in previous reports [128, 129]. Repetitive drop-wise addition of the aqueous salt solution to the IL solution was carried out until the detection of a cloudy biphasic solution, followed by the drop wise addition of water until the finding of a monophasic region. This procedure was carried under constant stirring. Each mixture composition was determined by the weight quantification of all components added within an uncertainty of ± 10^{-4} g (using an analytical balance, Mettler Toledo Excellence XS205 DualRange).

The tie-lines (TLs) of each phase diagram, and at the mixtures compositions for which the extraction of BSA was carried out, were determined by a gravimetric method originally described by Merchuk et al. [130]. The selected mixture, at the biphasic regime, was prepared by weighting the appropriate amounts of IL + salt + water and further vigorously stirred. Then, the mixture was submitted to centrifugation for 10 min and at controlled temperature (25 ± 1) °C. After centrifugation, the sample was left in equilibrium for more 10 min at (25 ± 1) °C to guarantee the equilibration of the coexisting phases. After this period, each phase was carefully separated and weighted. Each individual TL was determined by the application of the lever-arm rule to the relationship between the weight of the top and bottom phases and the overall system composition. The experimental binodal curves were fitted using Eq. 1 [130],

$$[\mathrm{IL}] = Aexp[(B[\mathrm{Salt}]^{0.5}) - (C[\mathrm{Salt}]^{3})] \quad (1)$$

where [IL] and [Salt] are the IL and salt weight fractions percentages, respectively, and A, B and C are fitted constants obtained by least-squares regression. Each individual TL was determined by a weight balance approach through the relationship between the top weight phase composition and the overall system composition. For the determination of TLs the following system of four equations (Eqs. 2 to 5) was used to estimate the concentration of IL and salt at each phase ($[\mathrm{IL}]_{\mathrm{IL}}$, $[\mathrm{IL}]_{\mathrm{Salt}}$, $[\mathrm{Salt}]_{\mathrm{Salt}}$ and $[\mathrm{Salt}]_{\mathrm{IL}}$) [130]:

$$[\mathrm{IL}]_{\mathrm{IL}} = Aexp\left[\left(B[\mathrm{Salt}]_{\mathrm{Salt}}^{0.5}\right) - \left(C[\mathrm{Salt}]_{\mathrm{Salt}}^{3}\right)\right] \quad (2)$$

$$[\mathrm{IL}]_{\mathrm{Salt}} = Aexp\left[\left(B[\mathrm{Salt}]_{\mathrm{Salt}}^{0.5}\right) - \left(C[\mathrm{Salt}]_{\mathrm{Salt}}^{3}\right)\right] \quad (3)$$

$$[\mathrm{IL}]_{\mathrm{IL}} = \frac{[\mathrm{IL}]_{\mathrm{M}}}{\alpha} - \left(\frac{1-\alpha}{\alpha}\right)[\mathrm{IL}]_{\mathrm{Salt}} \quad (4)$$

$$[\mathrm{Salt}]_{\mathrm{IL}} = \frac{[\mathrm{Salt}]_{\mathrm{M}}}{\alpha} - \left(\frac{1-\alpha}{\alpha}\right)[\mathrm{Salt}]_{\mathrm{Salt}} \quad (5)$$

where the subscripts salt and IL designate the salt- and IL-rich phases, respectively, and M is the initial mixture composition. The parameter α is the ratio between the top weight and the total weight of the mixture. The solution of this system provides the concentration (wt %) of the IL and salt in the top and bottom phases, and thus the, TLs can be easily represented. For the calculation of the tie-line length (TLL) Eq. 6 was applied.

$$\mathrm{TLL} = \sqrt{([\mathrm{Salt}]_{\mathrm{IL}} - [\mathrm{Salt}]_{\mathrm{Salt}})^2 + ([\mathrm{IL}]_{\mathrm{IL}} - [\mathrm{IL}]_{\mathrm{Salt}})^2} \quad (6)$$

For this approach, each experimental binodal curve was previously fitted by Eq. 1.

All the calculations considering the mass fraction or molality of the citrate-based salt were carried out discounting the complexed water.

In all systems, the IL-rich phase corresponds to the top phase while the bottom phase is mostly enriched in the organic salt.

2.2.2.3. pH measurements

The pH values of both the IL-rich and organic-salt-rich aqueous phases were measured at (25 ± 1) ºC using a METTLER TOLEDO SevenMulti pH meter within an uncertainty of ± 0.02.

2.2.2.4 Extraction Efficiencies of Bovine Serum Albumin

The ternary mixtures compositions used in the partitioning experiments of BSA were gravimetrically prepared at a fixed and common mixture composition: (22.4 ± 1.3) wt % of $[N_{4444}][GB]$ + (25.6 ± 2.6) wt% of salt and (39.4 ± 0.7) wt % of $[P_{4444}][GB]$ + (15.1 ± 0.9) wt % of salt. The aqueous solution added contained BSA at a concentration of *circa* 0.5 $g \cdot dm^{-3}$. Each mixture was vigorously stirred, centrifuged for 10 min, and left to equilibrate for at least 10 min at 25 (± 1) °C to achieve the complete BSA partitioning between the two phases. After, a careful separation of the phases was performed, and the amount of BSA in each phase was quantified by SE-HPLC (Size Exclusion High-Performance Liquid Chromatography) using a calibration curve specifically determined for this purpose (Appendix A). Each aqueous phase was diluted at a 1:10 (v:v) ratio in a phosphate buffer saline solution before injection. For the preparation of the phosphate buffer saline solution it was used: sodium phosphate monobasic (NaH_2PO_4) and sodium phosphate dibasic heptahydrated ($Na_2HPO_4 \cdot 7H_2O$). A Chromaster HPLC (VWR, Hitachi) coupled with an UV detector was used. RP-HPLC was performed on an analytical column (25 cm × 2 mm

i.d., 25 μm), Lichrospher 100 RP-18 from Merck. A 100 mM phosphate buffer in MiliQ water (mobile phase) was run isocratically with a flow rate of 1 mL·min^{-1}. The column oven temperature was kept constant at 25 °C as well as the auto-sampler temperature. The injection volume was of 25 μL. The wavelength was set at 280 nm whereas the retention time of BSA was found to be 9.31 min within an analysis time of 24 min. The quantification of BSA was carried out by an external standard calibration method in the range of 0.001 to 1 g·dm^{-3} of protein. At least three independent biphasic mixtures for each GB-IL-based system were prepared and 3 samples of each phase were quantified. The interference of the salts and ILs with the quantification method was also ascertained and blank control samples were initially analyzed.

The percentage extraction efficiency of BSA, $EE_{\mathrm{BSA}}\%$, is the percentage ratio between the amount of protein in the IL-rich aqueous phase to that in the total mixture, and is defined according to Eq. 7,

$$EE_{\mathrm{BSA}}\% = \frac{[\mathrm{BSA}]_{\mathrm{IL}} \times w_{\mathrm{IL}}}{[\mathrm{BSA}]_{\mathrm{IL}} \times w_{\mathrm{IL}} + [\mathrm{BSA}]_{\mathrm{Salt}} \times w_{\mathrm{Salt}}} \qquad (7)$$

where [BSA] is the concentration of protein, *w* is the weight of each phase, and the subscripts IL and Salt represent the IL- and salt-rich phases, respectively.

2.3 Results and Discussion

2.3.1. Characterization of synthetized Ionic Liquids

The macroscopical appearance and NMR characterization data for each GB-IL are described below.

[P_{4444}][Tricine]: From Tricine buffer (50.3 mmol), this compound was obtained as white solid. Water content < 0.05 wt%. ^{1}H NMR (300 MHz, D_2O/TSP): 3.37 (s, 6H), 3.12 (s, 2H), 2.00 (m, 8H), 1.27-1.44 (m, 16H), 0.77 (t. 12H). ^{13}C NMR (75.47 MHz, D_2O/TSP): 182.71, 63.12, 62.97, 47.68, 26.28, 20.79, 20.15, 15.42.

[P_{4444}][TES]: From TES buffer (45.1 mmol), this compound was obtained as a light viscous liquid. Water content < 0.05 wt%. ^{1}H NMR (300 MHz, D_2O/TSP): 3.31 (s, 6H), 2.82 (s, 2H), 2.57 (t, 2H), 2.10 (m, 8H), 1.29-1.49 (m,16H), 0.79 (t, 12H). ^{13}C NMR (75.47 MHz, D_2O/TSP): 60.65, 57.63, 51.58, 37.69, 26.28, 20.83, 20.17, 15.46.

[P_{4444}][MES]: From MES buffer (48.5 mmol), this compound was obtained as a white solid. Water content < 0.05 wt%. ^{1}H NMR (300 MHz, D_2O/TSP): 3.63 (t, 4H), 2.99 (t,

2H), , 2.72 (t, 2H), 2.50 (t, 4H), 2.02 (m, 8H), 1.27-1.42 (m, 16H), 0.78 (t,12H,). ^{13}C NMR (75.47 MHz, D_2O/TSP): 68.80, 55.44, 55.11, 50.02, 26.28, 20.80, 20.16, 15.44.

[P_{4444}][HEPES]: From HEPES buffer (44.3 mmol), this compound was obtained as as a light viscous liquid. Water content < 0.05 wt%. ^{1}H NMR (300 MHz, D_2O/TSP): 3.59 (t,4H), 2.97 (t, 2H), 2.94 (t, 2H), 2.67 (t, 2H), 2.46 (t, 8H), 2.03 (m, 8H), 1.28-1.45 (m, 16H), 0.79 (t, 12H). ^{13}C NMR (75.47 MHz, D_2O/TSP): 61.59, 60.87, 55.02, 54.78, 54.19, 50.39, 26.29, 20.80, 20.16, 15.44.

[P_{4444}][CHES]: From CHES buffer (47.2 mmol), this compound was obtained as a white solid. Water content < 0.05 wt%. ^{1}H NMR (300 MHz, D_2O/TSP); ^{1}H NMR (300 MHz, D_2O/TSP); 2.95 (m, 2H), 2.38-2.47 (*m*, 1*H*), 2.02 (m, 8H), 1.28-1.45 (m, 16H,), 0.94 (m, 10H), 0.78 (t, 12H). ^{13}C NMR (75.47 MHz, D_2O/TSP): 63.37, 63.09, 53.42, 39.56, 26.28, 26.08 , 25.60, 20.30, 20.15, 15.43.

[N_{4444}][Tricine]: From Tricine buffer (52.3 mmol), this compound was obtained as a white solid. Water content < 0.05 wt%. ^{1}H NMR (300 MHz, D_2O/TSP): 3.53 (s, 6H) 3.27 (s, 2H), 3.21 (t, 8H), 1.65 (quin, 8*H*), 1.37 (sext, 8*H*), 0.93 (t,12H). ^{13}C NMR (75.47 MHz, D_2O/TSP): 182.83, 63.15, 62.93, 60.97, 47.70, 26.00, 22.03, 15.71.

[N_{4444}][TES]: From TES buffer (49.0 mmol), this compound was obtained as a white solid. Water content < 0.05 wt%. ^{1}H NMR (300 MHz, D_2O/TSP): 3.32 (s,6H), 3.17 (t, 8H), 2.86 (t, 2H), 2.60 (2H, t), 1.55 (quin, 8H), 1.30 (sext,8 *H)* 0.91 (t,12 H). ^{13}C NMR (75.47 MHz, D_2O/TSP): 60.55, 60.49, 57.59, 51.50, 37.65, 23.20, 19.25, 13.52.

[N_{4444}][MES]: From MES buffer (48.5 mmol), this compound was obtained as a white solid. Water content < 0.05 wt%. ^{1}H NMR (300 MHz, D_2O/TSP): 3.53 (t, 4H), 3.17 (t, 8H); 2.51 (t, 2H,), 2.49 (t,2H,), 2.32 (t, 4H), 1.55 (quin 8H), 1.30 (sext, 8H), 0.93 (t,12H). ^{13}C NMR (75.47 MHz, D_2O/TSP): 68.94, 61.00, 55.53, 55.18, 50.19, 26.03, 22.07, 15.78.

[N_{4444}][HEPES]: From HEPES buffer (45.9 mmol), this compound was obtained as a white solid. Water content < 0.05 wt%. ^{1}H NMR (300 MHz, D_2O/TSP): 3.46 (t, 4H), 3.17 (t, 8H); 2.61 (t, 2H), 2.54 (t, 2H), 2.50 (t, 2H), 2.34 (t, 8H), 1.55 (quin, 8H), 1.33 (sext, 8H), 0.93 (t, 12H). ^{13}C NMR (75.47 MHz, D_2O/TSP): 61.66, 60.97, 60.97, 55.06, 54.83, 54.26, 50.45, 26.03, 22.06, 15.76.

[N_{4444}][CHES]: From CHES buffer (49.0 mmol), this compound was obtained as a white viscous liquid. Water content < 0.05 wt%. ^{1}H NMR (300 MHz, D_2O/TSP): 3.23 (*t*, 8H); 2.81 (*t*, 2H).[1] 2.58 (t, 2H), 2.39-2.44 (m, H), 1.34 (sext, 8H), 1.57 (quint, 8H), 0.99-

1.78 (m, 10H), 0.91 (t, 12H). ^{3}C NMR (75.47 MHz, D_2O/TSP): 57.41, 55.65, 50.43, 42.47, 32.22, 25.73, 24.23, 23.73, 19.12, 13.30.

The chemical structures of the synthesized ILs are presented in Figure 2.1.

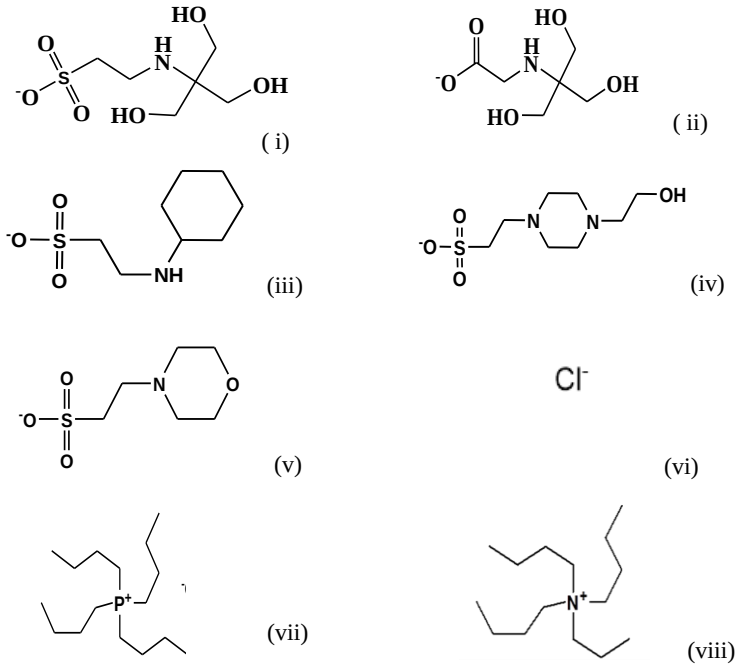

Figure 2.1. Chemical structures of the studied good buffers ionic liquids: (i) $[Tricine]^-$; (ii) $[TES]^-$, (iii) $[CHES]^-$; (iv) $[HEPES]^-$, (v) $[MES]^-$; (vi) Cl^-; (vii) $[P_{4444}]^+$; (viii) $[N_{4444}]^+$.

2.3.2 Phase Diagrams and Tie-lines

The new phase diagrams, at 25 ºC and at atmospheric pressure, for the systems composed of water, $K_3C_6H_5O_7$ and the ILs $[P_{4444}][GB]$ ($[P_{4444}][Tricine]$, $[P_{4444}][CHES]$, $[P_{4444}][MES]$, $[P_{4444}][HEPES]$ and $[P_{4444}][TES]$) and $[N_{4444}][GB]$ ($[N_{4444}][Tricine]$, $[N_{4444}][CHES]$, $[N_{4444}][MES]$, $[N_{4444}][HEPES]$ and $[N_{4444}][TES]$) are illustrated in Figures 2.2 and 2.3, respectively. The ternary phase diagrams previously reported for $[P_{4444}]Cl$ and $[N_{4444}]Cl$ [131] are also shown for comparison purposes. The experimental data are shown both in weight fraction and molality units. The molality units allows a better understanding of the impact of the ILs structure on the phase diagrams behaviour, avoiding differences that could result from different molecular weights. The detailed experimental data corresponding to the ternary phase diagrams determined in this work are presented in Appendix B.

For all studied ABS, the top phase corresponds to the IL-rich aqueous phase while the bottom phase is mainly composed of salt and water.

Considering the representations in Figures 2.2 and 2.3, the closer to the axis is located to the binodal curve, the easier it is to separate the IL from aqueous solution. Given the trends presented, the formation of ABS must be the result of the salting-out effect of the citrate-based salt, a strong salting-out salt composed of a trivalent charged anion, over the IL in aqueous media. For phosphonium-based ILs, and in molality units, the IL anions ability to form an ABS, for instance at 1.0 $mol \cdot kg^{-1}$ of $K_3C_6H_5O_7$, follows the order: $[P_{4444}][CHES] > [P_{4444}][MES] > [P_{4444}][HEPES] > [P_{4444}][TES] > [P_{4444}][Tricine]$. As expected, for ammonium IL-based (taking into account the anions), the order keeps the same: $[N_{4444}][CHES] > [N_{4444}][MES] > [N_{4444}][HEPES] > [N_{4444}][TES] > [N_{4444}][Tricine]$.

The formation of an aqueous biphasic system depends on the type of IL and its concentration, type of salt and its concentration, temperature and other features such as pH of the aqueous medium. The intensity of the phase-forming ability in each IL-based system relays on the basis of the complex and competing nature of the interactions occurring between the solutes (*i.e.*, ions from the inorganic salt and IL) and water or between the phase-forming components [2]. Since potassium citrate is a strong salting-out salt, according to the Hofmeister series [132], it has a higher affinity for water and thus there is a preferential exclusion of the IL from the aqueous solution, while promoting the two phases formation. Comparing to cations, anions have a higher aptitude for hydration since they are more polarizable and present a more diffuse valence electronic configuration [133], and thus the influence of the IL anion is more relevant to the phase diagrams behaviour than the influence derived from the IL cation as presented and discussed below. It was already demonstrated that the ability of an ionic liquid anion to produce ABS closely follows the decrease on their hydrogen-bond accepting strength or electron pair donation ability [134]. Anions with lower hydrogen bond basicity values present lower ability to create hydration complexes, and therefore are more easily salted-out by salts. Although no hydrogen-bond basicity values have been reported for these new ILs, some major conclusions can be drawn at this point using use of the water-octanol partition coefficients (K_{ow}) of each good buffer.

The phase diagrams for the ILs composed of the anions with more -OH groups ($[Tricine]^-$ and $[TES]^-$) are those that are more distant from origin, meaning that these

systems require more salt for phase separation. Then, $[HEPES]^-$, with one –OH group appears followed by $[MES]^-$ and $[CHES]^-$ with no –OH groups. The presence of –OH groups enhances the hydrogen-bonding with water and turns more difficult the salting-out process by the citrate-based salt. These affinities for water are reflected in the respective K_{ow} values of each buffer. Values for $\log(K_{ow})$ are as follow: CHES: -0.59; MES: -2.48; HEPES: -3.11; TES: -4.48; Tricine: -5.25. The higher the value of $\log(K_{ow})$ the higher the affinity of the anion for the octanol-rich phase and the lower its polarity. Therefore, higher $\log(K_{ow})$ values correspond to anions that are more easily separated into two aqueous phases (with a phase diagram situated near the binodal origin).

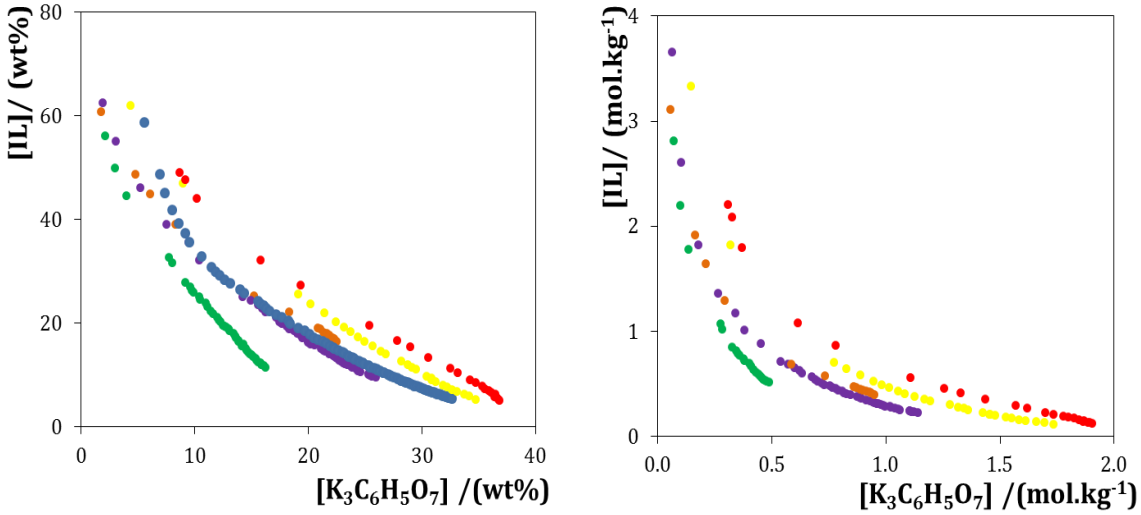

Figure 2.2. Ternary phase diagrams for the systems composed of IL + $K_3C_6H_5O_7$ + water at 25 °C and atmospheric pressure in wt% (left) and in mol.kg-1 (right): (●) $[P_{4444}]$[Tricine], (●) $[P_{4444}]$[MES], (●) $[P_{4444}]$[HEPES], (●) $[P_{4444}]$[TES], (●) $[P_{4444}]$[CHES], and (●) $[P_{4444}]$Cl [131].

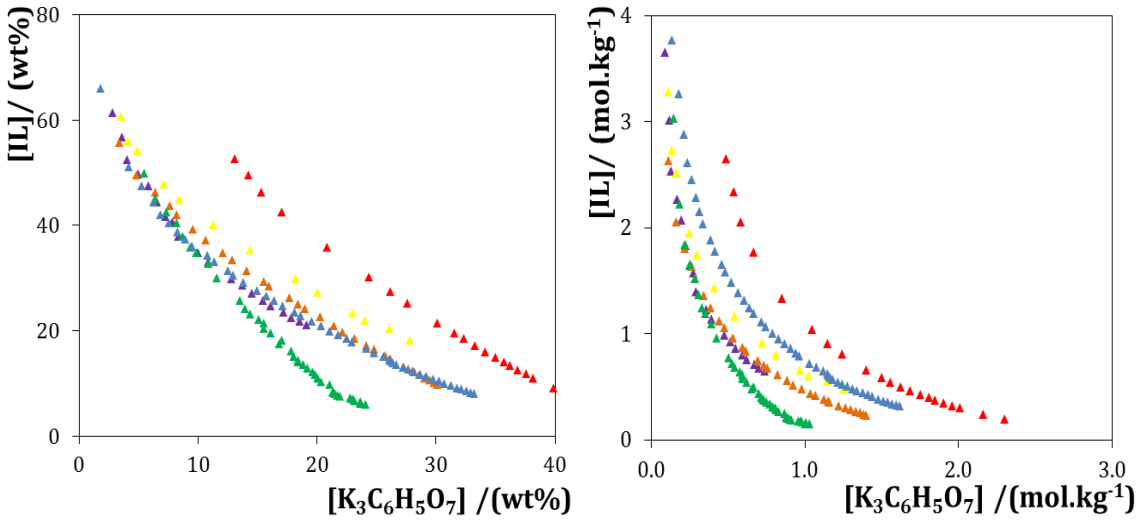

Figure 2.3. Phase Ternary phase diagrams for systems composed of IL + $K_3C_6H_5O_7$ + water at 25 °C and atmospheric pressure in wt% (left) and in mol.kg-1 (right): (▲) $[P_{4444}]$[Tricine], (▲) $[N_{4444}]$[MES], (▲) $[N_{4444}]$[HEPES], (▲) $[N_{4444}]$[TES], (▲) $[N_{4444}]$[CHES] and (▲) $[N_{4444}]$Cl [131].

The effect of the IL cation core is displayed in Figure 2.4. The $[P_{4444}]^+$ ability to form ABS with potassium citrate, for instance at 1.0 mol·kg^{-1} of $K_3C_6H_5O_7$, is higher than $[N_{4444}]^+$ for all cation-anion combinations. Although both types of compounds are composed of 4 alkyl chains of similar size, there are also some contributions derived from the central atom at the cation core. Similar results were obtained in ABS constituted by more conventional ILs and potassium phosphate [135], sodium carbonate [136] and potassium citrate [131] as the salting-out agents. In these investigations phosphonium-based ILs are also more effective in promoting ABS when compared to ammonium-based compounds. In addition, Neves et al. [137] reported that independently of the salt employed and of the pH of the aqueous media, the phosphonium-based ILs are always more effective in forming ABS [137, 138]. This is an expectable trend since none of the cations can suffer speciation at different pH values. Nevertheless, both cations are known for their high ability for ABS formation: they have highly shielded charges, located mostly on the heteroatom that is surrounded by four alkyl chains and no aromatic character, and hence possess a low affinity for water. The smaller the affinity for water and/or the more extensive hydrophobic nature of the IL, the more prone it is to be salted-out [136].

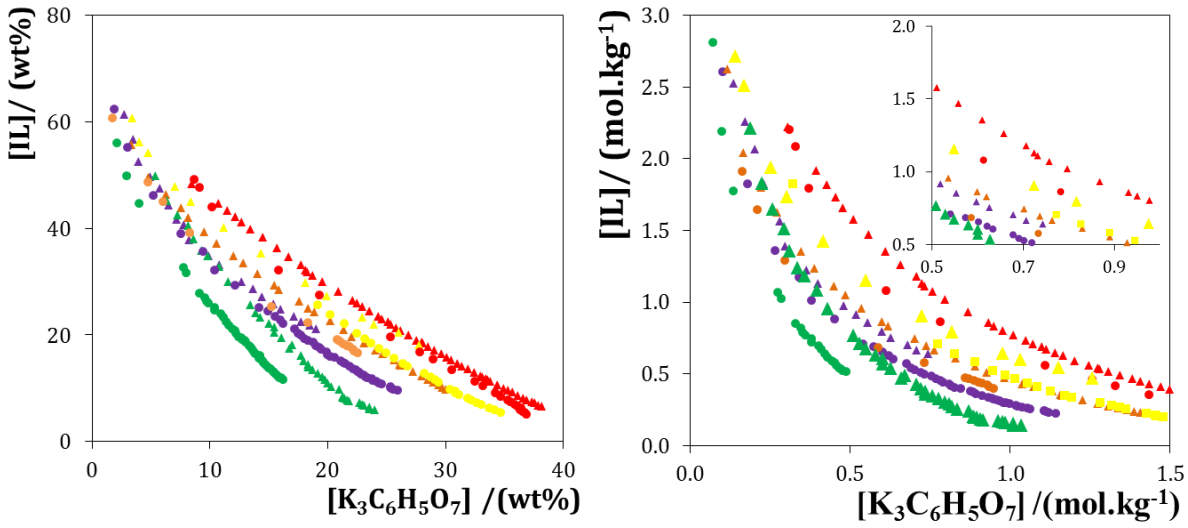

Figure 2.4. Evaluation of the cation nature in the ternary phase diagrams composed of IL + $K_3C_6H_5O_7$ + water at 25 °C and atmospheric pressure in wt% (left) and in mol.kg-1 (right): (●) $[P_{4444}]$[Tricine], (●) $[P_{4444}]$[MES], (●) $[P_{4444}]$[HEPES], (●) $[P_{4444}]$[TES], (●) $[P_{4444}]$[CHES], (▲) $[N_{4444}]$[Tricine], (▲) $[N_{4444}]$[MES], (▲) $[N_{4444}]$[HEPES], (▲) $[N_{4444}]$[TES], (▲) $[N_{4444}]$[CHES].

For the studied systems, the experimental binodal data were further fitted by the empirical relationship described by Eq.1. The regression parameters A, B and C, were estimated by the least-squares regression method, and their values and corresponding standard deviations (σ) are provided in Table 2.1. In general, good correlation coefficients were obtained for all systems, indicating that these fittings can be used to predict data in a given region of the phase diagram where no experimental results are available, as it is possible to confirm in Figure 2.5.

The experimental TLs, along with their respective length (TLL), are reported in Table 2.2. An example of the TLs obtained is depicted in Figure 2.6. In general, the TLs are closely parallel to each other.

Table 2.1. Correlation parameters used to describe the experimental binodal data by Eq. 1 and respective standard deviations (σ) and correlation coefficients.

IL	$A \pm \sigma$	$B \pm \sigma$	$10^5 (C \pm \sigma)$	R^2
$[N_{4444}][TES]$	96.0 ± 2.0	-0.256 ± 0.008	1.5 ± 0.2	0.9986
$[N_{4444}][Tricine]$	83.3 ± 1.1	-0.185 ± 0.004	2.4 ± 0.0	0.9926
$[N_{4444}][MES]$	116.5 ± 1.6	-0.382 ± 0.005	0.2 ± 0.1	0.9983
$[N_{4444}][HEPES]$	87.7 ± 0.7	-0.250 ± 0.003	2.9 ± 0.1	0.9996
$[N_{4444}][CHES]$	118.2 ± 4.1	-0.358 ± 0.010	9.3 ± 0.4	0.9974
$[P_{4444}][TES]$	113.0 ± 1.2	-0.287 ± 0.003	3.1 ± 0.0	0.9997
$[P_{4444}][Tricine]$	110.1 ± 8.5	-0.373 ± 0.002	2.4 ± 0.2	0.9963
$[P_{4444}][MES]$	98.3 ± 0.5	-0.328 ± 0.002	4.0 ± 0.1	0.9996
$[P_{4444}][HEPES]$	89.9 ± 1.65	-0.280 ± 0.008	3.05 ± 0.3	0.9987
$[P_{4444}][CHES]$	93.2 ± 1.0	-0.355 ± 0.005	15.4 ± 0.3	0.9991

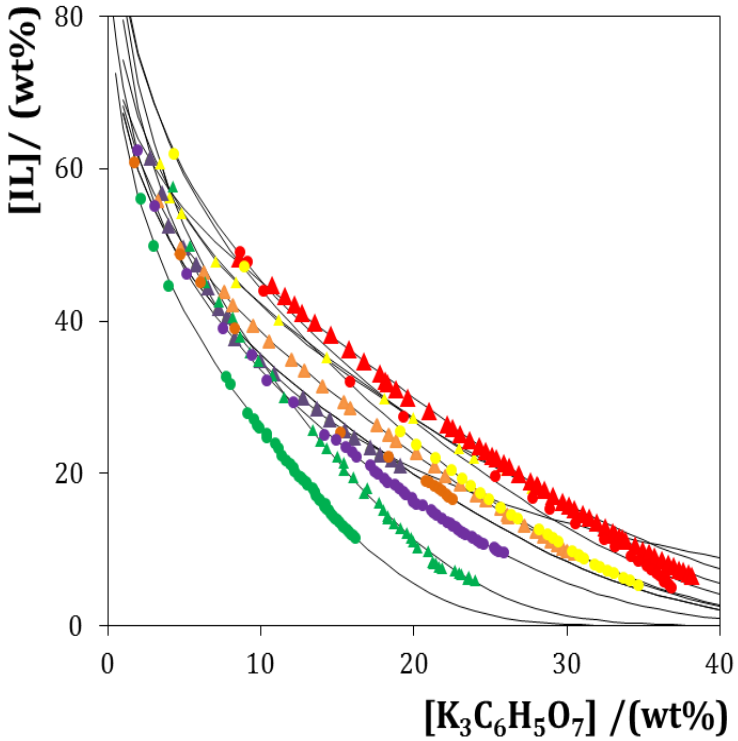

Figure 2.5. Phase diagram for the ternary systems composed of GB-IL + $K_3C_6H_5O_7$ + water, with the corresponding binodal fitting of data using Eq. 1 (-).

Table 2.2. Data for the tie-lines (TLs) and tie-line lengths (TLLs). Initial mixture compositions are represented as $[Salt]_M$ and $[IL]_M$ whereas $[Salt]_{Salt}$ and $[IL]_{Salt}$ are the composition of IL and salt at the IL-rich phase, respectively, and vice-versa.

IL	Weight fraction composition / wt %						
	$[IL]_{IL}$	$[Salt]_{IL}$	$[IL]_M$	$[Salt]_M$	$[IL]_{Salt}$	$[Salt]_{Salt}$	TLL
$[N_{4444}][TES]$	51.7296	5.7859	20.8895	28.1389	11.0112	35.2987	50.2892
	61.0784	3.1155	20.7819	29.0911	10.8459	35.4960	59.7645
$[N_{4444}][Tricine]$	65.2216	1.7079	28.6541	29.8436	0.8649	51.2251	81.2018
	32.7911	18.0888	21.4407	26.4080	10.4568	34.4595	27.6916
	38.1894	14.4785	22.4482	25.9560	9.4489	35.4343	35.5691
$[N_{4444}][MES]$	43.9481	6.5012	23.8439	23.3054	11.7814	33.3054	41.9237
	43.3294	6.6911	22.3808	24.2833	11.9457	33.0466	40.9822
$[N_{4444}][HEPES]$	54.1907	3.6776	23.8439	23.3054	5.6360	35.0821	57.8255
	51.9180	4.3472	23.5406	23.0112	6.0666	34.5039	54.8796
$[P_{4444}][TES]$	79.5109	1.511	39.4578	19.7654	5.0904	35.4285	78.3983
	55.664	5.9871	39.5184	14.4206	10.6396	29.5049	50.7967
$[P_{4444}][Tricine]$	81.4673	1.2599	39.7357	18.7737	13.2004	29.9100	89.8518
	55.8111	6.1947	38.9070	15.4753	14.3100	28.9804	67.5233
$[P_{4444}][HEPES]$	79.6613	0.1869	40.3970	18.2171	5.0206	34.4388	82.1245
	71.0696	0.7061	40.5886	14.9978	8.4631	30.082	69.1558
$[P_{4444}][CHES]$	81.2968	0.1491	39.8681	19.1759	0.0003	37.4859	89.4603
	77.4011	0.2751	42.9426	16.1162	0.0011	35.8500	41.4097
$[P_{4444}][MES]$	3.6038	33.0105	40.2318	17.7693	82.2216	0.2970	85.1524
	30.0802	5.5498	38.9783	16.3011	77.2079	0.5430	77.5070
$[P_{4444}]Cl$	76.7622	2.7018	38.3083	22.6123	2.4265	41.1911	83.7091
	56.5028	5.1675	38.9051	13.9931	8.1176	29.4337	54.1293
	57.7081	4.9733	39.2215	14.8860	7.3160	30.6090	56.5381

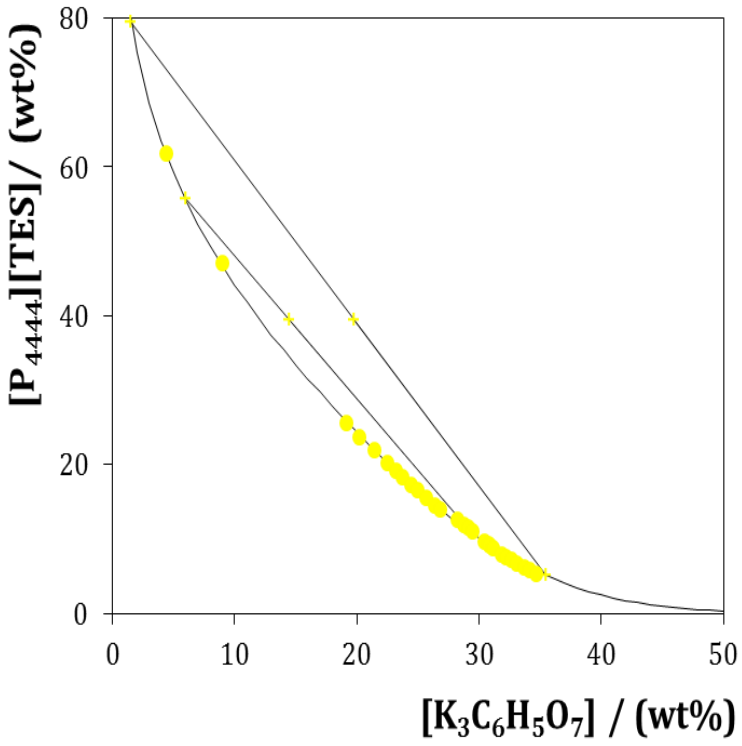

Figure 2.6. Phase diagram for the quaternary system composed of $K_3C_6H_5O_7$ + $[P_{4444}][TES]$ + Water at 25ºC and atmospheric pressure: binodal curve data (●); TL data (+); adjusted binodal data using Eq. 1 (-).

2.3.3 Extraction Efficiencies of BSA

Table 2.3 presents the extraction efficiencies of BSA in ABS composed of $[N_{4444}][GB]$ + $K_3C_6H_5O_7$ and $[P_{4444}][GB]$ + $K_3C_6H_5O_7$. The mixture compositions of each ABS are also provided in Table 2.3. This organic salt was chosen to perform the extraction experiments of BSA due to its biodegradable and non-toxic nature [131]. The macroscopic appearance of the studied ABS is shown in Figure 2.7.

During partitioning, the exposed groups of proteins come into contact with the phase components which determine the partitioning behaviour. This surface-dependent phenomenon is very complex since a protein can interact with the surrounding molecules within a given phase *via* hydrogen bonding, electrostatic interactions, π···π interactions between the aromatic groups and dispersive-type interactions between the aliphatic groups. The net effect of these interactions is likely to be different in the two phases and the protein will partition preferentially into one phase [139].

Figure 2.7. Visual appearance of the BSA extraction with an ABS formed by IL+ salt + water.

Table 2.3. Percentage extraction efficiencies of BSA, $EE_{BSA\%}$, and respective standard deviations (σ) in the ABS composed of $[N_{4444}][GB] + K_3C_6H_5O_7$ at 25 ºC and $[P_{4444}][GB] + K_3C_6H_5O_7$ at 25 ºC and atmospheric pressure. Initial mixture compositions and respective standard deviations (σ) are represented as $[IL]_M$ and $[Salt]_M$.

IL	Weight fraction composition / (wt%)		EE_{BSA}%
	$[IL]_M$	$[Salt]_M$	
$[N_{4444}]$[Tricine]	21.4 ± 1.2	26.4 ± 2.5	100
$[N_{4444}]$[HEPES]	22.8 ± 0.3	23.3 ± 0.2	100
$[N_{4444}]$[MES]	22.4 ± 0.8	23.3 ± 0.6	100
$[N_{4444}]$[TES]	20.9 ± 0.9	26.4 ± 2.0	100
$[P_{4444}]$Tricine]	38.8 ± 0.9	14.0 ± 0.5	100
$[P_{4444}]$[HEPES]	39.6 ± 0.5	13.9 ± 0.2	100
$[P_{4444}]$[CHES]	39.3 ± 0.8	13.7 ± 0.3	100
$[P_{4444}]$[MES]	38.9 ± 0.6	16.3 ± 1.5	100
$[P_{4444}]$[TES]	39.5 ± 0.3	15.3 ± 0.1	100
$[P_{4444}]$Cl	40.6 ± 0.6	14.4 ± 0.7	100

In all the studied examples it was observed that the IL-rich phase is able to completely extract the protein with extraction efficiencies of 100%. In fact, no protein was detected at the salt-rich phase. The high extraction efficiencies can be a direct result of the strong salting-out ability of $K_3C_6H_5O_7$ (high-charge density anion with an improved ability to create hydration complexes) which leads to the "exclusion" of BSA from the inorganic-salt-rich phase to the more "organic" IL-rich phase. Overall, BSA has a higher affinity for the IL-aqueous phases when compared with the salt-rich phase although this is a more hydrated phase.

The pH values of both phases in each ABS, and for the compositions for which the TLs were determined, and some examples are displayed in Table 2.4. In all situations, BSA is in a negative charged form (pH > pI) due to the buffered alkaline medium used in the extractions (Table 2.4). Nevertheless and even charged, the protein has more affinity for the IL-rich phase, and it seems that the electrostatic interactions between the salt cation (K^+) and the BSA negative form are not relevant, since the protein migrates preferentially to the IL-rich phase.

Table 2.4. pH values of the coexisting phases ABS formed by ILs + $K_3C_6H_5O_7$.

IL	pH (IL-rich phase)	pH (Salt-rich phase)
$[P_{4444}][MES]$	9.64	9.47
$[P_{4444}][HEPES]$	9.65	9.60
$[P_{4444}][Tricine]$	11.89	10.77
$[N_{4444}][Tricine]$	10.75	10.90

From weight balances to the protein (in all experiments), it was possible to infer that there are no major "losses" of protein by precipitation. The GB-IL–based systems studied, allowed to maintain the pH of each ABS while allowing a proper extraction free of protein denaturation or precipitation. The stability of the protein in presence of ILs aqueous solutions was also evaluated in this work and it will be presented latter. These results are even more relevant when compared with some literature works. Lin et al. [140], reported a study based on the extraction of different proteins, including BSA, resorting to the use of ABS formed by eight ILs combined with K_3PO_4, where 1-octyl-3-methylimidazolium bromide ($[C_8mim]Br$) was selected as the suitable IL. In this work, even with the application of the best IL, they were only able to achieve a 90.5% extraction efficiency [140]. In addition, another recent work evaluated the partitioning behaviour of BSA in an ABS composed by 1-hexyl-3-methylimidazolium chloride ($[C_6mim]Cl$) + K_2CO_3 [141] Still, despite the evaluation of the influence of several process parameters like the ionic liquid and salt concentrations, system temperature, tie-line length, phase volume ratio and neutral salts addition, they only achieved a maximum extraction of BSA of about 94% [141].

Overall, the systems proposed here are more efficient for the extraction of BSA while using a biodegradable salt and ILs with buffer characteristics.

2.4. Conclusions

It was possible to evaluate the novel GB-IL-based ABS combined with a biodegradable organic salt, ranging from their phase diagrams to their application in the extraction of proteins. In this section it was described the synthesis of a new class of ionic liquids, novel phase diagrams for ABS, and the respective TLs and TLLs. The large array of ILs investigated and the distinct phase behaviours observed, allowed not only to study the influence of the cation on the formation of ABS but also the anion influence. In general, an increase in either the cation or the anion hydrophobicity facilitates the formation of ABS, following the same trend of conventional ILs.

The obtained results confirm that GB-ILs–based ABS are a powerful technique for the separation and extraction of biomolecules sensitive to the pH of the medium. Consequently, these new systems are a promising extraction technique and worthy of further investigation when dealing with valued-added proteins or of high interest, such as cancer biomarkers.

.

3.Extraction of BSA using IL + polymer ABS

3.1. Introduction

The growing demand for biotechnological fine chemicals and biological molecules, in particular proteins which have been increasingly used in therapeutic and diagnostic applications, has led to the development of specific separation and purification methods. Conventional methods for purifying and separating proteins, as already discussed, present several disadvantages such as high complexity, time and cost-consuming and are not easily scaled-up. Since proteins are easily denatured and lose their biological activity when in contact with most organic solvents, the use of biocompatible ILs and polymers in ABS appear to be a viable alternative for concentrating the target high-value cancer biomarkers from biological fluids foreseen in this work. ABS based on the application of ionic liquids (ILs) emerged in recent years as an efficient extraction alternative compared to traditional organic-solvent-water systems. The most studied IL-based ABS are formed by ILs, water and inorganic salts [134, 135, 142, 143]. However, there are some environmental concerns associated with the use of inorganic salts which tend to be toxic and non-biodegradable. For this purpose, inorganic salts are being replaced by organic as previously shown in this work.

Aiming at overcoming the toxicity of some ILs, several studies [104, 144] have been conducted on the evaluation of their toxicity. All these works [104, 144] revealed that the ILs toxicity is primordially determined by the cation nature and it is directly correlated with the length of the alkyl side chains as well as with the number of alkyl groups. It is already well accepted that the toxicity of ILs increases with their hydrophobicity; so, toxic ILs are poorly water soluble at room temperature minimizing thus their environmental impact in aquatic streams [144]. It should be remarked that ILs used in ABS formulations are usually of lower toxicity since to be water-soluble they should be constituted by cations with short alkyl side chains. Nevertheless, this toxicity can be non-negligible and in order to overcome this major drawback, the use of non-toxic and more environmentally benign ILs from renewable materials is strongly recommended. Among these, cholinium-based salts are derived from natural resources and have emerged, in recent years, as completely bio-derived ILs [145]. These ILs usually contain cholinium cations combined with inorganic, amino-acid-based or carboxylic-acid-based anions [94].

Cholinium-based ILs are less expensive as a consequence of the lower cost of the cation starting material, and are more biocompatible and more biodegradable compared

with more common ILs, such as imidazolium- or pyridinium-based [145]. Cholinium-based ILs are usually derived from choline chloride, also known as 2-hydroxyethyltrimethyl ammonium chloride or vitamin B4. Choline chloride can be found in food obtained from vegetable or animal sources, and supports several essential biological functions [94]. Cholinium-based ILs have been studied in the isolation of suberin from cork, electrodeposition of zinc, tin, and zinc–tin alloys, catalytic reactions, and in extraction of antibiotics and proteins using ABS [94, 145]. In fact, cholinium-based ILs were already investigated as two-phase promoters in ABS either combined with salts or polymers [109, 115, 146] . The polymers investigated were polypropylene glycol and polyethylene glycol and chosen based on their biodegradability and biocompatibility [115]. However, it should be remarked that cholinium-based ILs are more hydrophilic than their imidazolium-, pyridinium or piperidinium-based counterparts, and thus ABS composed of cholinium-based ILs and salts were only achieved with strong salting-out species such as K_3PO_4 [135]. Regarding the systems formed by polymers, the authors [115] were able to show that not only these ABS constitute promising clean systems due to the substitution of the high-charge density salts and more toxic ILs, but are also efficient in the extraction and purification of proteins (89-100% of recovery efficiency in a single step), while being an excellent long-term storage media for proteins like trypsin. In addition, the activity of trypsin was found to increase in these aqueous IL solutions within 13 months, whereas in water only 30% of the activity of trypsin could be maintained [115].

The separation of biological molecules and particles in polymer-based ABS was initiated more than half a century ago by Albertsson [147], and later proved to be a highly useful tool for the extraction and purification of biomolecules, such as proteins, enzymes, blood cells and antibiotics [92, 102]. Polyethylene glycol (PEG) and dextran, both with high molecular weights, are two polymers frequently used to form ABS, mostly due to their stable nature and non-toxic characteristic for biological materials [148]. However, the dextran-rich phase in a PEG/dextran ABS usually displays a high viscosity which brings difficulties to the phase separation of polymer-polymer systems and raises the energetic consumption [148]. Dextran is also too expensive as a phase-forming component to scale-up the extraction process [148]. On the other hand, polypropylene glycol (PPG) or PEG are of lower cost and are often considered within the framework of green technologies [109]. Most studies addressed the use of PPG due to its higher propensity for liquid–liquid

demixing in presence of ‘‘salting-out’’ inducing ILs [109, 149]. PPGs are polymers usually more hydrophobic than PEGs due to the additional methyl group at the side chain and are hence more easily separated in ABS [91]. On the other hand, and being more hydrophilic, PEGs are less able to form ABS with ILs [149, 150]. PPGs are biodegradable and non-toxic and can be conveniently recovered by heating [109]. Further advantages can be associated with the use of these ABS, such as avoiding salt crystallization and corrosion problems [91]. Polymers also offer an additional degree of design, for instance, by varying the length of the polymeric chains or the structure of the monomer unit.

In this work, a series of environmentally-friendly ABS composed of cholinium-based ILs and propylene glycol with a molecular weight of 400 $g \cdot mol^{-1}$ (PPG 400) have been investigated. Either cholinium-based ILs composed of anions derived from carboxylic acids, inorganic or other organic anions, or from Good’s buffers were investigated. The respective ternary phase diagrams, as well as the tie-lines and tie-line lengths, were determined at 25 ºC. Finally, these systems were evaluated though their extractive performance for a model protein (BSA). The effects of the ILs chemical structure and phase-forming components concentration were deeply investigated aiming at reaching high extraction yields while not leading to protein denaturation.

3.2. Experimental Section

3.2.1. Chemicals

The ABS studied in this work were established by using the polymer polypropylene glycol of average molecular weight 400 g.mol-1, PPG 400, supplied by Aldrich and used as received. The choline hydroxide solution (40 wt%) and glycolic (99 wt % pure) were from Sigma-Aldrich, propanoic (≥ 99.5 wt % pure) acquired from Merck, butanoic (99 wt % pure) and lactate (88-92 wt % pure) acids (to perform as the IL anions) were acquired from Riedel-de-Haën. Cholinium ((2-hydroxyethyl)trimethylammonium) chloride, [Ch]Cl (99 wt% pure), cholinium acetate, [Ch][Ac] (98 wt% pure), cholinium dihydrogen phosphate, [Ch][DHPhs] (99 wt% pure), cholinium dihydrogen citrate, [Ch][DHCit] (98 wt % pure), and [Ch][Bit] (98 wt % pure) were commercially acquired. [Ch][DHPhs] and [Ch][Ac] were purchased from Iolitec. The remaining were acquired from Sigma-Aldrich. The following ILs were also studied and were synthetized in our laboratory according to standard protocols [151, 152], namely cholinium propionate, [Ch][Prop], cholinium glycolate, [Ch][Gly], cholinium butanoate, [Ch][But], and cholinium lactate, [Ch][Lac]. Cholinium-based ILs composed of Good's buffers anions were also synthesized in this work and include cholinium N-(2-hydroxy-1,1-bis(hydroxymethyl)ethyl, [Ch][Tricine], cholinium 2-(N-morpholino)ethanesulfonic acid, [Ch][MES], and cholinium N-cyclohexyl-2-aminoethanesulfonic acid, [Ch][HEPES]. It should be remarked that [Ch]Cl does not fall within the IL category due to its high melting point. However, it is included in the cholinium-based ILs group in all the results and discussions presented thereinafter for comparison purposes. Before use, all the ILs were purified and dried for a minimum of 24 h at constant agitation, at moderate temperature (≈ 60 °C) and under vacuum (to reduce their volatile impurities to negligible values). After this step, the purity of each IL was confirmed by ^{1}H and ^{13}C NMR spectra and found to be > 98 wt %. The water employed was ultra-pure water, double distilled, passed by a reverse osmosis system and further treated with a Milli-Q plus 185 water purification equipment.

3.2.2. Experimental Procedure

3.2.2.1. Synthesis and characterization of cholinum based ionic liquids

The choline hydroxide solution (40 wt%) and propanoic, butanoic, glycolic, and lactate acids, as well as tricine, MES and HEPES buffers were used without further

purification. All solutions were made up with Millipore-grade water. The GB-ILs were synthesized *via* neutralization of the base with the appropriate acid as explained in the previous chapter. The water was then removed under vacuum at 50 °C. Moreover, the unreacted acid in the prepared IL was further eliminated by precipitation with the solvents acetone or methanol. The solvents were evaporated under vacuum and the obtained IL was dried under vacuum at 70 °C for at least 24 h. All the above procedure was done under an inert atmosphere, thereby preventing the choline hydroxide degradation induced by oxygen (Figure 3.1). The ILs synthetized in this work showed high purity with no sign of decomposition. After this step, the purity of each IL was confirmed by ^{1}H and ^{13}C NMR spectra. The water content of the synthesized ILs was determined by coulometric Karl Fischer titration (Mettler Toledo DL 39) with the Hydranal Coulomat AG reagent (Riedel-de Haën).

Figure 3.1. Synthesis of ionic liquids in an inert atmosphere.

3.2.2.2. Phase diagrams and TLs

The ternary phase diagrams (PPG 400 + IL + water) were determined with the following ILs: [Ch]Cl, [Ch][Ac], [Ch][Pro], [Ch][Gly], [Ch][But], [Ch][Lac], [Ch][Cit], [Ch][MES], [Ch][HEPES], and [Ch][Tricine]. The experimental procedure adopted was similar to the one described in Section 2.2.2. Aqueous solutions of PPG 400 at ≈ 90 wt % and aqueous solutions of the different hydrophilic ILs at variable concentrations (from 60

to 80 wt %) were prepared gravimetrically and used for the determination of the binodal curves. Drop-wise addition of each aqueous IL solution to a PPG 400 aqueous solution was carried out until the detection of a cloudy solution (biphasic region), followed by the drop-wise addition of ultra-pure water until the detection of a clear and limpid solution (monophasic region). In some cases, the addition of the PPG solution to the IL was also carried out to complete the phase diagrams. The ternary system compositions were determined by weight quantification within ± 10^{-4} g.

The TLs and respective TLLs were determined by the gravimetric method described by Merchuk et al.[130] and presented in Section 2.2.2.

3.2.2.3. pH measurement

The pH values of both the IL-rich and PEG-rich aqueous phases were measured at (25 ± 1) ºC using a METTLER TOLEDO SevenMulti pH meter within an uncertainty of ± 0.02.

3.2.2.4. Extraction efficiencies of the BSA

The ternary mixtures compositions used in the partitioning experiments were chosen based on the phase diagrams determined here for each PPG-400-IL-water system. A ternary mixture with a common composition, and within the biphasic region, was prepared with 30 wt % of PPG 400, 30 wt % of IL and 40 wt % of water. Each mixture was vigorously stirred, centrifuged for 10 min, and left to equilibrate for at least 10 min at 25 ºC.

After a careful separation of both phases, the quantification of BSA in the two phases was carried by HPLC, using the same procedure presented in section 2.2.3.

The percentage extraction efficiency of BSA, $EE_{\mathrm{BSA}}\%$, is the percentage ratio between the amount of protein in the IL-rich aqueous phase to that in the total mixture, and is defined according to Eq. 7.

In the studied ABS, the top phase corresponds to the PPG-rich aqueous phase while the bottom phase is mainly composed of IL and water – a reverse phase density on the IL-rich phase when compared to the IL-salt ABS presented before.

3.3 Results and Discussion

3.3.1. Characterization of synthetized choline based ILs

The macroscopical appearance, NMR characterization and water content data for each Choline based-IL is described below.

[Ch][But]: From butyric acid (92.6 mmol); this compound was obtained as a light yellow viscous liquid. Water content: 0.364 wt%. ^{1}H NMR (300 MHz, DMSO): 3.85 (m, 2H), 3.42 (m, 2H), 3.13 (s, 9H), 1.85 ppm (t, 2H), 1.42, 0.81(t, 3H). ^{13}C NMR (75.47 MHz, DMSO): 176.7, 67.6, 55.4, 40.6, 20.0, 14.8 ppm.

[Ch][Prop] From propionic acid (96.5 mmol); this compound was obtained as a white to pale yellow viscous liquid. Water content: 0.064 wt%. ^{1}H NMR (300 MHz, DMSO): 3.84 (m, 2H), 3.42 (m, 2H), 3.13 (s, 9H), 3.12 (s, 9H), 1.89 ppm (q, 2H). ^{13}C NMR (75.47 MHz, DMSO): 176.8, 67.2, 54.9, 53.0, 30.5, 11.4 ppm.

[Ch][Lac]: From lactic acid (118.0 mmol); this compound was obtained as a yellow dark viscous liquid. Water content: 0.073 wt%. ^{1}H NMR (300 MHz, DMSO): 3.84 (m, 2H), 3.53 (q, 1H), 3.42 (m, 2H), 3.12 (s, 9H), 1.08 ppm (t, 3H). ^{13}C NMR (75.47 MHz, DMSO): 178.2, 67.3, 67.2, 55.1, 53.1, 21.6 ppm.

[Ch][Gly]: From glycolic acid (90.8 mmol); this compound was obtained as a pale yellow viscous liquid. Water content: 0.10 wt% ^{1}H NMR (300 MHz, DMSO): 5.17 (m, 2H), 3.86 (m, 2H), 3.44 (m, 2H), 3.15 (s, 9H). ^{13}C NMR (75.47 MHz, DMSO): 175.3, 67.5, 55.4, 53.4, 40.13 ppm.

[Ch][Tricine]: From tricine buffer (77.0 mmol); this compound was obtained as a white solid. Water content: <0.05%. ^{1}H NMR (300 MHz, D_2O/TSP): 3.93 (m, 2H), 3.42 (s, 6H), 3.38 (m, 2H), 3.17 (s, 2H), 3.08 (s, 9H). ^{13}C NMR (75.47 MHz, D_2O/TSP): 182.19, 70.28, 63.30, 63.03, 58.47, 56.73, 47.62 ppm.

[Ch][Mes]: From MES buffer (60.1 mmol); this compound was obtained as a white spleen viscous liquid. Water content: <0.05 wt%. ^{1}H NMR (300 MHz, D_2O/TSP): 3.94 (m, 2H), 3.64 (t, 4H), 3.40(m, 2H), 3.08(s, 9H), 3.01 (t, 2H), 2.70 (t, 2H), 2.48(s, 1H).
^{13}C NMR (75.47 MHz, D_20/TSP): 70.29, 68.86, 58.50, 56.76, 55.49, 55.17, 50.23 ppm.

[Ch][HEPES]: From HEPES buffer (50.8 mmol); this compound was obtained as a yellow viscous liquid. Water content: <0.05% wt%. ^{1}H NMR (300 MHz, D_2O/TSP): 3.93 (m, 2H), 3.62 (t, 4H), 3.39 (m, 2H), 3.07 (s, 9H), 3.07 (s, 9H), 2.99 (t, 2H), 2.70(m, 2H),

2.53(t, 8H) ppm (t, 3H). ^{13}C NMR (75.47 MHz, D_2O/TSP): 70.28, 61.57, 60.69, 58.48, 56.74, 55.00, 54.74, 54.06, 50.40 ppm.

3.3.2 Phase diagrams and tie-lines

Ternary phase diagrams were determined for several ILs ([Ch][DHPhs], [Ch][DHCit], [Ch][Ac], [Ch]Cl, [Ch][Bit], [Ch][Prop], [Ch][Lac], [Ch][But], [Ch][Gly], [Ch][Tricine], [Ch][MES], and [Ch][HEPES]) + water + PPG 400 at (25 ± 1) °C and at atmospheric pressure. The chemical structures of the ILs used as phase-forming components of ABS with PPG 400 are shown in Figure 3.2.

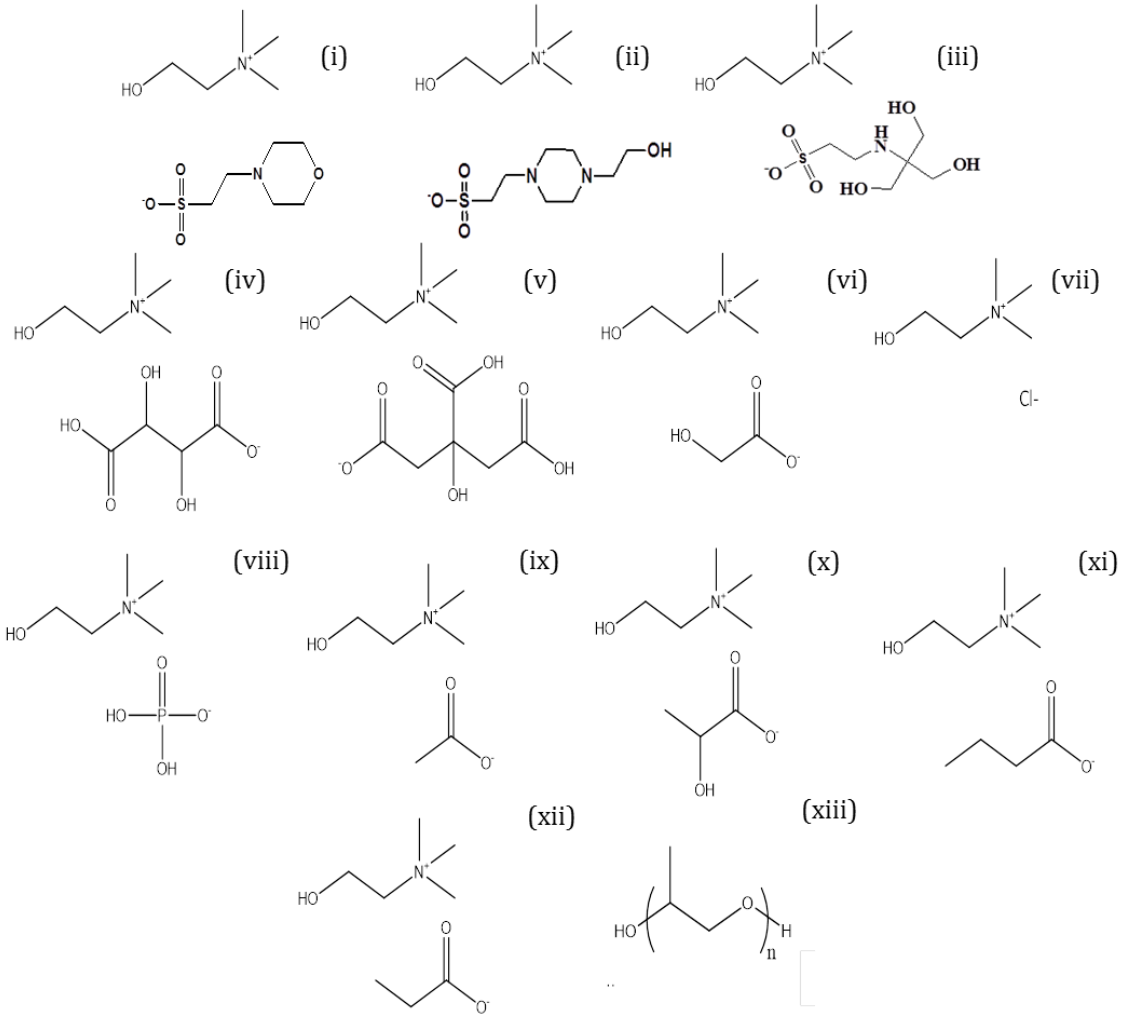

Figure 3.2. Chemical structure of the studied ILs and PPG: i) [Ch][MES]; (ii) [Ch][HEPES]; (iii) [Ch][Tricine]; (iv) [Ch][Bit]; (v) [Ch][DHCit]; (vi) [Ch][Gly]; (vii) [Ch]Cl (viii) [Ch][DHPhs], (ix) [Ch][Ac], (x) [Ch][Lac], (xi) [Ch][But], (xii) [Ch][Prop], (xiii) PPG.

Since it has been established in the previous chapter that the combination of buffers with common IL cations can be a good alternative to create biocompatible and efficient ABS, here they were also implemented, yet combined with the cholinium cation. These ILs were also investigated as phase-forming promoters with polymers of different molecular weight as well as with the biodegradable organic salt, $K_3C_6H_5O_7$, studied before. The combinations tested are presented in Table 3.1. However, cholinium-based ILs are more hydrophilic than the tetrabutylphosphonium and tetrabutylammonium-based ILs studied before, and are thus not able to form ABS with conventional salts. Up to date, ABS composed of cholinium-based ILs and salts were only achieved with the strong salting-out K_3PO_4 [91].

The ternary phase diagrams obtained in this work are illustrated in Figure 3.4, 3.5 and 3.6. The experimental weight fraction data of each phase diagram are reported in appendix B. In addition to weight fraction, the solubility curves are also presented in molality units for a better understanding of the anion impact on the phase diagrams behaviour. The biphasic or two-phase region is localized above the solubility curve, and the larger this regime, the higher is the ability of the IL to undergo liquid-liquid demixing in presence of PPG 400 in aqueous environments.

Table 3.1. Identification of the systems able (✓), not able (×) or not tried (◯) to form two-phase systems with PPG with different molecular weights (400, 600, 1200) and the organic salt $K_3C_6H_5O_7$.

	PPG 400	PPG 600	PPG 1200	$K_3C_6H_5O_7$
[Ch]Cl	✓	×	×	×
[Ch][Ac]	✓	×	×	×
[Ch][Gly]	✓	×	×	×
[Ch][DHPhs]	✓	×	×	×
[Ch][DHCit]	✓	×	×	×
[Ch][But]	✓	×	×	×
[Ch][Prop]	✓	◯	◯	×
[Ch][Lac]	✓	◯	◯	×
[Ch][Bit]	✓	◯	◯	×
[Ch][Tricine]	✓	◯	◯	×
[Ch][MES]	✓	◯	◯	×
[Ch][HEPES]	✓	◯	◯	×
[Ch][CHES]	×	◯	◯	×

In general, the ability of the IL to form ABS in presence of a fixed PPG concentration, for instance at 8 $mol.kg^{-1}$ of PPG 400, decreases in the following order: [Ch][DHPhs] > [Ch][Ac] > [Ch][Gly] > [Ch][Lac] ≈ [Ch][Prop] > [Ch][But] > [Ch][Bit] > [Ch][DHCit] > [Ch][Cl] > [Ch][MES] > [Ch][HEPES] > [Ch][Tricine]. Considering the fact that all ILs share the same cation, yet combined with different anions, this pattern could be explained by the decreased hydrophobic nature and therefore the higher affinity for water of the IL anion [115].

For a better inspection of the IL anion effect, the phase diagrams obtained for the carboxylic-acid-derived ILs, commercial ILs and those obtained for the GB-based ILs are shown in separated figures, namely Figures 3.3, 3.4 and 3.5.

The phase diagrams of the systems composed of ILs with anions derived from carboxylic acids allow to conclude that shorter alkyl side chains have higher affinity for water and thus hydrate more easily and induce the formation of a second liquid phase in the presence of highly hydrophobic polymers, such as PPG [91]. This trend is confirmed with the ILs comprising the anions acetate, propanoate and butanoate. For this type of anions (derived from carboxylic acids) the fowling trend was observed: [Ch][Ac] > [Ch][Gly] > [Ch][Lac] ≈ [Ch][Prop] > [Ch][But] > [Ch][DHCit]. Despite the anions propanoate and lactate having the same alkyl chain length, the latter presents an additional hydroxyl group, which will favor the formation of hydrogen bonds and therefore will provide a more hydrophilic character to the ionic liquid. This is confirmed by Figure 3.4, since the lactate diagram is slightly closer to the origin.

[Ch[DHCit] is the IL with the lower ability to form ABS with PPG 400 amongst the several ILs derived from carboxylic acids. The [Ch][DHCit] anion is derived from citric acid, which has a high ability to act as an H-bond and/or an H-acceptor anion, and as as consequence it is expected to behave has a strong salting-out agent. However, similar to what happens in systems formed by PEG [153], this IL shows a small ability to form ABS when compared with other anions derived from carboxylic acids. This can be explained based on the crystal structure previously studied by Glusker et al. [154]. They reported that citrate anions can suffer some phenomena of self-aggregation, as a result of the presence of intermolecular hydrogen bonds between the hydroxyl hydrogen atoms and one of the oxygens of the central carboxyl group. This will result in a more hydrophobic character of the anion and decreases its interaction with water [154].

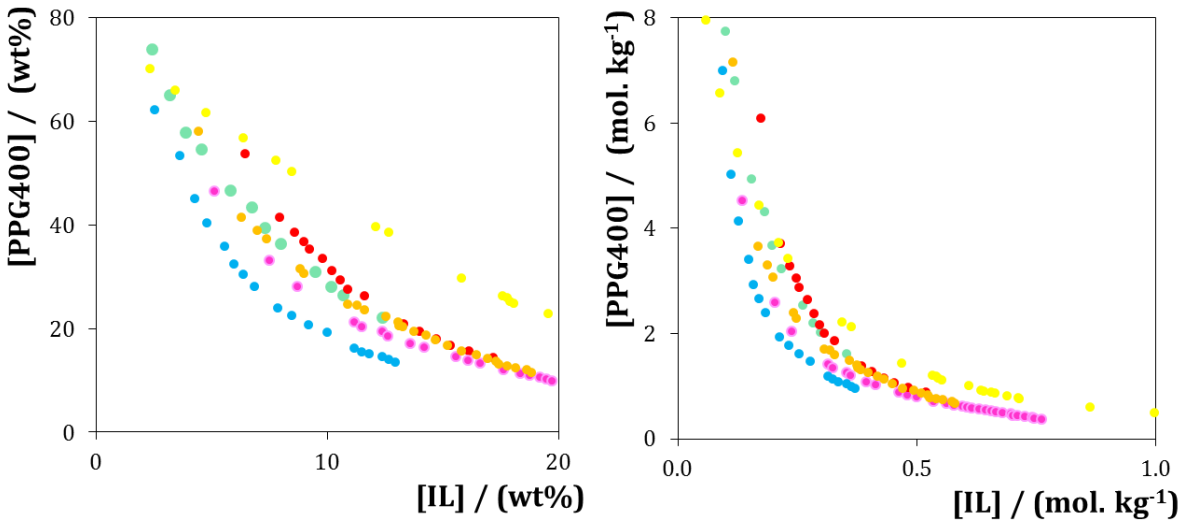

Figure 3.3. Phase diagrams for systems composed of PPG 400 + IL + water at 25ºC and atmospheric pressure in wt% (left) and in mol.kg-1 (right): (●) [Ch][Ac]; (●) [Ch][Gly]; (●) [Ch][lac]; (●) [Ch][Prop]; (●) [Ch][But]; (●) [Ch][DHCit].

In the studied ABS formed by commercial ILs, [Ch][DHPhs] showed the highest ability to promote ABS, whereas [Ch]Cl exhibited the lowest (Figure 3.4). This trend complies to the idea that an increase in the anion polar surface improves the ability of each IL to induce ABS. ILs with higher affinity for water are more capable to exclude PPG to a second liquid phase. This fact suggests that these interactions are mainly governed by solvation in water, where a higher affinity for water implies a higher ability to promote phase separation. This behaviour is in close agreement with what was previously observed in the PEG–IL ABS, in which the anions with higher charge density are more able to create ion–water complexes and larger repulsive interactions with the ether oxygens of the PEG [153].

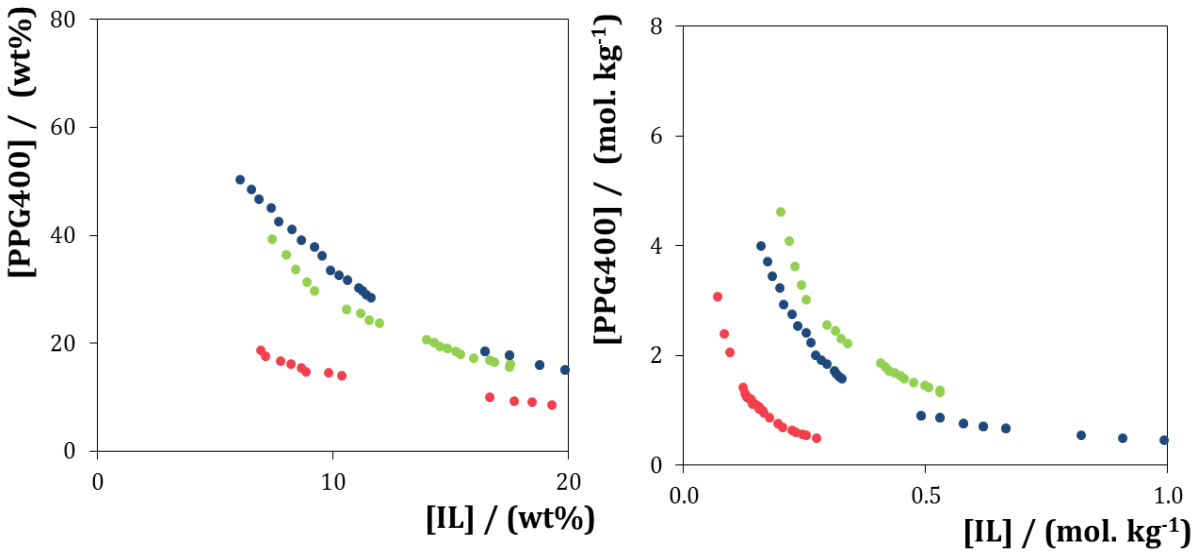

Figure 3.4. Phase diagrams represented in molality for the systems composed of PPG + IL + water in units wt% (left) and in mol.kg-1 (right): (●) [Ch]DHPhs]; (●) [Ch][Bit]; (●) [Ch]Cl.

Finally, when evaluating the ABS formed by GB-ILs, the following trend was found: [Ch][MES] > [Ch][HEPES] > [Ch][Tricine] (Figure 3.5). The respective phase diagrams are depicted in Figure 3.6. This trend can be explained based on the log(K_{ow}) values of each buffer: MES-2.48; HEPES-3.11; Tricine-5.25. On the contrary to what happens in IL + salt ABS, since polymers are the phase components with a more hydrophobic character, the higher the anion value log(K_{ow}), the lower the ability of IL to promote the ABS formation.

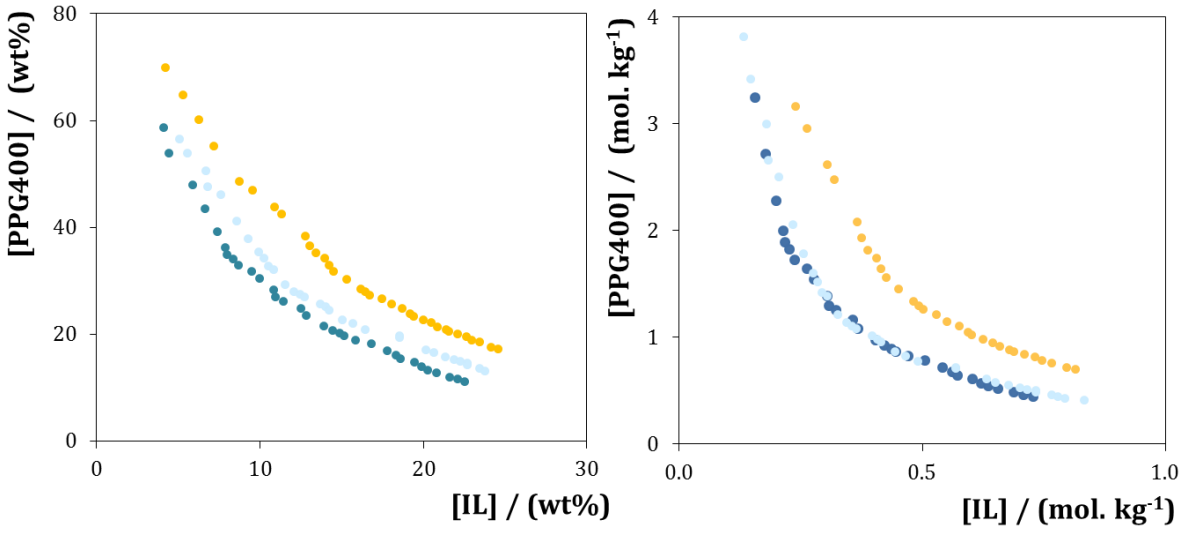

Figure 3.5. Phase diagrams represented in molality for the systems composed of PPG + IL + water in units wt% (left) and in mol.kg-1 (right): (●) [Ch][Tricine]; (●) [Ch][HEPES]; (●) [Ch][MES].

It was already shown that in contrast to what is observed in IL + salt systems, in aqueous systems of polymers and ILs, the hydrophilic ILs are more prone to act as "salting-out" species and thus reverse orders on the ILs ability to form ABS are commonly found. However, the underlying mechanisms on the formation of IL-polymer-based ABS are by far more complex and still not completely understood. Recent studies are proving that unlike the salt + IL systems, the salting-out phenomenon is not the main inducer of ABS formation but the liquid-liquid demixing mainly results from the polymer−IL mutual miscibilities and interactions [155]. Tomé et al. [156] showed that a very small amount of water (depending on the binary mixture and temperature) is enough to trigger the liquid–liquid phase separation of a completely miscible binary system composed of [C_4mim]Cl and PEG 1500. In polymer-IL binary systems ([C_4mim]Cl + PEG) the main interactions occurring are the hydrogen bonds established between Cl^- and the OH^- groups of PEG, and also some bonds between the polymer and the IL cation at the level of the hydrogen atoms of the imidazolium ring [156]. However, the authors [156] proved that the introduction of water in this binary system will disrupt the IL ions and polymer hydrogen bonds (interfering however to a lesser extent with the interactions between the non-polar moieties of the cation and the polymer) and will be replaced by more favourable and stronger water–IL anion hydrogen bonds, leading to a ‘‘washing-out’’ phenomenon. Therefore, it is

also expected that the phase separation of the systems studied in this work are also mainly driven by the formation of stronger water–IL anion hydrogen bonds (allowing the separation of the anion from the PPG), and that both the IL and the polymer become independently solvated by water and two aqueous-rich phases can be formed [156]. Nevertheless, no major conclusions can be derived at this point since there is still a lack in literature regarding the understanding of the molecular-level phenomenon involving PPG and other ILs different from imidazolium-based. ABS formed by PPG 400 and ILs were already reported [109], however only using imidazolium-based ILs. In general, the authors concluded that with the increase of the ILs hydrophilicity lower concentrations of ILs are needed to create an ABS.

For the studied systems, the experimental binodal data were further fitted by the empirical relationship described by Eq. 1 [130]. The regression parameters were estimated by least-squares regression, and their values and corresponding standard deviations (σ) are provided in Table 3.2. The experimental TLs, along with their TLLs, are reported in Table 3.3 as well as the initial composition of each system. An example of the TLs obtained is shown in Figure 3.6.

Table 3.2. Correlation parameters used to describe the experimental binodal data by Eq. 1 and respective standard deviations (σ) and correlation coefficients.

IL	$A \pm \sigma$	$B \pm \sigma$	$10^5 (C \pm \sigma)$	r^2
[Ch][DHPhs]	215.0 ± 5.2	-0.81 ± 0.01	1.00± 0.85	0.9989
[Ch][Ac]	240.4 ± 15.1	-0.81 ± 0.00	1.00 ± 1.86	0.9938
[Ch][Bit]	205.8 ± 13.9	-0.57 ± 0.0	1.00 ± 0.43	0.9962
Ch][Lac]	235.0 ± 8.5	0.67 ± 0.01	1.05 ± 0.00	0.9979
[Ch][Prop]	162.0 ± 6.1	-0.50 ± 0.02	12.25 ± 2.83	0.9981
[Ch][But]	452.9 ± 33.6	-0.84 ± 0.03	0.01 ± 1.12	0.9984
[Ch][DHCit]	342.6 ± 2.3	- 0.62 ± 0.01	0.03 ± 0.00	0.9991
[Ch]Cl	265.4 ± 16.1	-0.69 ± 0.00	1.08 ± 0.20	0.9902
[Ch][Tricine]	179.3 ± 5.4	-0.56 ± 0.01	1.00 ± 0.4	0.9972
[Ch][MES]	169.2 ± 3.9	-0.42 ± 0.01	1.69 ± 0.16	0.9971
[Ch][HEPES]	187.1 ± 9.1	-0.52 ± 0.02	1.00 ± 0.40	0.9936

Table 3.3. Data for the tie-lines (TLs) and tie-line lengths (TLLs). Initial mixture compositions are represented as $[Salt]_M$ and $[PPG]_M$ whereas $[Salt]_{Salt}$ and $[PPG]_{Salt}$ are the composition of IL and salt at the IL-rich phase, respectively, and vice-versa.

IL	Weight fraction composition / wt %						TLL
	$[PPG]_{PPG}$	$[Salt]_{PPG}$	$[PPG]_M$	$[Salt]_M$	$[PPG]_{Salt}$	$[Salt]_{Salt}$	
[Ch][DHPhs]	40.8214	4.1447	20.0916	19.2240	1.4111	32.8214	44.1466
[Ch][DHPhs]	81.4241	1.4169	30.0568	29.9829	0.3007	46.5305	92.8237
[Ch][Ac]	95.7430	1.3007	30.1093	29.9757	0.5527	42.8888	103.8786
[Ch][Ac]	91.7995	1.3119	24.9112	24.9477	3.7843	29.3653	90.2118
[Ch][Gly]	63.2805	3.2068	30.4085	29.7656	0.2953	54.0955	80.9741
[Ch][MES]	77.0069	3.5595	56.1147	9.9973	20.4344	22.2437	57.3042
[Ch][Bit]	98.3921	1.6971	30.3889	31.0858	2.2065	43.2653	104.7835
[Ch][Lac]	90.5132	1.1171	30.0546	30.4477	2.0271	44.0508	98.7808
[Ch][Prop]	88.5791	1.4479	29.488	31.5532	2.4200E-05	46.5765	99.4125
[Ch][But]	96.5904	3.3854	29.9202	30.0195	2.0697	41.0608	101.7526
[Ch][HEPES]	96.6420	1.5832	29.9242	30.0627	3.1079	41.5100	101.6995
[Ch][DHCit]	82.4292	5.3832	29.8696	29.9531	6.6731	40.7967	83.6248
[Ch]Cl	96.7066	1.4471	29.9440	29.9679	3.9281	40.9909	100.8542
[Ch][Tricine]	91.2958	1.5648	30.0874	30.0874	1.9926	42.7543	98.3445
[Ch][Tricine]	81.0250	2.0125	49.8924	10.1744	13.957	19.595	69.3350

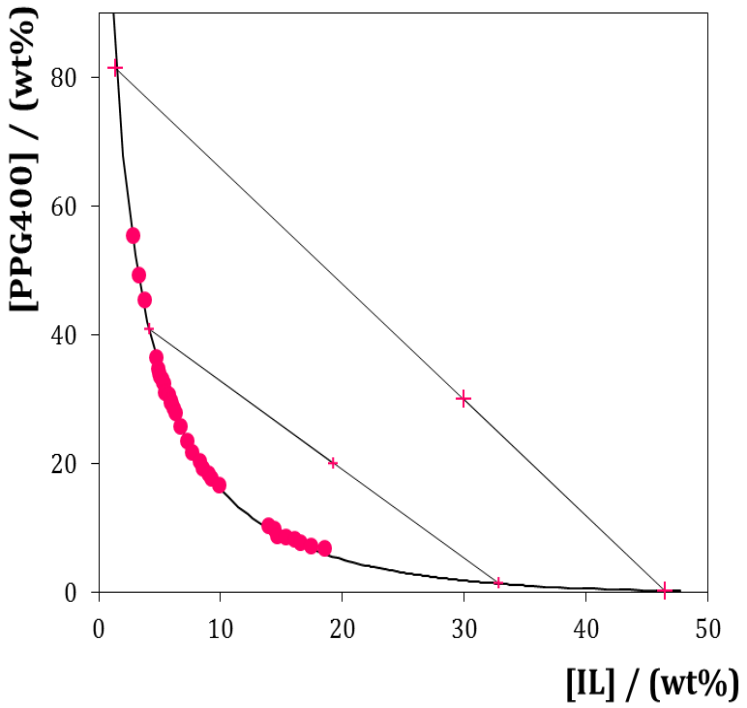

Figure 3.6. Phase diagram for the ternary system composed of PPG 400+ [Ch][DHPhs] + water at 25 ºC: binodal curve data (●); TL data (+); adjusted binodal data using Equation 1 (-).

3.3.3. Extraction efficiencies of BSA

In the present work, the BSA partition in the ABS composed of cholinium-based ILs + PPG 400 at 25 ºC has been examined. The extraction efficiencies of BSA, at 25 ºC and at a common TLL ≈ 30-30, are shown in Table 3.4.

In all systems it is observed a preferential partitioning of BSA for the IL-rich aqueous phase. In general, the partitioning of proteins between the two phases of an ABS is a complex phenomenon, guided mainly by several competing interactions of the partitioned solute and the phase components [91]. During partitioning, the exposed groups of proteins come into contact with the phase components and therefore determine the partitioning behaviour. This surface-dependent phenomenon is very complex since a protein can interact with the surrounding molecules through hydrogen-bonding, electrostatic interactions, van der Waals forces, hydrophobic interactions and steric effects. The net effect of these interactions is likely to be different in the two phases and the protein will partition preferentially into one phase. In this case, the preferential migration of BSA for the IL-rich phase can be explained by the protein affinity for the most hydrophilic phase

(IL-rich phase) of the ABS. In fact, the complete extraction of BSA in a single-step procedure was achieved with several ILs, such as [Ch][MES], [Ch][Tricine], [Ch][DHCit], [Ch][Prop], [Ch][But] and [Ch][Ac]. Remarkably, the extraction efficiencies of BSA vary between 91.79% to 100%, and increase in the following order: [Ch][Lac] < [Ch][DHPhs] < [Ch][Bit] < [Ch][HEPES] < [Ch][MES] ≈ [Ch][Tricine] ≈ [Ch][DHCit] ≈ [Ch][Prop] ≈ [Ch][But] ≈ [Ch][Ac]. Rito- Palomares et al. [157] reported the application of ABS formed by polymer (PEG) and phosphate salt for BSA extraction of whole bovine blood. They obtained a maximum overall protein recovery of 62%, results that are not very significant compared with the ones described in this work. In 2010, another work reported the use of polymers, namely PEG and PPG, combined with three inorganic salts for the extraction of BSA. The maximum extraction obtained was 90.4 %, with the ABS formed by PPG + $MgSO_4$ + water [158]. In this work, the combination of polymers and ionic liquids leads to higher extraction efficiencies overall.

Table 3.4. Percentage extraction efficiencies of BSA , EE_{BSA}% and respective standard deviations (σ), in the ABS composed of IL + PPG 400 at 25 ºC. Initial mixture compositions and respective standard deviations (σ) are represented as $[IL]_M$ and $[PPG400]_M$.

IL	Weight fraction composition / (wt %)		EE_{BSA}%
	$[IL]_M$	$[PPG400]_M$	
[Ch][Ac]	30.06 ± 0.09	30.11 ± 0.12	100.0
[Ch][Ac]	24.43 ± 0.24	24.67 ± 0.27	100.0
[Ch][Ac]	20.23 ± 0.21	19.94 ± 0.27	100.0
[Ch][Prop]	29.70 ± 0.58	29.05 ± 0.78	100.0
[Ch][But]	29.92 ± 0.27	30.39 ± 0.32	100.0
[Ch][Tricine]	29.93 ± 0.14	30.02 ± 0.07	100.0
[Ch][MES]	29.80 ± 0.02	29.88 ± 0.04	100.0
[Ch][DHCit]	29.70 ± 0.33	29.72 ± 0.37	100.0
[Ch][HEPES]	30.12 ± 1.43	31.64 ± 1.58	99.76 ± 0.24
[Ch][Bit]	30.26 ± 0.23	30.03 ± 0.35	98.02 ± 0.21
[Ch][DHPhs]	29.73 ± 0.05	30.30 ± 0.60	96.10 ± 1.09
[Ch][Lac]	30.34 ± 0.11	29.99 ± 0.07	91.79 ± 0.05

Figure 3.7 displays some examples of the obtained chromatograms. For instance, for [Ch][Ac], the complete extraction is verified since there is no evidence of the presence of BSA in the top (PPG 400) phase. Also, it is represented the complete extraction of BSA in [Ch][DHCit]; however, despite the good extraction results, it was observed some precipitation of protein in the systems formed by this ILs (Figure 3.8).

An example where the complete extraction ([Ch][Phs] was not verified is also depicted in Figure 3.7, and where the peak corresponding to BSA at the polymer-rich phase is visible.

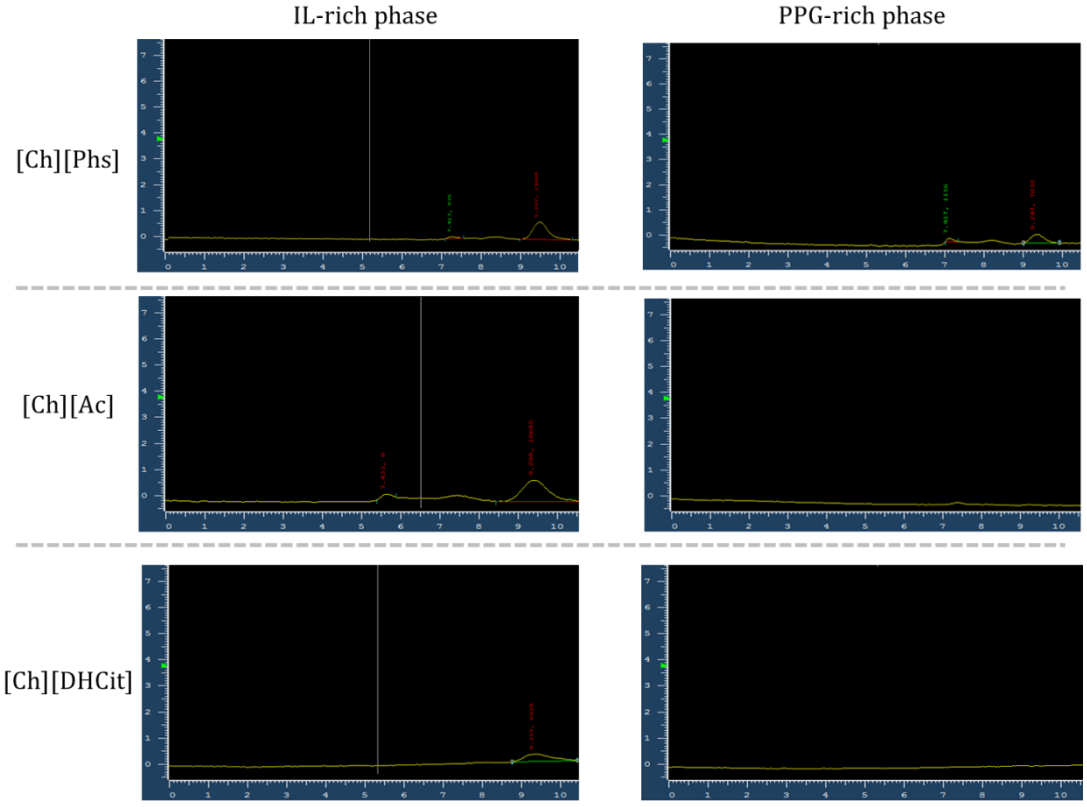

Figure 3.7. Size exclusion chromatograms of BSA in ternary system composed of PPG 400+ IL + water at 25 ºC. X-axis – Absorbance 280 (mV) a y-axis - Elution time (min).

In figure 3.8 are also represented others examples of systems with protein precipitation, and in some cases extend to the PPG-rich phase.

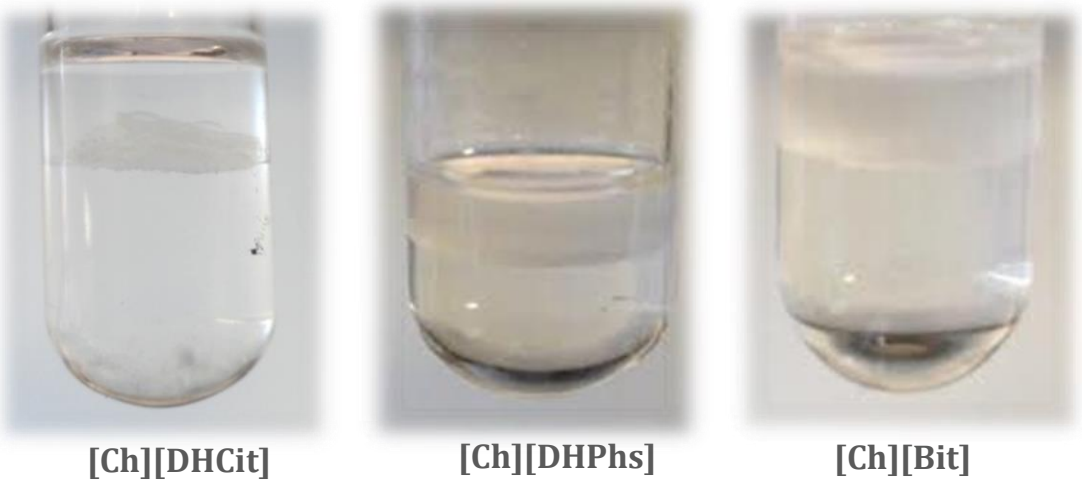

Figure 3.8. BSA extraction with ABS formed by PPG + IL + water with visible protein precipitation at the interface.

From the overall results it is evident that the cholinium-based ILs composed of anions derived from carboxylic acids and with anions derived from Good's buffers present a better performance since they lead to a complete extraction of BSA with no precipitation or loss of protein.

Despite the hydrogen-bonding interactions as the main driving force for the partitioning of BSA into the ionic liquid phase, protein partitioning can be also favored by electrostatic interactions. Proteins are composed of sequences of amino acids that carry charged groups (depending upon their acidic or alkaline character); the net electric charge on a protein surface represents the sum of all electric charges present on the amino acids. The net charge on the protein varies with the pH of the ABS, and depending on the isoelectric point (pI) of the protein it influences the partitioning between the two phases. All systems studied (except the ones formed by GB-IL) in this work were done under controlled pH (≈7.0) using a PBS buffer solution. The pI of BSA is 4.7, and above this value the protein carries a negative net charge which will promote electrostatic interactions with the IL. However, and in addition to the different phase-forming components studied, in this type of systems BSA also has a higher affinity for the IL-rich phase.

It is known that the TLL can affect the protein affinity for the phases by changing the hydrophobicity and interfacial tension between the phases of a given ABS. As the TLL increases the top- and bottom-phases show increasing differences in compositions [159].

The ABS becomes more hydrophobic with an increase in the TLL due to a reduction in the water content. With a reduction in the water content the saturation solubility of the proteins in a given phase can be reached and thus the protein can precipitate as commonly observed [159]. After the study at a common TLL on the ability of the PPG-IL-based ABS to extract BSA, it was further evaluated the effect of the two phase compositions on the extraction efficiency of BSA. The IL chosen was [Ch][Ac] because it presents an extraction efficiency of 100% and leads to a negligible protein precipitation. The new TLLs chosen were ≈ 25 and 20, in order to avoid a decrease in extraction efficiency associated with the protein solubility in water. With these two TLLs the water content is increased while reducing the amount of IL and PPG required for extraction. The mixture compositions used in partitioning experiments are presented in Table 3.3 whereas the respective phases' compositions and TLLs are presented in Table 3.4. It is clear in Table 3.3 that the extraction efficient of BSA is not affected by changing the TLL (at least at the TLLs considered).

3.3.4 Stability of BSA

The stability of proteins during extraction is a prerequisite for the application of this technique. In fact, small changes in the protein environment such as temperature, pH and type of solvent can alter the native fold of the protein; so, it is important to confirm the protein stability in the extracted phase. Several studies on proteins interactions with ILs and their stability have been performed [117, 160, 161]. Rodrigues et al. [160] have already shown that cholinium-based ILs can either increase lysozyme stability or have a negligible effect on protein stability. Furthermore, it was also proved that low levels of [Ch][Ac] do not affect the conformation of proteins like lipase [160].

In our work, the samples of the IL-rich top phase were investigated by HPLC and a careful analysis of the resulting chromatograms allowed the study of the BSA stability in a PBS solution composed of 20 wt% of IL. [Ch][Ac] proved to be the most suitable IL for the extraction of BSA. The chromatogram depicted in Figure 3.9 revealed that the peak intensity and shape do not change significantly, supporting thus the stability of the protein when in the IL-rich phase after ≈ 30 min. In order to support the stability of BSA solution in [Ch][Ac] (Table 3.5) the area of the peak of the standard BSA in the PBS buffer was calculated and compared with the area obtained for a solution of BSA in 20 wt% of IL. As clearly shown by the relative standard deviation (RSD <= 5), the peak area remains constant, which ensures the stability of the protein in the presence of [Ch][Ac].

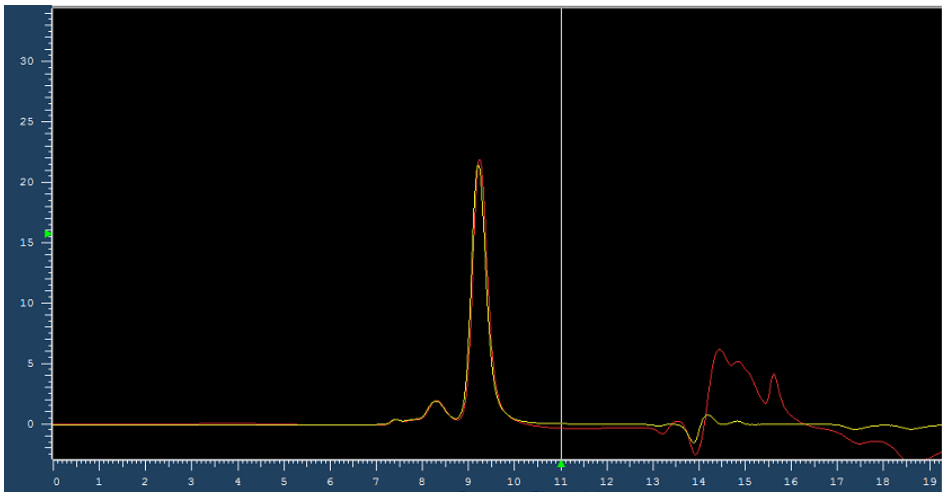

Figure 3.9. Size exclusion chromatogram of BSA in PBS solution with 20% of [Ch][Ac]. Yellow line: BSA in PBS; Red line: BSA in 20% of [Ch][Ac].

Table 3.5. BSA stability test in 20% solution of IL conducted in HPLC.

Solution	[BSA] / ($g.L^{-1}$)	Peak area ± σ	RSD / (%)
PBS	0.005	4450 ± 195	5.05
20 wt% IL		4143 ± 30	
PBS	0.5	509746 ± 3964	0.57
20 wt% IL		513775 ± 17460	

The protein stability can be strongly influenced by the type of ILs present in aqueous solution. Although the interactions between ILs and protein are not well understood, there are some discussions indicating that ILs follow the Hofmeister series [162]. An IL can be constituted by a kosmotropic anion and a chaotropic cation - and this combination can stabilize proteins. In this work, we used cholinium-based ILs which are constituted by a chaotropic quaternary ammonium cation. Rodrigues et al. [160] have already shown in a systematic study on the stability of lysozyme that the cholinium-based ILs can increase the protein stability. Furthermore, it was also proved that low levels of [Ch][Ac] do not affect the conformation of proteins like lipase, and also a study on the stability of lipase in sodium di-2-ethylhexylsulfoccinate (AOT) reverse micelles indicated that the IL is able to maintain the activity of lipase up to a certain extent [161]. The effect of [Ch][Ac] is thus consistent with that predicted based on the Hofmeister series [161].

3.4 Conclusions

In the present work, the effect of the IL anion on the phase forming ability of ABS was evaluated. The following order represent the overall trend: [Ch][DHPhs] > [Ch][Ac] > [Ch][Lac] ≈ [Ch][Prop] > [Ch][But] > [Ch][Bit] > [Ch][Ac] > [Ch][DHCit] > [Ch]Cl > [Ch][MES] > [Ch][HEPES] > [Ch][Tricine]. The data obtained with the extraction of BSA also shown that cholinium-based ILs + PPG400 ABS can be used to efficiently extract proteins in a single-step. Moreover, a proper choice of the IL avoids the protein precipitation or denaturation. Since both the cholinium-based ILs and PPG400 tend to be less toxic and more biodegradable, these ABS offer a greener and highly efficient technique for extracting and concentrating proteins of high interest-

4. Concentration of BSA using optimized IL-based ABS

4.1. Introduction

As pointed out before, one of the major concerns related with the biomarkers analysis, identification and/or quantification is related to their low concentration in body fluids. Most of the biomarkers assays on the market are formulated for use in specific immunoassay tests in clinical chemistry laboratories [163]. Moreover, they require skilled personnel and are associated with a time-consuming sample processing so that results are not instantly available [163]. Also, the investment in time (several weeks) and resources required to generate such immunoassays are considerable, what often obstructs the development of clinically useful protein-based assays in the absence of compelling pre-clinical data [6]. Furthermore, differences in the choice of the antibody, the method design and the method robustness will inevitably contribute to the between-method variation in results that are observed even for accurately calibrated equimolar assays [163]. Therefore, these tests are not ideally suited for the establishment of large screening programs to be potentially carried out in urological clinics and general medical practices [163].

IL-based ABS represent an appealing alternative to the current request for fast, economic, and easy-to-implement processes and besides their extraction ability, IL-based ABS have also shown to be a promising concentration technique. Passos et al. [146] reported that IL-based ABS can be used to concentrate endocrine disruptors from biological fluids up to 100-times in a single-step. These results can revolutionize the clinical analyses with the pre-concentration of most proteins from biological fluids [164]. Therefore, IL-based ABS offer the opportunity to combine the extraction and concentration of proteins in a single-step procedure for the detection of cancer biomarkers present in human fluids.

4.2. Experimental Section

4.2.1. Chemicals

The salt potassium citrate tribasic monohydrate ($K_3C_6H_5O_7 \cdot H_2O$, purity ≥ 99 wt%), and the polymer PPG 400 were obtained from Sigma–Aldrich Chemical Co. BSA/fraction V, pH = 7.0, was obtained from Acros Organics. Methanol (HPLC grade, purity > 99.9%) was obtained from Fisher Scientific. Acetonitrile (purity > 99.7%) was supplied from Lab-Scan. The buffer Tricine (purity > 99 wt%) was purchased from Sigma–Aldrich Chemical Co. The choline hydroxide solution (40 wt %, in H_2O) hydroxide-based compound,

[N_{4444}][OH] (40 wt% in H_2O), was also supplied by Sigma–Aldrich Chemical Co.. The ILs [Ch][Tricine] and [N_{4444}][Tricine] were synthesized according to the procedure described in section 3.2.2.1. Purified water passed through a reverse osmosis and a Milli-Q plus 185 water purifying system was used in all experiments.

4.2.2. Experimental Procedure

4.2.2.1. Lever-Arm Rule

The lever-arm rule was used to determine the weight percentages ratio of the coexisting phases in the respective phase diagram. Several extractions were carried out at different compositions in the same TL (Figure 4.1) which correspond to different concentration factors. Along the same TL the composition of the phases is maintained while varying the weight or volume ratio between them. First, a fixed and long TL was selected and a weight balance approach, as described in section 2.2.2.1, was used to determine the weight fraction of each phase-forming component ([Ch][Tricine] and PPG400 or [N_{4444}][Tricine] and $K_3C_6H_5O_7$).

For each mixture the salt concentration was varied to obtain the desired concentration factor (f_c, equation (11)),

$$f_c = \%H_2O_{PM}/(w_{ABS} \times \%ILphase) \quad (8)$$

where $\%H_2O_{PM}$, w_{ABS} and $\%ILphase$ correspond to the water percentage in the mixture point, ABS total weight and IL weight percentage in the top phase.

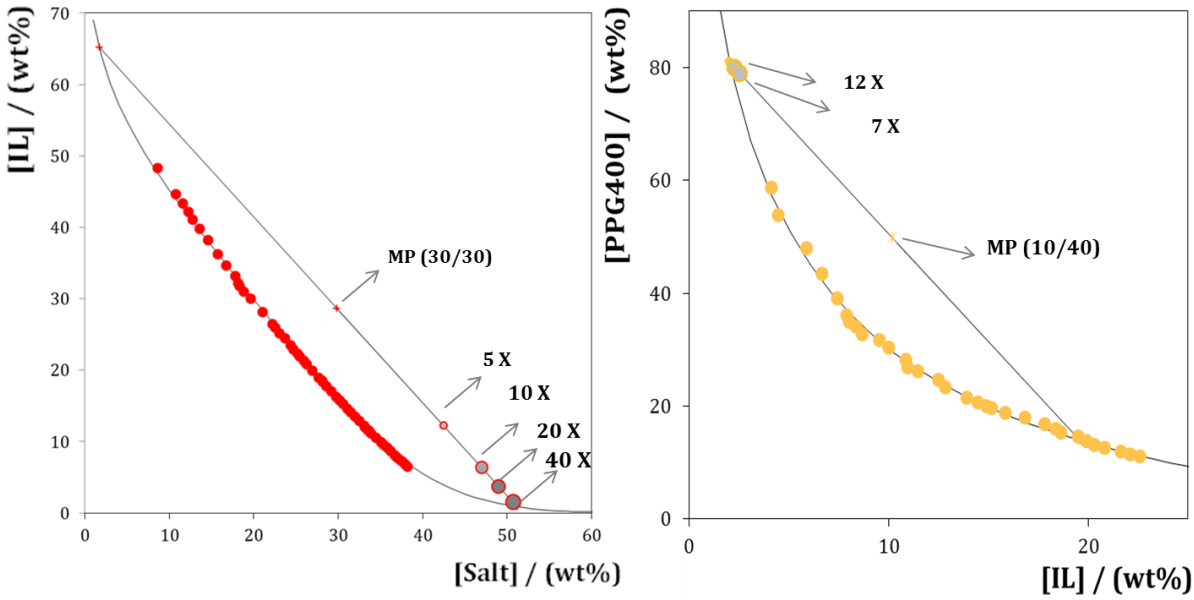

Figure 4.1. Different compositions along the same the same TL obtained by applying the lever-arm rule. Salt + IL + water ABS (left), and PPG 400 + IL + water (right). MP: mixture point; 5x, 7x, 10x, 12x, 20x, 40x corresponds to concentration factors.

4.2.2.2. Concentration Factors of BSA

The ternary mixtures compositions used in the partitioning experiments were chosen based on the phase diagrams determined here for each PPG-400-IL-water system and salt - IL-water system. Several ternary mixtures within the biphasic region were prepared, namely 3 wt % of IL, 78 wt % of PPG400 and 19 wt % of water (f_c = 7) and 2.5 wt % of IL, 18.5 wt % of PPG400 and 48 wt % of water (f_c = 12) for PPG 400-IL-water systems. Considering the salt-IL-water systems, ternary mixtures with the following compositions were prepared: 12 wt % of IL, 43 wt % of salt and 48 wt % of water (f_c = 2), 6 wt % of IL, 47 wt % of salt and 47 wt % of water (f_c = 5), 4 wt % of IL, 49 wt % of salt and 47 wt % of water (f_c = 10), 2 wt % of IL, 50 wt % of salt and 47 wt % of water (f_c = 20), 2 wt % of IL, 51 wt % of salt and 48 wt % of water (f_c = 40). Each mixture was vigorously stirred, centrifuged for 30 min, and left to equilibrate for at least 10 min at (25 ± 1) ºC.

After a careful separation of the phases, the quantification of BSA in the two phases was carried by HPLC, using the same procedure presented in section 2.2.3.

The percentage extraction efficiency of BSA, EE_{BSA}%, is the percentage ratio between the amount of protein in the IL-rich aqueous phase to that in the total mixture, and is

defined according to Eq. 7 Further, the final concentration of BSA in the IL-rich phase was determined and compared to the initial concentration in water solution aiming at calculating each concentration factor.

4.3. Results and Discussion

4.3.1. Concentration Factors of BSA

In order to optimize the liquid-liquid extraction method for the biomarkers concentration, more specifically PSA, several extractions of the model protein (BSA) were carried out at different compositions along the same TLL (Figure 4.1). This procedure reduces the volume of the IL-rich phase down to a minimum capable of concentrating the BSA that is actually present in a larger volume of an initial aqueous solution (for instance, biological fluids). The several initial compositions are along the same TL; yet, different initial concentrations lead to a different volume/weight ratio.

The results obtained are depicted in Figures 4.2 and 4.3. At first, the PPG-400-IL-water system was used (TLL for 49 wt% of salt and 10 wt % of IL), where two concentration factors were tested, and using a system that allows the 100% of extraction ([Ch][Tricine] + PPG 400 + water). The results shown in Figure 4.2 reveal that this system is not ideal for the final goal since it wasn´t possible to achieve the desired concentration levels. Probably, the high viscosity of PPG 400 turns more difficult the complete/accurate phase separation, even after centrifugation. When increasing the concentration factor we are decreasing the volume of the IL-rich phase turning more difficult the accurate separation and weight of this phase. This difficulty is more evident with the higher concentration factor since it was necessary to increase the total volume of the mixture (from 10g to 60g) to obtain a larger IL-rich phase that would be easier to separate. However, this resulted in a significant increase in the amount of PPG 400 which in turns makes more difficult the phases separation. However, it should be noted that no BSA was detected in the PPG phase in all experiments meaning that the extraction remained at 100% for all the concentration tests performed.

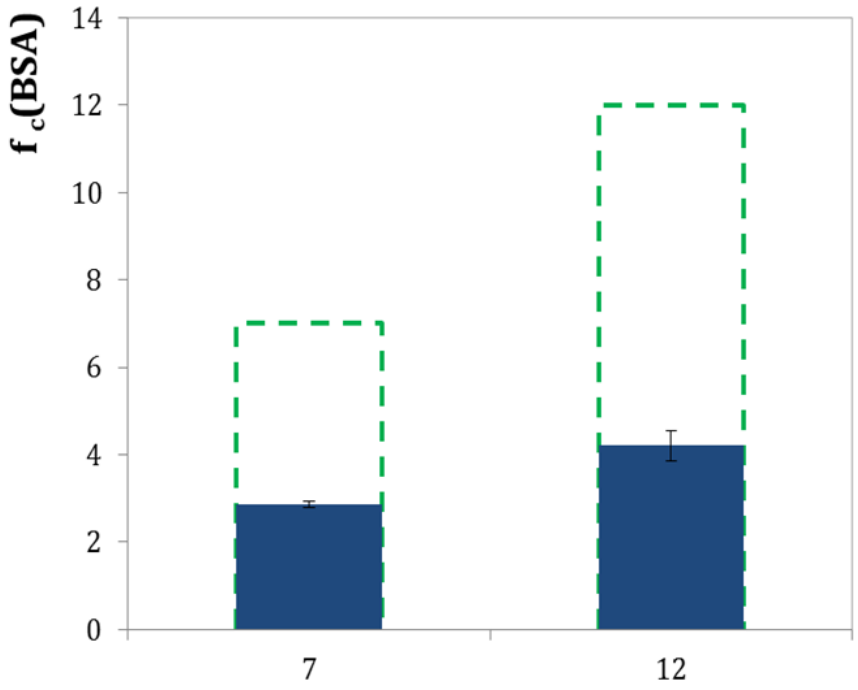

Figure 4.2. Concentration factors (f_c) of BSA ($E_{BSA\%}$) in the systems composed of [Ch][Tricine] + PPG400 + water: f_c=7 and f= 12; p1 and p2 represent the different experiments. The filled line: experimental values; dashed green line: theoretical values.

Aiming at overcoming this problem of phase separation, that seems to derive mainly from the polymer high viscosity, the same concentration procedure was employed with a salt-IL-water system. As with the PPG-400-IL-water system, a common TLL was chosen (for the initial composition of 29.8 wt% of salt and 28.7 wt% of IL). $[N_{4444}]$[Tricine] and $K_3C_6H_5O_7$ were the IL and salt selected and concentration factors equal to 2, 5, 10, 20 and 40 were tested. In Figure 4.3, it is possible to observe that up to a concentration of 20 times the results obtained are very close to the predicted ones by the level-arm rule. Only at the concentration factor of 40 the results start to deviate. At this point more experimental investigations are required as well as the development of a more convenient separation technique. The IL-rich liquid phase formed in the system corresponding to a 40 times concentration was too small (0.662 g for a total of 60 g), and probably losses through the walls of the tubes used for extraction may be in the origin of these results. However, similarly to the PPG-400-IL-water system, at all tested concentrations the extraction efficiency of BSA remained at 100%.

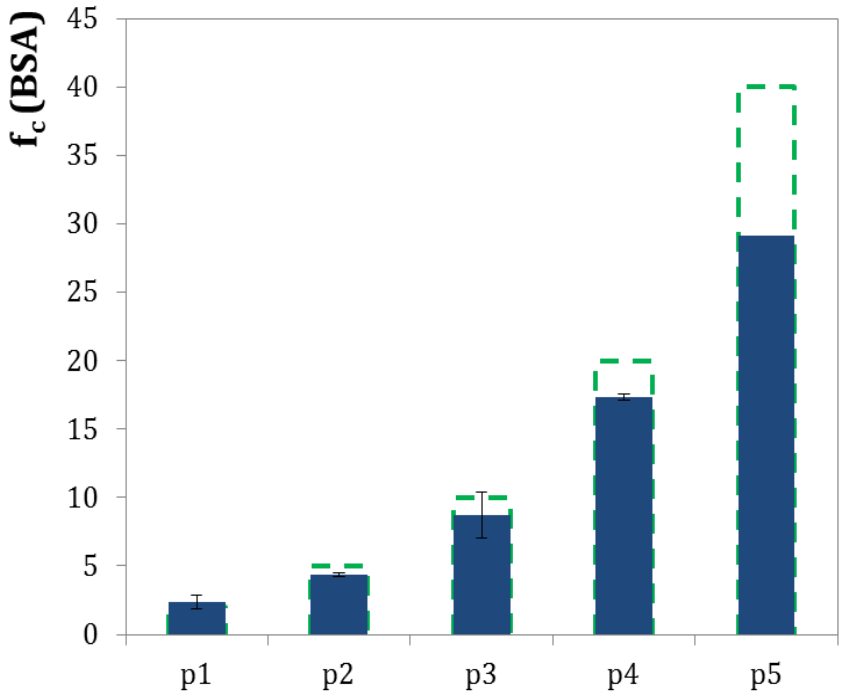

Figure 4.3. Concentration factors (f_c) of BSA (EE_{BSA}%) in the systems composed of [N_{4444}][Tricine] + salt + water: fc=2, 5, 10, 20 and 40; p1;p2;p3;p4;p5 represents the different experiments. Filled lines: experimental values; dashed green line: theoretical values.

Still, based in the latest results (Figure 4.3) it can be affirmed that controlling the volume ratio of the aqueous phases, aiming at decreasing the volume of the IL-rich phase, makes possible the concentration of proteins while keeping the complete extraction in a single-step. Therefore, different mixture compositions along the same TL always led to the complete extraction of BSA. In this context, the concentration of BSA can be increased at least up to 900 × by the reduction of the total volume of the extractive phase (from a theoretical calculation and for the mixture point composed of 0.90 wt% of IL and 51.1 wt% of salt). Nevertheless, additional experiments are still required in what concerns the optimization of the procedure employed for separating the coexisting phases. As already discussed, the pre-concentration of biomarkers from biological fluids is traditionally carried out by highly cost techniques and according to well-known protocols. Therefore, the alternative process presented in this work is, in comparison to the later, simpler and more economical and certainly deserves further investigations.

4.4. Conclusions

Based on the theoretical concentration factors that can be achieved, small kits containing the optimized ILs and $K_3C_6H_5O_7$ in fixed amounts can be conceptualized as analytical/clinical strategies where the identification/quantification of cancer biomarkers is required. Nevertheless, it is still required to optimize the separation of the coexisting phases. PSA, as most biomarkers, is found in very low concentrations in biological fluids, and often below the detection limits of conventional devices. The possibility created by the application of this type of ABS, eliminates the need of using very expensive equipment, such as ELISA, and specialized personnel in conducting screening tests that overload the national health system.

5. Extraction of PSA using optimized IL-based ABS

5.1. Introduction

Since PSA discovery and introduction into clinical use, it has become one of the most important tumor markers in cancer detection [20]. In general, a PSA value of > 4.0 µg/L has been defined in the literature [29] as abnormal and it is frequently used as a cut-off. This value is below the detection limit of most quantification equipment, making the selection of extraction/concentration techniques relevant in order to prevent the cancer progression to advanced states [15]. Although, as has been carefully reviewed in Chapter 1, some of the conventional tests and techniques used for clinical analysis, presents serious drawbacks. Currently, immunoassays are the most common type of assays commercially available, such as ELISA [46], but this type of techniques require the identification and characterization of immunoassay-qualified antibodies and highly qualified technical operators [5]. Also, the investment on time and resources required to generate such immunoassays are considerable and must be developed on clinically specific chemistry laboratories [6]. In addition to these, it was reported the use of fluorescence and electrochemistry-based techniques, but these also have disadvantages like a high detection limit and the need to modify the target analyte - a step that could result in sample loss consequently affecting the quantification results [83].Therefore, is of great need to develop an alternative platform for the extraction and concentration of PSA from human urine samples.

At this point of the work, the ABS formed by $[N_{4444}][GB]$ + salt + water were chosen as the improved system. With the aim to support the potential application of this type of ABS as alternative techniques for the extraction and concentration of cancer biomarkers, the ABS formed by $K_3C_6H_5O_7$ and $[N_{4444}][Tricine]$ was here used in an isolated experiment for the extraction of PSA.

.

5.2. Experimental Section

5.2.1. Chemicals

The salt potassium citrate tribasic monohydrate ($K_3C_6HO_4 \cdot H_2O$, purity ≥ 99 was obtained from Sigma–Aldrich Chemical Co. PSA (purity ≥ 95%,) was obtained from Sigma–Aldrich Chemical Co.. The buffer Tricine (purity > 99 wt%) was purchased from Sigma–Aldrich Chemical Co. The choline hydroxide solution (40 wt %, in H_2O) hydroxide-based compound, $[N_{4444}][OH]$ (40 wt% in H_2O), was also supplied by Sigma–

Aldrich Chemical Co. The IL [N_{4444}][Tricine] was synthesized according to the procedure described in section 3.2.2.1. Purified water passed through a reverse osmosis and a Milli-Q plus 185 water purifying system was used in all experiments.

5.2.2. Experimental Procedure

5.2.2.1. Extraction efficiencies of PSA

The ternary mixture composition used in this partitioning experiment was chosen based on the previous results carried out with BSA. A ternary mixture with a common composition, and within the biphasic region, was prepared with 30 wt % of PPG 400, 30 wt % of IL and 40 wt % of water. The mixture was vigorously stirred, centrifuged for 10 min, and left to equilibrate for at least 10 min at 25 ºC.

After a careful separation of both phases, the quantification of PSA in the two phases was carried by UV-spectroscopy, either using a Shimadzu UV-1700, Pharma-Spec Spectrometer (to gather the whole spectrum from 190-800 nm and from which it was possible to select the wavelength correspondent to the highest absrovance value (280 nm) or a microplate reader from BioTec, SYNERGY|HT.

Two samples with three readings were used in order to determine the average in the partition coefficient and extraction efficiency, as well as the corresponding standard deviations. The interference of the salts and ILs with the quantification method was also ascertained and blank control samples were always employed.

The percentage extraction efficiency determined by UV-spectroscopy is defined as the percentage ratio between the amount of PSA (absorbance obtained in the IL-rich aqueous phase time the weight of the corresponding phase) to that in the total mixture, and is defined according to Equation 9,

$$EE_{\mathrm{PSA}}\% = \frac{\mathrm{Abs}_{\mathrm{PSA}}^{\mathrm{IL}} \times \mathrm{w}_{\mathrm{IL}}}{\mathrm{Abs}_{\mathrm{PSA}}^{\mathrm{IL}} \times \mathrm{w}_{\mathrm{IL}} + \mathrm{Abs}_{\mathrm{PSA}}^{\mathrm{Salt}} \times \mathrm{w}_{\mathrm{Salt}}} \quad (9)$$

where w_{IL} and $\mathrm{w}_{\mathrm{Salt}}$ are the weight of the IL-rich phase and the weight of the salt-rich phase, respectively. $\mathrm{Abs}_{\mathrm{PSA}}^{\mathrm{IL}}$ and $\mathrm{Abs}_{\mathrm{PSA}}^{\mathrm{Salt}}$ are the absorbance of PSA at the maximum wavelength, adjusted by the respective dilution factor, in the IL-rich and in the salt-rich aqueous phases, respectively.

5.3. Results and Discussion

5.3.1. Extraction efficiencies of PSA

In the previous chapters it was proven the possibility of extracting 100% of BSA, a protein chosen as a model, for the IL-rich phase, and in a single-step procedure. This was achieved wither with salt + IL or polymer + IL ABS.

The concentration of BSA to the IL-rich phase up to ≈ 30 x was attained resorting to the use of ABS formed by salts and ionic liquids as improved systems. The combination of these results allowed us to define the $K_3C_6H_5O_7$ + $[N_{4444}]$[Tricine] ABS as an optimized system that can be applied in the extraction of PSA. Hereupon, the PSA partition in the ABS composed of 30 wt % of $K_3C_6H_5O_7$ + 30 wt% of $[N_{4444}]$[Tricine] ABS at 25 ºC was performed. The extraction efficiencies of PSA were obtained from the results gathered by two different analytical instruments to have more confidence on the final results. At this point it should be stated that the HPLC technique was not used due to some faced operational problems that were not solved up to the end of this work. The extraction efficiencies of PSA at 25 ºC are displayed in Figure 5.1.

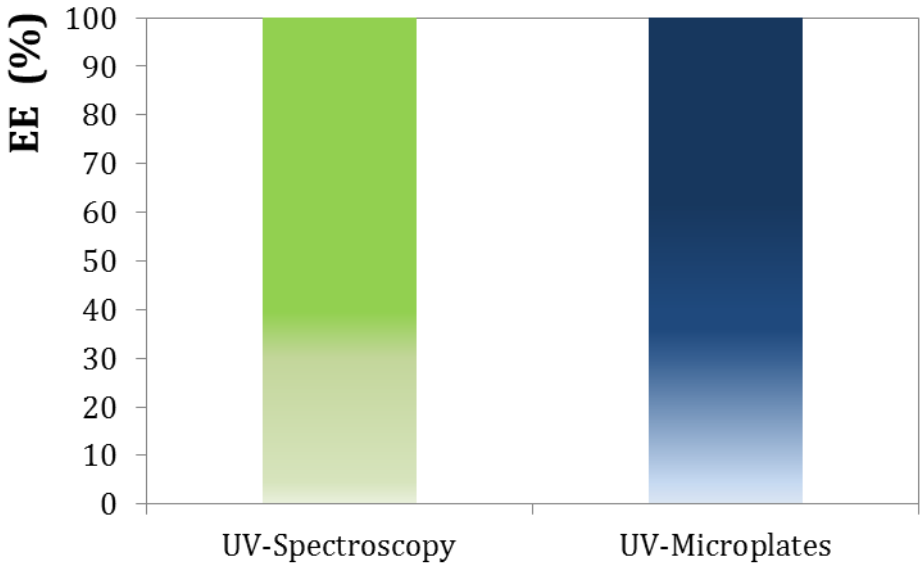

Figure 5.1. Extraction efficiencies of PSA (EE_{PSA}%) for the IL-rich phase in the systems composed of $K_3C_6H_5O_7$ + $[N_{4444}]$[Tricine] + water at 25 (±1)º C and atmospheric pressure determined from the two different techniques

As expected and based on what has been previously discussed, it was observed the complete partitioning of PSA for the IL-rich aqueous phase without any signs of denaturation and protein precipitation. The study on other ABS and the respective concentration factors of PSA is of paramount importance and should be carried out in the near future.

5.4. Conclusions

To the best of our knowledge, the remarkable ability of IL-based ABS to extract the PSA biomarker in a single-step procedure was reported here for the first time.

Huge advances were obtained in this work allowing to conclude that IL-based ABS are improved liquid-liquid systems for extracting and further concentrating proteins. The studies carried out with BSA led to the identification of the best systems to be used in the extraction and concentration of PSA aiming at attaining the biomarker in detectable levels that could be quantified by conventional methods.

6. Final remarks

6.1. Conclusions

The main purpose of this work consisted on the development of novel aqueous biphasic systems composed of ionic liquids that could allow not only an efficient extraction and a high concentration factor but also able to maintain the protein stability.

At first, new GB-IL-based ABS combined with the biodegradable organic salt, $K_3C_6H_5O_7$, were tested. More specifically, [P_{4444}][Tricine], [P_{4444}][CHES], [P_{4444}][MES], [P_{4444}][HEPES], [P_{4444}][TES], [N_{4444}][Tricine], [N_{4444}][CHES], [N_{4444}][MES], [N_{4444}][HEPES] and [N_{4444}][TES] were used to form ABS at a controlled/buffered pH. Their phase diagrams were initially ascertained, followed by extraction experiments using BSA as a model protein. In all systems, 100% of extraction of BSA for the IL-rich phase was reached in a single-step procedure with no denaturation or precipitation effects observed.

As a second approach, and with the intent of finding more benign and sustainable extraction/concentration systems, several ABS composed of cholinium-based ILs, representative materials from renewable resources, and a biodegradable and biocompatible polymer, were evaluated. The ternary phase diagrams (PPG 400 + IL + water) were determined with the following ILs: [Ch]Cl, [Ch][Ac], [Ch][Prop], [Ch][Gly], [Ch][But], [Ch][Lac], [Ch][Cit], [Ch][MES], [Ch][HEPES] and [Ch][Tricine]. After, their extraction ability for BSA was evaluated. ABS composed of [Ch][Ac], [Ch][Tricine], [Ch][But], [Ch][MES], [Ch][DHCit] and [Ch][Prop] revealed to be a promising separation process since they provide a complete extraction while maintaining a suitable aqueous environment for the protein.

In order to optimize the liquid-liquid extraction method for biomarkers concentration, more specifically PSA, several concentration factors for the model protein (BSA) were experimentally investigated. These were performed with different ABS formed at different compositions along the same TL and with two systems that allowed a 100% extraction of BSA: [Ch][Tricine] + PPG 400 + water and [N_{4444}][Tricine] + $K_3C_6H_5O_7$ + water. It was shown that the ABS formed by [N_{4444}][Tricine] and $K_3C_6H_5O_7$ is the better choice when evaluating the ABS as a concentration technique.

Finally, in order to support the potential application of the studied ABS as alternative techniques for the extraction and concentration of cancer biomarkers, the ABS formed by $K_3C_6H_5O_7$ and [N_{4444}][Tricine] was used in an isolated experiment for the extraction of

PSA and where it was confirmed the complete extraction of the biomarker for the IL-rich phase by UV-spectroscopy.

In summary, small kits containing the optimized ILs and $K_3C_6H_5O_7$ in fixed amounts can be conceptualized analytical/clinical strategies where the identification/quantification of cancer biomarkers is required. Nevertheless, much more work is still required, particularly on the concentration factors of PSA from aqueous solutions and making use of biological-fluids-type samples.

6.2. Future work

Once validated this method for general protein extraction, it is also important to study a protein structurally and functionally analogous to PSA, such as chymotrypsin, to predict the biomarker results.

The next step is to study and implement the optimized systems in the extraction and concentration of PSA.

It is necessary, at an early stage, to optimize the quantification process, similar to what was done in this work with BSA. Then, the concentration factors should be studied in more detail and it is still required to optimize the experimental phases' separation. After, the same procedure should be applied to urine-type samples. Since PSA is a biomarker with more clinical relevance in serum, the selected ABS should be finally evaluated with serum-type samples. At these stages, the partitioning and interference of other proteins in biological fluids need to be deeply evaluated. With this, the following objective is the implementation of these systems not only in PSA analyses, but also to other types of biomarkers which face the same quantification problem, such as α-fetoprotein and β-microglobulin (biomarkers of hepatocellular carcinoma and multiple myeloma/lymphoma, respectively).

7. References

1. Siegel, R., Naishadham, D., and Jemal, A., *Cancer statistics, 2013.* CA: a cancer journal for clinicians, 2013. **63**(1): p. 11-30.
2. Ilic, D., Neuberger, M. M., Djulbegovic, M., and Dahm, P. f. p. c., *Screening for prostate cancer.* The Cochrane database of systematic reviews, 2013. **1**: p. CD004720-CD004720.
3. Nam, R. K., Saskin, R., Lee, Y., Liu, Y., Law, C., Klotz, L. H., Loblaw, D. A., Trachtenberg, J., Stanimirovic, A., Simor, A. E., Seth, A., Urbach, D. R., and Narod, S. A., *Increasing hospital admission rates for urological complications after transrectal ultrasound guided prostate biopsy.* The Journal of urology, 2013. **189**(1): p. 12-17.
4. Hoffman, R. M., *Clinical practice. Screening for prostate cancer.* The New England journal of medicine, 2011. **365**(21): p. 9.
5. Acevedo, B., Perera, Y., Ruiz, M., Rojas, G., Benítez, J., Ayala, M., and Gavilondo, J., *Development and validation of a quantitative ELISA for the measurement of PSA concentration.* Clinica chimica acta; international journal of clinical chemistry, 2002. **317**(1-2): p. 55-63.
6. Adel Ahmed, H. and Azzazy, H. M. E., *Power-free chip enzyme immunoassay for detection of prostate specific antigen (PSA) in serum.* Biosensors and Bioelectronics, 2013. **49**: p. 478-484.
7. Siegel, R., Naishadham, D., and Jemal, A., *Cancer statistics, 2012.* CA: a cancer journal for clinicians. **62**(1): p. 10-29.
8. Malvezzi, M., Bertuccio, P., Levi, F., La Vecchia, C., and Negri, E., *European cancer mortality predictions for the year 2013.* Annals of oncology : official journal of the European Society for Medical Oncology / ESMO, 2013. **24**(3): p. 792-800.
9. McNeal, J. E. and Gleason, D. F., *[Gleason's classification of prostatic adenocarcinomas].* Annales de pathologie, 1991. **11**(3): p. 163-8.
10. Bostwick, D. G., Burke, H. B., Djakiew, D., Euling, S., Ho, S.-m., Landolph, J., Morrison, H., Sonawane, B., Shifflett, T., Waters, D. J., and Timms, B., *Human prostate cancer risk factors.* Cancer, 2004. **101**(10 Suppl): p. 2371-490.
11. Shen, M. M. and Abate-Shen, C., *Molecular genetics of prostate cancer: new prospects for old challenges.* Genes & development, 2010. **24**(18): p. 1967-2000.
12. *Cancer Facts & Figures 2013*. 2013 [cited 2013 November]; available from: http://www.cancer.org/research/cancerfactsfigures/cancerfactsfigures/cancer-facts-figures-2013.
13. Messing, E. M., Manola, J., Sarosdy, M., Wilding, G., Crawford, E. D., and Trump, D., *Immediate hormonal therapy compared with observation after radical prostatectomy and pelvic lymphadenectomy in men with node-positive prostate cancer.* The New England journal of medicine, 1999. **341**(24): p. 1781-8.
14. Schröder, F. H., Hugosson, J., Roobol, M. J., Tammela, T. L. J., Ciatto, S., Nelen, V., Kwiatkowski, M., Lujan, M., Lilja, H., Zappa, M., Denis, L. J., Recker, F., Berenguer, A., Määttänen, L., Bangma, C. H., Aus, G., Villers, A., Rebillard, X., van der Kwast, T., Blijenberg, B. G., Moss, S. M., and Koning, D., *Screening and prostate-cancer mortality in a randomized European study.* The New England journal of medicine, 2009. **360**(13): p. 1320-8.
15. Ilic, D., O'Connor, D., Green, S., and Wilt, T., *Screening for prostate cancer.* The Cochrane database of systematic reviews, 2006(3): p. CD004720-CD004720.
16. *Survival rates for prostate cancer*. 2013 [cited 2013 november]; available from: http://www.cancer.org/cancer/prostatecancer/detailedguide/prostate-cancer-survival-rates.
17. Verma, S. and Rajesh, A., *A clinically relevant approach to imaging prostate cancer: review.* AJR. American journal of roentgenology, 2011. **196**(3): p. 1-10

18. You, J., Cozzi, P., Walsh, B., Willcox, M., Kearsley, J., Russell, P., and Li, Y., *Innovative biomarkers for prostate cancer early diagnosis and progression.* Critical Reviews in Oncology/Hematology, 2010. **73**: p. 10-22.
19. Loeb, S., Carter, H. B., Catalona, W. J., Moul, J. W., and Schroder, F. H., *Baseline prostate-specific antigen testing at a young age.* European urology, 2012. **61**(1): p. 1-7.
20. Pinsky, P. F., Andriole, G., Crawford, E. D., Chia, D., Kramer, B. S., Grubb, R., Greenlee, R., and Gohagan, J. K., *Prostate-specific antigen velocity and prostate cancer gleason grade and stage.* Cancer, 2007. **109**(8): p. 1689-95.
21. Eckersberger, E., Finkelstein, J., Sadri, H., Margreiter, M., Taneja, S. S., Lepor, H., and Djavan, B., *Screening for Prostate Cancer: A Review of the ERSPC and PLCO Trials.* Reviews in urology, 2009. **11**(3): p. 127-33.
22. *National Cancer Institute. NCI Dictionary of Cancer Terms*. [cited 2013 november]; available from: http://www.cancer.gov/dictionary?cdrid=45618.
23. Velonas, V. M., Woo, H. H., Remedios, C. G. D., and Assinder, S. J., *Current status of biomarkers for prostate cancer.* International journal of molecular sciences, 2013. **14**(6): p. 11034-60.
24. Panini, N. V., Messina, G. A., Salinas, E., Fernández, H., and Raba, J., *Integrated microfluidic systems with an immunosensor modified with carbon nanotubes for detection of prostate specific antigen (PSA) in human serum samples.* Biosensors & bioelectronics, 2008. **23**(7): p. 1145-51.
25. Gutman, A. B. and Gutman, E. B., *An acid phosphatase occurring in the serum of patients with metastasizing carcinoma of the prostate gland.* The Journal of clinical investigation, 1938. **17**(4): p. 473-8.
26. Graddis, T. J., McMahan, C. J., Tamman, J., Page, K. J., and Trager, J. B., *Prostatic acid phosphatase expression in human tissues.* International journal of clinical and experimental pathology, 2011. **4**(3): p. 295-306.
27. Wang, M. C., Valenzuela, L. A., Murphy, G. P., and Chu, T. M., *Purification of a human prostate specific antigen.* Investigative urology, 1979. **17**(2): p. 159-63.
28. Catalona, W. J., Smith, D. S., Ratliff, T. L., Dodds, K. M., Coplen, D. E., Yuan, J. J., Petros, J. A., and Andriole, G. L., *Measurement of prostate-specific antigen in serum as a screening test for prostate cancer.* The New England journal of medicine, 1991. **324**(17): p. 1156-61.
29. Heidenreich, A., Bellmunt, J., Bolla, M., Joniau, S., Mason, M., Matveev, V., Mottet, N., Schmid, H.-P., van der Kwast, T., Wiegel, T., and Zattoni, F., *EAU guidelines on prostate cancer. Part 1: screening, diagnosis, and treatment of clinically localised disease.* European urology, 2011. **59**(1): p. 61-71.
30. Gretzer, M. B. and Partin, A. W., *PSA Levels and the Probability of Prostate Cancer on Biopsy.* European Urology Supplements, 2002. **1**(6): p. 21-27.
31. Reed, A., Ankerst, D. P., Pollock, B. H., Thompson, I. M., and Parekh, D. J., *Current age and race adjusted prostate specific antigen threshold values delay diagnosis of high grade prostate cancer.* The Journal of urology, 2007. **178**(5): p. 1929-32; discussion 1932.
32. Oesterling, J. E., Jacobsen, S. J., Chute, C. G., Guess, H. A., Girman, C. J., Panser, L. A., and Lieber, M. M., *Serum prostate-specific antigen in a community-based population of healthy men. Establishment of age-specific reference ranges.* JAMA : the journal of the American Medical Association, 1993. **270**(7): p. 860-4.
33. Anderson, J. R., Strickland, D., Corbin, D., Byrnes, J. A., and Zweiback, B. S. E., *Age-specific reference ranges for serum prostate-specific antigen.* Urology, 1995. **46**(1): p. 54-57.
34. Stamey, T. A., Yang, N., Hay, A. R., McNeal, J. E., Freiha, F. S., and Redwine, E., *Prostate-specific antigen as a serum marker for adenocarcinoma of the prostate*, 1987. p. 909-16.
35. Grossklaus, D. J., Smith, J. A., Shappell, S. B., Coffey, C. S., Chang, S. S., and Cookson, M. S., *The free/total prostate-specific antigen ratio (%fPSA) is the best predictor of tumor*

involvement in the radical prostatectomy specimen among men with an elevated PSA. Urologic oncology. **7**(5): p. 195-198.

36. Diamandis, E. P., *Prostate-specific Antigen: Its Usefulness in Clinical Medicine.* Trends in Endocrinology & Metabolism, 1998. **9**(8): p. 310-316.
37. Richardson, T. D., Wojno, K. J., Liang, L. W., Giacherio, D. A., England, B. G., Henricks, W. H., Schork, A., and Oesterling, J. E., *Half-life determination of serum free prostate-specific antigen following radical retropubic prostatectomy.* Urology, 1996. **48**(6A Suppl): p. 40-4.
38. Lange, P. H., Ercole, C. J., Lightner, D. J., Fraley, E. E., and Vessella, R., *The value of serum prostate specific antigen determinations before and after radical prostatectomy.* The Journal of urology, 1989. **141**(4): p. 873-9.
39. Hugosson, J., Carlsson, S., Aus, G., Bergdahl, S., Khatami, A., Lodding, P., Pihl, C.-G., Stranne, J., Holmberg, E., and Lilja, H., *Mortality results from the Göteborg randomised population-based prostate-cancer screening trial.* The Lancet Oncology, 2010. **11**(8): p. 725-732.
40. Loeb, S., Vonesh, E. F., Metter, E. J., Carter, H. B., Gann, P. H., and Catalona, W. J., *What is the true number needed to screen and treat to save a life with prostate-specific antigen testing?* Journal of clinical oncology : official journal of the American Society of Clinical Oncology, 2011. **29**(4): p. 464-7.
41. Ulmert, D., Cronin, A. M., Björk, T., O'Brien, M. F., Scardino, P. T., Eastham, J. A., Becker, C., Berglund, G., Vickers, A. J., and Lilja, H., *Prostate-specific antigen at or before age 50 as a predictor of advanced prostate cancer diagnosed up to 25 years later: a case-control study.* BMC medicine, 2008. **6**: p. 6-6.
42. Lilja, H., Ulmert, D., Björk, T., Becker, C., Serio, A. M., Nilsson, J.-A., Abrahamsson, P.-A., Vickers, A. J., and Berglund, G., *Long-term prediction of prostate cancer up to 25 years before diagnosis of prostate cancer using prostate kallikreins measured at age 44 to 50 years.* Journal of clinical oncology : official journal of the American Society of Clinical Oncology, 2007. **25**(4): p. 431-6.
43. Murphy, D., *The Melbourne consensus statment Prostate cancer testing.* BJU International, 2013.
44. Polascik, T. J., Oesterling, J. E., and Partin, A. W., *Prostate specific antigen: a decade of discovery--what we have learned and where we are going.* The Journal of urology, 1999. **162**(2): p. 293-306.
45. Balk, S. P., Ko, Y.-J., and Bubley, G. J., *Biology of Prostate-Specific Antigen.* Journal of Clinical Oncology, 2003. **21**(2): p. 383-391.
46. Sumi, S., Arai, K., and Yoshida, K.-i., *Separation methods applicable to prostate cancer diagnosis and monitoring therapy.* Journal of Chromatography B: Biomedical Sciences and Applications, 2001. **764**(1): p. 445-455.
47. McCormack, R. T., Wang, T. J., Rittenhouse, H. G., Wolfert, R. L., Finlay, J. A., Lilja, H., Okoloff, R. L., and Oesterling, J. E., *Molecular forms of prostate-specific antigen and the human kallikrein gene family: A new era.* Urology, 1995. **45**(5): p. 729-744.
48. Parracino, A., Neves-Petersen, M. T., di Gennaro, A. K., Pettersson, K., Lövgren, T., and Petersen, S. B., *Arraying prostate specific antigen PSA and Fab anti-PSA using light-assisted molecular immobilization technology.* Protein science : a publication of the Protein Society, 2010. **19**(9): p. 1751-9.
49. Lilja, H., Ulmert, D., and Vickers, A. J., *Prostate-specific antigen and prostate cancer: prediction, detection and monitoring.* Nature reviews. Cancer, 2008. **8**(4): p. 268-78.
50. Vermassen, T., Speeckaert, M. M., Lumen, N., Rottey, S., and Delanghe, J. R., *Glycosylation of prostate specific antigen and its potential diagnostic applications.* Clinica Chimica Acta, 2012. **413**(19): p. 1500-1505.

51. Armbruster, D. A., *Prostate-specific antigen: biochemistry, analytical methods, and clinical application.* Clinical chemistry, 1993. **39**(2): p. 181-95.
52. Yousef, G. M. and Diamandis, E. P., *An overview of the kallikrein gene families in humans and other species: emerging candidate tumour markers.* Clinical Biochemistry, 2003. **36**(6): p. 443-452.
53. Akiyama, K., Nakamura, T., Iwanaga, S., and Hara, M., *The chymotrypsin-like activity of human prostate-specific antigen, gamma-seminoprotein.* FEBS letters, 1987. **225**(1-2): p. 168-72.
54. Denmeade, S. R., Lou, W., Lövgren, J., Malm, J., Lilja, H., and Isaacs, J. T., *Specific and efficient peptide substrates for assaying the proteolytic activity of prostate-specific antigen.* Cancer research, 1997. **57**(21): p. 4924-30.
55. Lilja, H., Oldbring, J., Rannevik, G., and Laurell, C. B., *Seminal vesicle-secreted proteins and their reactions during gelation and liquefaction of human semen.* The Journal of clinical investigation, 1987. **80**(2): p. 281-5.
56. Lilja, H., *A kallikrein-like serine protease in prostatic fluid cleaves the predominant seminal vesicle protein.* The Journal of clinical investigation, 1985. **76**(5): p. 1899-903.
57. Bischoff, R., Satheesh Babu, A. K., Vijayalakshmi, M. A., Smith, G. J., and Chadha, K. C., *Thiophilic-interaction chromatography of enzymatically active tissue prostate-specific antigen (T-PSA) and its modulation by zinc ions.* Journal of Chromatography B, 2008. **861**(2): p. 227-235.
58. Cohen, P., Graves, H. C., Peehl, D. M., Kamarei, M., Giudice, L. C., and Rosenfeld, R. G., *Prostate-specific antigen (PSA) is an insulin-like growth factor binding protein-3 protease found in seminal plasma.* The Journal of clinical endocrinology and metabolism, 1992. **75**(4): p. 1046-53.
59. Kumar, V., Hassan, M. I., Singh, A. K., Dey, S., Singh, T. P., and Yadav, S., *Strategy for sensitive and specific detection of molecular forms of PSA based on 2DE and kinetic analysis: A step towards diagnosis of prostate cancer.* Clinica Chimica Acta, 2009. **403**(1): p. 17-22.
60. Zhang, W. M., Leinonen, J., Kalkkinen, N., Dowell, B., and Stenman, U. H., *Purification and characterization of different molecular forms of prostate-specific antigen in human seminal fluid.* Clinical chemistry, 1995. **41**(11): p. 1567-73.
61. Wang, T. J., Hill, T. M., Sokoloff, R. L., Frankenne, F., Rittenhouse, H. G., and Wolfert, R. L., *Dual monoclonal antibody immunoassay for free prostate-specific antigen.* The Prostate, 1996. **28**(1): p. 10-6.
62. Hori, S., Blanchet, J.-S., and McLoughlin, J., *From prostate-specific antigen (PSA) to precursor PSA (proPSA) isoforms: a review of the emerging role of proPSAs in the detection and management of early prostate cancer.* BJU international, 2013. **112**(6): p. 717-28.
63. Christensson, A., Laurell, C. B., and Lilja, H., *Enzymatic activity of prostate-specific antigen and its reactions with extracellular serine proteinase inhibitors.* European journal of biochemistry / FEBS, 1990. **194**(3): p. 755-63.
64. Peter, J., Unverzagt, C., and Hoesel, W., *Analysis of Free Prostate-specific Antigen (PSA) after Chemical Release from the Complex with {alpha}1-Antichymotrypsin (PSA-ACT).* Clin. Chem., 2000. **46**(4): p. 474-482.
65. Woodrum, D., French, C., and Shamel, L. B., *Stability of free prostate-specific antigen in serum samples under a variety of sample collection and sample storage conditions.* Urology, 1996. **48**(6A Suppl): p. 33-9.
66. Mikolajczyk, S. D., Marks, L. S., Partin, A. W., and Rittenhouse, H. G., *Free prostate-specific antigen in serum is becoming more complex.* Urology, 2002. **59**(6): p. 797-802.
67. Jung, K., Brux, B., Lein, M., Rudolph, B., Kristiansen, G., Hauptmann, S., Schnorr, D., Loening, S. A., and Sinha, P., *Molecular Forms of Prostate-specific Antigen in Malignant*

and Benign Prostatic Tissue: Biochemical and Diagnostic Implications. Clin. Chem., 2000. **46**(1): p. 47-54.

68. Mikolajczyk, S. D., Millar, L. S., Wang, T. J., Rittenhouse, H. G., Wolfert, R. L., Marks, L. S., Song, W., Wheeler, T. M., and Slawin, K. M., *"BPSA," a specific molecular form of free prostate-specific antigen, is found predominantly in the transition zone of patients with nodular benign prostatic hyperplasia.* Urology, 2000. **55**(1): p. 41-5.
69. Mikolajczyk, S. D., Grauer, L. S., Millar, L. S., Hill, T. M., Kumar, A., Rittenhouse, H. G., Wolfert, R. L., and Saedi, M. S., *A precursor form of PSA (pPSA) is a component of the free PSA in prostate cancer serum.* Urology, 1997. **50**(5): p. 710-4.
70. Jansen, F. H., Roobol, M., Jenster, G., Schröder, F. H., and Bangma, C. H., *Screening for Prostate Cancer in 2008 II: The Importance of Molecular Subforms of Prostate-Specific Antigen and Tissue Kallikreins.* European Urology, 2009. **55**(3): p. 563-574.
71. Filella, X. and Giménez, N., *Evaluation of [-2] proPSA and Prostate Health Index (phi) for the detection of prostate cancer: a systematic review and meta-analysis.* Clinical chemistry and laboratory medicine : CCLM / FESCC, 2013. **51**(4): p. 729-39.
72. Emami, N. and Diamandis, E. P., *Human kallikrein-related peptidase 14 (KLK14) is a new activator component of the KLK proteolytic cascade. Possible function in seminal plasma and skin.* The Journal of biological chemistry, 2008. **283**(6): p. 3031-41.
73. España, F., Gilabert, J., Estellés, A., Romeu, A., Aznar, J., and Cabo, A., *Functionally active protein C inhibitor/plasminogen activator inhibitor-3 (PCI/PAI-3) is secreted in seminal vesicles, occurs at high concentrations in human seminal plasma and complexes with prostate-specific antigen.* Thrombosis research, 1991. **64**(3): p. 309-20.
74. Cartledge, Thompson, Verril, Clarkson, and Eardley, *The stability of free and bound prostate-specific antigen.* BJU International, 2001. **84**(7): p. 810-814.
75. Reed, A. B., Ankerst, D. P., Leach, R. J., Vipraio, G., Thompson, I. M., and Parekh, D. J., *Total Prostate Specific Antigen Stability Confirmed After Long-Term Storage of Serum at −80C.* The Journal of Urology, 2008. **180**(2): p. 534-538.
76. Arneth, B. M., *Clinical Significance of Measuring Prostate-Specific Antigen.* Laboratory Medicine, 2009. **40**(8): p. 487-491.
77. Kuriyama, M., Wang, M. C., Papsidero, L. D., Killian, C. S., Shimano, T., Valenzuela, L., Nishiura, T., Murphy, G. P., and Chu, T. M., *Quantitation of prostate-specific antigen in serum by a sensitive enzyme immunoassay.* Cancer research, 1980. **40**(12): p. 4658-62.
78. Tang, L., Dong, C., and Ren, J., *Highly sensitive homogenous immunoassay of cancer biomarker using silver nanoparticles enhanced fluorescence correlation spectroscopy.* Talanta, 2010. **81**(4): p. 1560-1567.
79. Uludag, Y. and Tothill, I. E., *Cancer biomarker detection in serum samples using surface plasmon resonance and quartz crystal microbalance sensors with nanoparticle signal amplification.* Analytical chemistry, 2012. **84**(14): p. 5898-904.
80. Oh, S. W., Kim, Y. M., Kim, H. J., Kim, S. J., Cho, J.-S., and Choi, E. Y., *Point-of-care fluorescence immunoassay for prostate specific antigen.* Clinica Chimica Acta, 2009. **406**(1): p. 18-22.
81. Miano, R., Mele, G. O., Germani, S., Bove, P., Sansalone, S., Pugliese, P. F., and Micali, F., *Evaluation of a new, rapid, qualitative, one-step PSA Test for prostate cancer screening: the PSA RapidScreen test.* Prostate cancer and prostatic diseases, 2005. **8**(3): p. 219-23.
82. R A Ferguson, H. Y., *Ultrasensitive detection of prostate-specific antigen by a time-resolved immunofluorometric assay and the Immulite immunochemiluminescent third-generation assay: potential applications in prostate and breast cancers.* Clinical chemistry, 1996. **42**(5): p. 675-84.

83. Poon, C.-Y., Chan, H.-M., and Li, H.-W., *Direct detection of prostate specific antigen by darkfield microscopy using single immunotargeting silver nanoparticle.* Sensors and Actuators B: Chemical, 2014. **190**: p. 737-744.
84. Ito, K., Nishimura, W., Maeda, M., Gomi, K., Inouye, S., and Arakawa, H., *Highly sensitive and rapid tandem bioluminescent immunoassay using aequorin labeled Fab fragment and biotinylated firefly luciferase.* Analytica Chimica Acta, 2007. **588**(2): p. 245-251.
85. Peter, J., Unverzagt, C., Lenz, H., and Hoesel, W., *Purification of Prostate-Specific Antigen from Human Serum by Indirect Immunosorption and Elution with a Hapten.* Analytical Biochemistry, 1999. **273**(1): p. 98-104.
86. Fortin, T., Salvador, A., Charrier, J. P., Lenz, C., Lacoux, X., Morla, A., Choquet-Kastylevsky, G., and Lemoine, J., *Clinical quantitation of prostate-specific antigen biomarker in the low nanogram/milliliter range by conventional bore liquid chromatography-tandem mass spectrometry (multiple reaction monitoring) coupling and correlation with ELISA tests.* Molecular & cellular proteomics : MCP, 2009. **8**(5): p. 1006-15.
87. Kawinski, E., Levine, E., and Chadha, K., *Thiophilic interaction chromatography facilitates detection of various molecular complexes of prostate-specific antigen in biological fluids.* The Prostate, 2002. **50**(3): p. 145-53.
88. Matsumoto, K., Konishi, N., Hiasa, Y., Kimura, E., Takahashi, Y., Shinohara, K., and Samori, T., *A highly sensitive enzyme-linked immunoassay for serum free prostate specific antigen (f-PSA).* Clinica Chimica Acta, 1999. **281**(1): p. 57-69.
89. Beijerinck, M. W., *1896*, 1896. p. 698-699.
90. Albertsson, P. A., *Particle fractionation in liquid two-phase systems; the composition of some phase systems and the behaviour of some model particles in them; application to the isolation of cell walls from microorganisms.* Biochimica et biophysica acta, 1958. **27**(2): p. 378-95.
91. Freire, M. G., Cláudio, A. F. M., Araújo, J. M. M., Coutinho, J. A. P., Marrucho, I. M., Canongia Lopes, J. N., and Rebelo, L. P. N., *Aqueous biphasic systems: a boost brought about by using ionic liquids.* Chemical Society reviews, 2012. **41**(14): p. 4966-95.
92. Raja, S., Murty, R. V., Thivaharan, V., Rajasekar, V., and Ramesh, V., *Aqueous Two Phase Systems for the Recovery of Biomolecules –A Review.* Scientific & Academic Publishing Co, 2011. **1**(1): p. 7-16.
93. Ventura, S. P. M., de Barros, R. L. F., de Pinho Barbosa, J. M., Soares, C. M. F., Lima, Á. S., and Coutinho, J. A. P., *Production and purification of an extracellular lipolytic enzyme using ionic liquid-based aqueous two-phase systems.* Green Chemistry, 2012. **14**(3): p. 734-734.
94. Pereira, J. F. B., Vicente, F., Santos-Ebinuma, V. C., Araújo, J. M., Pessoa, A., Freire, M. G., and Coutinho, J. A. P., *Extraction of tetracycline from fermentation broth using aqueous two-phase systems composed of polyethylene glycol and cholinium-based salts.* Process Biochemistry, 2013. **48**(4): p. 716-722.
95. Walter, H. and Johansson, G., *Aqueous Two-phase Systems*. Aqueous two-phase systems1994: Academic Press.
96. Zhi, W., Song, J., Bi, J., and Ouyang, F., *Partial purification of alpha-amylase from culture supernatant of Bacillus subtilis in aqueous two-phase systems.* Bioprocess and biosystems engineering, 2004. **27**(1): p. 3-7.
97. Peters, T. J., *Partition of cell particles and macromolecules: Separation and purification of biomolecules, cell organelles, membranes and cells in aqueous polymer two phase systems and their use in biochemical analysis and biotechnology. P-A. Albertsson. Third Edition.* Cell Biochemistry and Function, 1987. **5**(3): p. 233-234.
98. Aguilar, O., Albiter, V., Serrano-Carreón, L., and Rito-Palomares, M., *Direct comparison between ion-exchange chromatography and aqueous two-phase processes for the partial*

purification of penicillin acylase produced by E. coli. Journal of chromatography. B, Analytical technologies in the biomedical and life sciences, 2006. **835**(1-2): p. 77-83.

99. Naganagouda, K. and Mulimani, V. H., *Aqueous two-phase extraction (ATPE): An attractive and economically viable technology for downstream processing of Aspergillus oryzae α-galactosidase.* Process Biochemistry, 2008. **43**(11): p. 1293-1299.
100. Nitsawang, S., Hatti-Kaul, R., and Kanasawud, P., *Purification of papain from Carica papaya latex: Aqueous two-phase extraction versus two-step salt precipitation.* Enzyme and Microbial Technology, 2006. **39**(5): p. 1103-1107.
101. Gutowski, K. E., Broker, G. A., Willauer, H. D., Huddleston, J. G., Swatloski, R. P., Holbrey, J. D., and Rogers, R. D., *Controlling the aqueous miscibility of ionic liquids: aqueous biphasic systems of water-miscible ionic liquids and water-structuring salts for recycle, metathesis, and separations.* Journal of the American Chemical Society, 2003. **125**(22): p. 6632-3.
102. Pereira, J. F. B., Rebelo, L. P. N., Rogers, R. D., Coutinho, J. A. P., and Freire, M. G., *Combining ionic liquids and polyethylene glycols to boost the hydrophobic-hydrophilic range of aqueous biphasic systems.* Physical chemistry chemical physics : PCCP, 2013. **15**(45): p. 19580-3.
103. Cláudio, A. F. M., Freire, M. G., Freire, C. S. R., Silvestre, A. J. D., and Coutinho, J. A. P., *Extraction of vanillin using ionic-liquid-based aqueous two-phase systems.* 2010. **75**(1): p. 39-47.
104. Ventura, S. P. M., Gonçalves, A. M. M., Sintra, T., Pereira, J. L., Gonçalves, F., and Coutinho, J. A. P., *Designing ionic liquids: the chemical structure role in the toxicity.* Ecotoxicology (London, England), 2013. **22**(1): p. 1-12.
105. Walden, P., *Molecular weights and electrical conductivity of several fused salts*, 1914. p. 405-422.
106. Charles, G., *Cellulose solution.* 1934.
107. Wier, T. P., 1948, US Patent 4446349.
108. Hurley, F. H., *Electrodeposition of Aluminium.* 1948.
109. Zafarani-Moattar, M. T., Hamzehzadeh, S., and Nasiri, S., *A new aqueous biphasic system containing polypropylene glycol and a water-miscible ionic liquid.* Biotechnology progress, 2012. **28**(1): p. 146-156.
110. He, C., Li, S., Liu, H., Li, K., and Liu, F., *Extraction of testosterone and epitestosterone in human urine using aqueous two-phase systems of ionic liquid and salt.* Journal of Chromatography A, 2005. **1082**(2): p. 143-149.
111. Du, Z., Yu, Y.-L., and Wang, J.-H., *Extraction of proteins from biological fluids by use of an ionic liquid/aqueous two-phase system.* Chemistry (Weinheim an der Bergstrasse, Germany), 2007. **13**(7): p. 2130-7.
112. Dreyer, S., Salim, P., and Kragl, U., *Driving forces of protein partitioning in an ionic liquid-based aqueous two-phase system.* Biochemical Engineering Journal, 2009. **46**(2): p. 176-185.
113. Earle, M. J., Esperança, J. M. S. S., Gilea, M. A., Lopes, J. N. C., Rebelo, L. P. N., Magee, J. W., Seddon, K. R., and Widegren, J. A., *The distillation and volatility of ionic liquids.* Nature, 2006. **439**(7078): p. 831-4.
114. Flecha, F. L. G. and Valeria, L., *Determination of the molecular size of BSA by fluorescence anisotropy.* Biochemistry and Molecular Biology Education, 2003. **31**(5): p. 319-322.
115. Li, Z., Liu, X., Pei, Y., Wang, J., and He, M., *Design of environmentally friendly ionic liquid aqueous two-phase systems for the efficient and high activity extraction of proteins.* Green Chemistry, 2012. **14**(10): p. 2941-2941.
116. Taha, M., e Silva, F. A., Quental, M. V., Ventura, S. P. M., Freire, M. G., and Coutinho, J. A. P., *Good's buffers as a basis for developing self-buffering and biocompatible ionic liquids for biological research.* Green Chemistry, 2014.

117. Desai, R. K., Streefland, M., Wijffels, R. H., and H. M. Eppink, M., *Extraction and stability of selected proteins in ionic liquid based aqueous two phase systems.* Green Chemistry, 2014.
118. Bing, D. H. and Research, C. f. B., *The chemistry and physiology of the human plasma proteins*1979: Pergamon Press.
119. Quiming, N. S., Vergel, R. B., Nicolas, M. G., and Villanueva, J. A., *Interaction of Bovine Serum Albumin and Metallothionein.* Journal of health science, 2005. **51**(1): p. 8-15.
120. Chang, Y.-K., Chou, S.-Y., Liu, J.-L., and Tasi, J.-C., *Characterization of BSA adsorption on mixed mode adsorbent: I. Equilibrium study in a well-agitated contactor.* Biochemical Engineering Journal, 2007. **35**(1): p. 56-65.
121. Ge, S., Kojio, K., Takahara, A., and Kajiyama, T., *Bovine serum albumin adsorption onto immobilized organotrichlorosilane surface: influence of the phase separation on protein adsorption patterns.* J Biomater Sci Polym Ed, 1998. **9**(2): p. 131-50.
122. Majorek, K. A., Porebski, P.J., Chruszcz, M., Almo, S.C., Minor, W., *Crystal structure of Bovine Serum Albumin*: Structural Genomics Research Consortium
123. Patel, R., Kumari, M., and Khan, A. B., *Recent Advances in the Applications of Ionic Liquids in Protein Stability and Activity: A Review.* Appl Biochem Biotechnol, 2014. **6**: p. 6.
124. Zeng, Q., Wang, Y., Li, N., Huang, X., Ding, X., Lin, X., Huang, S., and Liu, X., *Extraction of proteins with ionic liquid aqueous two-phase system based on guanidine ionic liquid.* Talanta, 2013. **116**(0): p. 409-416.
125. Domínguez-Pérez, M., Tomé, L. I. N., Freire, M. G., Marrucho, I. M., Cabeza, O., and Coutinho, J. A. P., *(Extraction of biomolecules using) aqueous biphasic systems formed by ionic liquids and aminoacids.* Separation and Purification Technology, 2010. **72**(1): p. 85-91.
126. Jiang, X., Ye, W., Song, X., Ma, W., Lao, X., and Shen, R., *Novel ionic liquid with both Lewis and Bronsted acid sites for Michael addition.* Int J Mol Sci, 2011. **12**(11): p. 7438-44.
127. Good, N. E., Winget, G. D., Winter, W., Connolly, T. N., Izawa, S., and Singh, R. M. M., *Hydrogen Ion Buffers for Biological Research*.* Biochemistry, 1966. **5**(2): p. 467-477.
128. Freire, M. G., Neves, C. M. S. S., Canongia Lopes, J. N., Marrucho, I. M., Coutinho, J. A. P., and Rebelo, L. P. N., *Impact of Self-Aggregation on the Formation of Ionic-Liquid-Based Aqueous Biphasic Systems.* J. Phys. Chem. B 2012. **116**(26): p. 7660-7668.
129. Mourão, T., Cláudio, A. F. M., Boal-Palheiros, I., Freire, M. G., and Coutinho, J. A. P., *Evaluation of the impact of phosphate salts on the formation of ionic-liquid-based aqueous biphasic systems.* J. Chem. Thermodyn. , 2012. **54**(0): p. 398-405.
130. Merchuk, J. C., Andrews, B. A., and Asenjo, J. A., *Aqueous two-phase systems for protein separation. Studies on phase inversion.* J Chromatogr B Biomed Sci Appl, 1998. **711**(1-2): p. 285-93.
131. Passos, H., Ferreira, A. R., Cláudio, A. F. M., Coutinho, J. A. P., and Freire, M. G., *Characterization of aqueous biphasic systems composed of ionic liquids and a citrate-based biodegradable salt.* Biochemical Engineering Journal, 2012. **67**(0): p. 68-76.
132. Pegram, L. M. and Record, M. T., *Hofmeister Salt Effects on Surface Tension Arise from Partitioning of Anions and Cations between Bulk Water and the Air−Water Interface.* The Journal of Physical Chemistry B, 2007. **111**(19): p. 5411-5417.
133. Ventura, S. P. M., Neves, C. M. S. S., Freire, M. G., Marrucho, I. M., Oliveira, J., and Coutinho, J. A. P., *Evaluation of Anion Influence on the Formation and Extraction Capacity of Ionic-Liquid-Based Aqueous Biphasic Systems.* The Journal of Physical Chemistry B, 2009. **113**(27): p. 9304-9310.
134. Mourão, T., Cláudio, A. F. M., Boal-Palheiros, I., Freire, M. G., and Coutinho, J. A. P., *Evaluation of the impact of phosphate salts on the formation of ionic-liquid-based aqueous biphasic systems.* The Journal of Chemical Thermodynamics, 2012. **54**(0): p. 398-405.

135. Louros, C. L. S., Cláudio, A. F. M., Neves, C. M. S. S., Freire, M. G., Marrucho, I. M., Pauly, J., and Coutinho, J. A. P., *Extraction of Biomolecules Using Phosphonium-Based Ionic Liquids + K3PO4 Aqueous Biphasic Systems.* International journal of molecular sciences, 2010. **11**(4): p. 1777-1791.
136. Marques, C. F., Mourao, T., Neves, C. M., Lima, A. S., Boal-Palheiros, I., Coutinho, J. A., and Freire, M. G., *Aqueous biphasic systems composed of ionic liquids and sodium carbonate as enhanced routes for the extraction of tetracycline.* Biotechnol Prog, 2013. **29**(3): p. 645-54.
137. Neves, C. M. S. S., Ventura, S. P. M., Freire, M. G., Marrucho, I. M., and Coutinho, J. A. P., *Evaluation of Cation Influence on the Formation and Extraction Capability of Ionic-Liquid-Based Aqueous Biphasic Systems.* The Journal of Physical Chemistry B, 2009. **113**(15): p. 5194-5199.
138. Bridges, N. J., Gutowski, K. E., and Rogers, R. D., *Investigation of aqueous biphasic systems formed from solutions of chaotropic salts with kosmotropic salts (salt-salt ABS).* Green Chemistry, 2007. **9**(2): p. 177-183.
139. Franco, T. T., Andrews, A. T., and Asenjo, J. A., *Use of chemically modified proteins to study the effect of a single protein property on partitioning in aqueous two-phase systems: Effect of surface hydrophobicity.* Biotechnology and Bioengineering, 1996. **49**(3): p. 300-308.
140. Lin, X., Wang, Y. Z., Zeng, Q., Ding, X. Q., and Chen, J., *Extraction and separation of proteins by ionic liquid aqueous two-phase system.* Analyst, 2013. **138**(21): p. 6445-6453.
141. Regupathi, I. and Monteiro, S. L., *1-Hexyl-3-Methylimidazolium Chloride-Potassium Carbonate Aqueous Two Phase System: Equilibrium Characteristics and BSA Partitioning Behavior.* Journal of Dispersion Science and Technology, 2013. **35**(3): p. 418-427.
142. Deive, F. J., Rodriguez, A., Pereiro, A. B., Araujo, J. M. M., Longo, M. A., Coelho, M. A. Z., Lopes, J. N. C., Esperanca, J. M. S. S., Rebelo, L. P. N., and Marrucho, I. M., *Ionic liquid-based aqueous biphasic system for lipase extraction.* Green Chemistry, 2011. **13**(2): p. 390-396.
143. Cláudio, A. F. M., Ferreira, A. M., Freire, C. S. R., Silvestre, A. J. D., Freire, M. G., and Coutinho, J. A. P., *Optimization of the gallic acid extraction using ionic-liquid-based aqueous two-phase systems.* Separation and Purification Technology, 2012. **97**(0): p. 142-149.
144. Docherty, K. M. and Kulpa, J. C. F., *Toxicity and antimicrobial activity of imidazolium and pyridinium ionic liquids.* Green Chemistry, 2005. **7**(4): p. 185-185.
145. Khan, I., Kurnia, K. A., Sintra, T. E., Saraiva, J. A., Pinho, S. P., and Coutinho, J. A. P., *Assessing the activity coefficients of water in cholinium-based ionic liquids: Experimental measurements and COSMO-RS modeling.* Fluid Phase Equilibria, 2014. **361**: p. 16-22.
146. Passos, H., Sousa, A. C. A., Pastorinho, M. R., Nogueira, A. J. A., Rebelo, L. P. N., Coutinho, J. A. P., and Freire, M. G., *Ionic-liquid-based aqueous biphasic systems for improved detection of bisphenol A in human fluids.* Analytical Methods, 2012. **4**(9): p. 2664-2664.
147. P-A, A., *Partition of cell particles and macromolecules, 3rd ed. New York: Wiley; 1986.* Acta Biotechnologica, 1986. **7**(2): p. 146-146.
148. Liu, Y., Wu, Z., Zhang, Y., and Yuan, H., *Partitioning of biomolecules in aqueous two-phase systems of polyethylene glycol and nonionic surfactant.* Biochemical Engineering Journal, 2012. **69**: p. 93-99.
149. Freire, M. G., Pereira, J. F. B., Francisco, M., Rodríguez, H., Rebelo, L. P. N., Rogers, R. D., and Coutinho, J. A. P., *Insight into the interactions that control the phase behaviour of new aqueous biphasic systems composed of polyethylene glycol polymers and ionic liquids.* Chemistry (Weinheim an der Bergstrasse, Germany), 2012. **18**(6): p. 1831-9.

150. Pereira, J. F., Kurnia, K. A., Cojocaru, O. A., Gurau, G., Rebelo, L. P., Rogers, R. D., Freire, M. G., and Coutinho, J. A., *Molecular interactions in aqueous biphasic systems composed of polyethylene glycol and crystalline vs. liquid cholinium-based salts.* Phys Chem Chem Phys, 2014. **16**(12): p. 5723-31.
151. Pernak, J., Syguda, A., Mirska, I., Pernak, A., Nawrot, J., Pradzynska, A., Griffin, S. T., and Rogers, R. D., *Choline-derivative-based ionic liquids.* Chemistry, 2007. **13**(24): p. 6817-27.
152. Muhammad, N., Hossain, M. I., Man, Z., El-Harbawi, M., Bustam, M. A., Noaman, Y. A., Mohamed Alitheen, N. B., Ng, M. K., Hefter, G., and Yin, C.-Y., *Synthesis and Physical Properties of Choline Carboxylate Ionic Liquids.* Journal of Chemical & Engineering Data, 2012. **57**(8): p. 2191-2196.
153. Pereira, J. F. B., Kurnia, K. A., Cojocaru, O. A., Gurau, G., Rebelo, L. P. N., Rogers, R. D., Freire, M. G., and Coutinho, J. A. P., *Molecular interactions in aqueous biphasic systems composed of polyethylene glycol and crystalline vs. liquid cholinium-based salts.* Physical Chemistry Chemical Physics, 2014. **16**(12): p. 5723-5731.
154. Glusker, J. P., *Citrate conformation and chelation: enzymic implications.* Accounts of Chemical Research, 1980. **13**(10): p. 345-352.
155. Rodriguez, H., Francisco, M., Rahman, M., Sun, N., and Rogers, R. D., *Biphasic liquid mixtures of ionic liquids and polyethylene glycols.* Phys Chem Chem Phys, 2009. **11**(46): p. 10916-22.
156. Tome, L. I. N., Pereira, J. F. B., Rogers, R. D., Freire, M. G., Gomes, J. R. B., and Coutinho, J. A. P., *"Washing-out" ionic liquids from polyethylene glycol to form aqueous biphasic systems.* Physical Chemistry Chemical Physics, 2014. **16**(6): p. 2271-2274.
157. Rito-Palomares, M., Dale, C., and Lyddiatt, A., *Generic application of an aqueous two-phase process for protein recovery from animal blood.* Process Biochemistry, 2000. **35**(7): p. 665-673.
158. Salabat, A. R., Abnosi, M. H., and Motahari, A., *Application of aqueous mixtures of polypropylene glycol or polyethylene glycol with salts in proteomic analysis.* Journal of the Iranian Chemical Society, 2010. **7**(1): p. 142-149.
159. Arafat, M. G., Yang, H., Cui, M., and Li, C., *Aqueous Two-Phase Extraction Advances for Bioseparation.* Journal of Bioprocessing & Biotechniques, 2013.
160. Rodrigues, J. V., Prosinecki, V., Marrucho, I., Rebelo, L. P. N., and Gomes, C. M., *Protein stability in an ionic liquid milieu: on the use of differential scanning fluorimetry.* Physical Chemistry Chemical Physics, 2011. **13**(30): p. 13614-13616.
161. Xue, L., Zhao, Y., Yu, L., Sun, Y., Yan, K., Li, Y., Huang, X., and Qu, Y., *Choline acetate enhanced the catalytic performance of Candida rogusa lipase in AOT reverse micelles.* Colloids and Surfaces B: Biointerfaces, 2013. **105**(0): p. 81-86.
162. Kumar, A. and Venkatesu, P., *Does the stability of proteins in ionic liquids obey the Hofmeister series?* International Journal of Biological Macromolecules, 2014. **63**(0): p. 244-253.
163. Healy, D. A., Hayes, C. J., Leonard, P., McKenna, L., and O'Kennedy, R., *Biosensor developments: application to prostate-specific antigen detection.* Trends in Biotechnology, 2007. **25**(3): p. 125-131.
164. Markham, D. A., Waechter, J. M., Wimber, M., Rao, N., Connolly, P., Chuang, J. C., Hentges, S., Shiotsuka, R. N., Dimond, S., and Chappelle, A. H., *Development of a method for the determination of bisphenol A at trace concentrations in human blood and urine and elucidation of factors influencing method accuracy and sensitivity.* Journal of analytical toxicology. **34**(6): p. 293-303.

8. List of publications

Co-author in:

Taha, M., e Silva, F. A., Quental, M. V., Ventura, S. P. M., Freire, M. G., and Coutinho, J. A. P., *Good's buffers as a basis for developing self-buffering and biocompatible ionic liquids for biological research.* Green Chemistry, 2014 **16**(6): p. 3149-3159.

Taha, M., e Silva, F. A., Quental, M. V., Ventura, S. P. M., Freire, M. G., and Coutinho, J. A. P., *Efficient aqueous biphasic systems designed by new Good's buffer ionic Liquids for protein extraction*. (in preparation).

Quental, V. Maria, Caban, Magda, Pereira, Matheus M., Stepnowski, Piotr, Coutinho, J. A. P and M., Freire, *Extraction of bovine serum albumin (BSA) by aqueous two-phase systems composed of cholinium-based ionic liquids and polymers.* (in preparation).

Quental, V. Maria, Passos, Helena, Kurnia, Kiki A., Coutinho, J. A. P and M., Freire, *Aqueous biphasic systems formed by ionic liquids and organic salts: influence of pH.* (in preparation).

Quental, V. Maria, Coutinho, J. A. P and M., Freire, *Selective separation of aminoacids using aqueous biphasic systems constituted by ionic liquid*s. (in preparation).

Appendix A
HPLC Calibration Curve

A.1. HPLC Calibration Curve for BSA

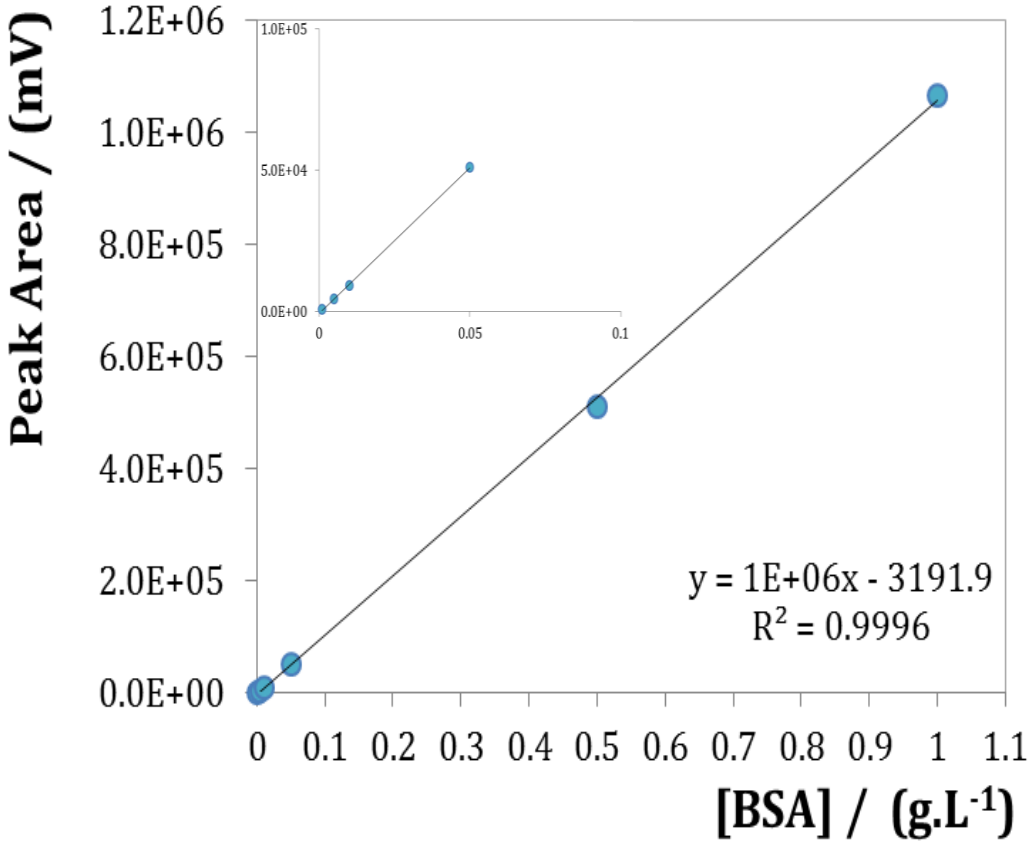

Figure A 1. Calibration curve for BSA in PBS solution by HPLC at λ = 278 nm.

Appendix B
Experimental binodal data

B.1. Experimental Binodal Data for Systems Composed of IL + salt + H_2O.

Table B.1.1. Experimental weight fraction data for the binodal curve of the systems composed of $[P_{4444}][GB]$ (1) + $K_3C_6H_5O_7$ (2) at (25 ± 1) °C

$[P_{4444}][TES]$		$[P_{4444}][MES]$				$[P_{4444}][HEPES]$	
Mw = 453.66 g.mol^{-1}		Mw = 453.66 g.mol^{-1}				Mw = 496.72 g.mol^{-1}	
$100w_1$	$100\ w_2$	$100w_1$	$100\ w_2$	$100\ w_1$	$100\ w_2$	$100\ w_1$	$100\ w_2$
61.8678	4.36723	62.3717	1.9534	14.4682	21.4879	60.6808	1.7776
47.0190	8.97101	55.0746	3.0687	14.0210	21.8603	48.7062	4.7776
25.5215	19.1506	46.1457	5.2053	13.5973	22.2147	44.9539	6.0756
23.7507	20.2187	38.9888	7.5466	13.3496	22.436	39.0405	8.3030
22.0028	21.4418	35.5324	9.4461	13.1172	22.5457	25.2803	15.2525
20.3078	22.4654	32.1736	10.4337	12.8557	22.7482	22.1920	18.3454
19.2364	23.1661	29.2351	12.177	12.6174	22.8941	19.0199	20.8474
18.3514	23.7213	25.0058	14.2196	12.3314	23.0981	18.7982	21.059
17.3671	24.4091	24.3730	14.9448	12.1281	23.2549	18.2316	21.3805
16.5209	24.9562	23.4465	15.5913	11.9372	23.4139	17.9539	21.6286
15.4982	25.6797	22.7324	15.9857	11.6437	23.7911	17.6748	21.8651
14.5372	26.3873	22.1010	16.2701	11.4069	23.8702	17.1974	22.1548
13.9789	26.7876	21.0463	17.2067	11.1862	24.1448	16.9076	22.2605
12.6568	28.2183	20.1913	17.4856	10.8123	24.4067	16.5236	22.5372
11.9845	28.7496	19.8753	17.7077	10.6356	24.5665		
11.4811	29.1502	19.296	18.0770	10.2575	25.3191		
11.0247	29.4545	18.8178	18.3213	10.0548	25.3267		
9.7313	30.4098	18.4771	18.7802	9.90130	25.4396		
9.3105	30.8228	17.9601	19.0542	9.76240	25.5814		
9.0700	30.8791	17.5589	19.3400	9.4916	25.9226		
8.7344	31.1791	17.1589	19.5134				
7.9971	31.8818	16.7271	19.9010				
7.6370	32.2070	16.3047	20.0070				
7.1529	32.6797	15.9311	20.2144				
6.7983	33.0729	15.7730	20.5767				
6.2622	33.6999	15.0549	21.1613				
5.8512	34.1718	14.7790	21.3413				
5.2969	34.7178	14.4682	21.4879				
		14.0210	21.8603				
		13.5973	22.2147				
		13.3496	22.436				
		13.1172	22.5457				
		12.8557	22.7482				
		12.6174	22.8941				

Table B.1.2 Experimental weight fraction data for the binodal curve of the systems composed of $[P_{4444}][GB]$ (1) + $K_3C_6H_5O_7$ (2) at (25 ± 1) °C.

$[P_{4444}][CHES]$ Mw = 465.71 g.mol^{-1}				$[P_{4444}][Tricine]$ Mw = 437.59 g.mol^{-1}	
$100w_1$	$100w_2$	$100w_1$	$100w_2$	$100w_1$	$100w_2$
56.0295	2.1514	16.4509	13.8854	49.0588	8.6992
49.8386	2.9995	15.9852	14.2903	43.9675	10.2137
44.5654	4.0045	15.5886	14.1837	47.6961	9.1530
32.6368	7.7831	15.3380	14.3336	32.0490	15.8351
31.6348	8.0459	15.0681	14.4827	27.3453	19.3309
27.8080	9.1536	14.6794	14.6118	19.5583	25.3643
26.9733	9.6042	14.3922	14.7490	16.6714	27.8062
26.3242	9.7600	14.0809	14.8845	15.3375	28.9483
25.9007	9.9304	13.7886	15.0419	13.3246	30.5587
25.1314	10.3976	13.4654	15.1744	11.2654	32.4796
24.6113	10.4534	13.1300	15.3955	10.3802	33.1815
23.8957	10.9677	12.8337	15.4474	9.0383	34.2280
23.1845	11.1648	12.5353	15.6245	8.4519	34.7186
22.3504	11.4097	12.2196	15.7977	7.7450	35.2786
21.7190	11.6700	11.9575	15.9053	7.3003	35.5413
21.0972	11.9757	11.8131	16.0626	6.9272	35.8852
20.6540	12.1558	11.5101	16.2111	6.5390	36.1197
20.2407	12.2667			6.2128	36.4294
19.6123	12.4833			5.8104	36.3621
19.4026	12.6567			5.5379	36.6229
19.1298	12.7742			5.3077	36.7289
18.8311	13.0228			5.0206	36.8553
18.4910	13.0977				
17.9544	13.4087				
17.4981	13.5529				
17.0529	13.6584				
16.6000	13.8609				

Table B.1.2. Experimental data mass fraction for the binodal curve of the system composed of $[N_{4444}][GB]$ (1) + $K_3C_6H_5O_7$ (2) at (25 ± 1) °C.

$[N_{4444}][TES]$		$[N_{4444}][MES]$		$[N_{4444}][HEPES]$			
Mw = 470.7 g.mol^{-1}		Mw = 436.69 g.mol^{-1}		Mw = 479.75 g.mol^{-1}			
100 w_1	100 w_2	100 w_1	100 w_2	100 w_1	100 w_2	100 w_1	100 w_2
60.6248	3.5221	61.4054	2.8040	49.4787	4.8618	29.2137	15.5311
56.1248	4.1141	56.7183	3.5916	46.2898	6.3893	28.4070	15.9580
54.1559	4.8890	52.4237	4.0263	43.764	7.6769	26.2531	17.6910
47.7225	7.1459	49.6251	5.0111	42.0049	8.2477	24.9637	18.4296
44.9413	8.4650	47.3829	5.8218	39.2991	9.6115	24.1665	18.9653
40.1389	11.2892	44.3436	6.5954	37.1717	10.6517		
35.2034	14.3904	41.6020	7.2906	34.7759	12.0841		
29.8266	18.1741	40.5412	7.8690	33.3929	12.9164		
27.2017	20.0343	37.7732	8.3407	31.3675	14.1100		
23.2966	23.0217	34.7701	9.9901	29.2137	15.5311		
21.9686	24.0255	33.0372	10.9006	28.4070	15.9580		
20.3775	26.0993	29.8618	12.7984	26.2531	17.6910		
18.0592	27.8101	28.5029	13.7175	24.9637	18.4296		
60.6248	3.5221	27.1237	14.5163	24.1665	18.9653		
		25.6895	15.4944	22.5916	20.2709		
		24.6592	16.1094	20.9033	21.4207		
		23.4150	17.2196	19.6424	22.1288		
		22.4664	17.8083	18.4485	23.1335		
		21.7983	18.5649	17.0663	24.1471		
		21.0613	19.1106	16.3445	24.7717		
				15.2264	25.7542		
				14.4333	26.1961		
				14.2421	26.2555		
				13.0309	27.3161		
				12.2152	28.0560		
				11.5620	28.5904		
				10.9958	29.0709		
				10.5826	29.5005		
				10.0336	29.8162		
				9.7698	30.1147		
				9.3672	30.6088		
				31.3675	14.1100		

Table B.1.3. Experimental data mass fraction for the binodal curve of the system composed of $[N_{4444}][GB]$ (1) + $K_3C_6H_5O_7$ (2) at (25 ± 1) °C.

$[N_{4444}][CHES]$ Mw = 448.74 g.mol^{-1}				$[N_{4444}][Tricine]$ Mw = 420.62 g.mol^{-1}			
100 w_1	100 w_1	100 w_1	100 w_1	100 w_1	100 w_2	100 w_1	100 w_2
57.5741	4.3595	8.2864	21.3362	48.2463	8.5815	17.0513	29.1451
49.7951	5.4885	8.1364	21.3748	44.6489	10.7724	16.3110	29.7432
45.0789	6.4316	8.0764	21.5365	43.3425	11.5793	15.7645	30.1447
42.4844	7.3569	7.6322	21.7491	42.1253	12.2497	15.2459	30.5384
40.4427	8.2403	7.4752	21.9145	41.0591	12.7489	14.6169	31.0718
37.8860	8.7157	7.1446	22.7635	39.8372	13.5505	14.1015	31.4787
35.7309	9.3461	6.9200	23.0455	38.1933	14.6085	13.5202	31.9596
34.6828	9.9063	6.7012	23.1616	36.2742	15.7678	12.8619	32.5152
32.7218	10.8505	6.3725	23.6590	34.6087	16.7694	12.2324	33.0209
29.9862	11.6212	6.0739	23.6358	33.1372	17.7943	12.0106	33.1806
25.5988	13.5087	5.8788	24.0770	32.1573	18.1785	11.6513	33.4869
24.1441	13.9681			31.7469	18.3389	11.4962	33.6289
23.1690	14.3891			31.0114	18.8360	11.1564	33.8981
22.0879	15.0957			29.9834	19.6339	10.4995	34.4976
21.3568	15.5439			28.1113	20.9998	9.9389	35.0097
20.3457	15.5442			26.4768	22.2000	9.4991	35.3803
19.4087	16.1333			25.9227	22.5364	9.1337	35.7540
18.0468	17.0493			25.2101	23.0306	8.6148	36.2365
17.3541	16.8495			24.4242	23.6589	8.0910	36.6959
16.0194	17.8183			23.4762	24.3404	7.7570	36.9904
15.0623	18.0782			22.9368	24.7026	7.3539	37.3906
14.3852	18.3897			22.3403	25.1777	7.1370	37.6344
13.9453	18.4047			21.8922	25.4478	6.7822	37.9600
13.4255	18.8291			21.3077	25.9037	6.4953	38.2110
12.7435	19.2393			20.7949	26.2962		
12.0429	19.6324			19.8940	26.9181		
11.5476	19.8836			18.9674	27.6444		
10.9424	20.0558			18.5053	28.0635		
10.2330	20.3634			18.3376	28.1522		
9.7194	21.0633			17.7885	28.5883		

B.2. Experimental Binodal Data for the IL-based ABS Systems Composed of IL + PPG 400 + H_2O.

Table B.2.1. Experimental data mass fraction for the binodal curve of the system composed of IL (1) + PPG400 (2) at (25 ± 1) °C.

[Ch][DHCit]		[Ch][DHPhs]		[Ch]Cl		[Ch][Ac]	
Mw = 295.29 g.mol^{-1}		Mw = 407.48 g.mol^{-1}		Mw = 139.62 g.mol^{-1}		Mw = 163.21 g.mol^{-1}	
100 w_1	100 w_2	100 w_1	100 w_2	100 w_1	100 w_2	100 w_1	100 w_2
70.1536	2.3417	55.4325	2.7881	48.7073	6.2832	59.387	4.6520
65.9819	3.4383	49.3628	3.2744	43.0658	6.9546	53.524	5.7410
61.6203	4.7738	45.4998	3.7429	39.1209	7.4608	49.188	6.7000
56.6761	6.3941	36.5270	4.7463	36.279	8.0541	37.388	9.4050
52.3928	7.8162	33.5006	4.9368	33.5576	8.4440	35.046	9.6350
50.2383	8.4651	32.4385	5.2692	31.3208	8.9212	33.690	10.2290
39.6114	12.1179	31.1122	5.4413	29.6235	9.2445	31.875	10.5070
38.4475	12.6739	29.4377	5.9556	26.2245	10.6186	27.986	12.1730
29.5967	15.8001	27.9268	6.3037	25.4599	11.2173	26.771	12.9600
26.1514	17.5801	25.8670	6.7016	24.2382	11.5553	25.409	13.5720
25.8432	17.7910	23.5555	7.2560	23.571	12.0105	24.351	14.1490
25.1537	17.9041	21.8186	7.6481	20.4964	14.0182	23.482	14.9080
24.8347	18.0937	20.3480	8.2812	19.9674	14.3353	22.483	15.2510
22.7529	19.5688	19.2992	8.5568	19.3311	14.5712	21.587	16.0310
21.4427	20.2485	18.4855	9.0082	18.8858	14.8972	20.564	16.3290
20.8654	20.3651	17.7096	9.2539	18.4645	15.2441	19.758	16.9150
20.5197	20.7738	16.6752	9.9229	17.9548	15.4338	18.977	17.5720
20.2059	21.0008	10.3907	13.9265	17.2173	16.0146	18.259	18.0890
19.3468	21.5827	9.8248	14.3877	16.7918	16.6792	17.354	19.2490
18.5068	22.1900	8.8675	14.6940	16.4596	16.8786	16.929	20.0760
18.3322	22.2421	8.6881	15.3362	15.9752	17.5472	16.316	20.672
15.0601	25.6635	8.2300	16.0529	15.4786	17.5268	15.3800	21.2250
12.5891	28.5293	7.8176	16.5972	6.9155	39.2329	14.7210	21.9620
11.2100	30.5431	7.1779	17.4248	5.7351	44.6712	13.9560	22.7510
9.72180	33.14760	6.9475	18.5105			13.3020	23.1640
						12.8000	23.8880
						12.1860	24.6520
						11.5650	25.3420
						10.9020	26.1680

Table B.2.2. Experimental data mass fraction for the binodal curve of the system composed of IL (1) + PPG400 (2) at (25 ± 1**) C** °

[Ch][Bit] *Mw* = 253.247 g.mol^{-1}		[Ch][Prop] *Mw* = 177.24 g.mol^{-1}			
100 w_1	100 w_2	100 w_1	100 w_2	100 w_1	100 w_2
54.6562	5.7383	6.5518	35.6425	73.8795	2.4499
50.2356	6.0681	5.7408	39.0975	65.1232	3.2181
48.4004	6.5524	4.4054	44.5808	57.8134	3.8680
46.5267	6.9060	14.1015	31.4787	54.6503	4.5710
44.9571	7.4007	13.5202	31.9596	46.6709	5.8241
42.5266	7.7080	12.8619	32.5152	43.3357	6.7603
41.0379	8.2784	12.2324	33.0209	39.3911	7.3039
39.0351	8.7010	12.0106	33.1806	36.3439	8.0177
37.8387	9.2356	11.6513	33.4869	30.9154	9.4875
36.0547	9.5499	11.4962	33.6289	27.9846	10.1696
33.4898	9.9097	11.1564	33.8981	26.3380	10.6931
32.5690	10.2686	10.4995	34.4976	22.1174	12.3729
31.6897	10.6442	9.9389	35.0097		
30.1394	11.1050	9.4991	35.3803		
29.6221	11.2820	9.1337	35.7540		
28.9419	11.4563	8.6148	36.2365		
28.4316	11.6253	8.0910	36.6959		
22.7443	13.4543	7.7570	36.9904		
21.4948	14.1535	7.3539	37.3906		
20.4860	14.7502	7.1370	37.6344		
19.8450	15.3551	6.7822	37.9600		
18.6803	16.3650	6.5518	35.6425		
17.9659	16.9610	5.7408	39.0975		
17.2787	17.2906	4.4054	44.5808		
16.3757	18.0381				
16.0134	18.2056				
15.4307	18.4583				
14.8828	18.9417				
14.4190	21.0743				
11.9483	24.7771				
11.0418	26.6543				
10.0298	28.4367				
9.1865	30.2331				

Table B.2.3. Experimental data mass fraction for the binodal curve of the system composed of IL (1) + PPG400 (2) at (25 ± 1) °C.

[Ch][MES] *Mw* = 298.40 g.mol^{-1}		[Ch][HEPES] *Mw* = 341.46 g.mol^{-1}		[Ch][Tricine] *Mw* = 282.33 g.mol^{-1}			
100 x1	100 x2	100 x1	100 x2	100 x1	100 x2	100 x1	100 x2
69.8838	4.2285	56.5128	5.0882	97.8736	1.2991	16.6959	18.0693
64.7860	5.3217	53.8068	5.5568	69.4904	3.1259	16.0723	18.5787
60.1333	6.2874	50.5166	6.7184	60.1858	3.6327	15.4576	19.0313
55.1965	7.1847	47.5280	6.8257	56.7761	4.2760	14.7720	19.5331
48.5012	8.7696	45.9982	7.6268	54.1640	4.7039	14.2343	20.0327
46.7958	9.5501	41.1425	8.6022	51.5482	5.4519	13.6790	20.5952
43.7971	10.9016	37.7310	9.3213	49.2567	5.7598	12.9267	21.3824
42.4334	11.3568	35.2451	9.9419	47.5950	6.2286	12.4041	21.9015
38.2685	12.7829	34.1140	10.2609	45.8467	6.6634	11.7706	22.6844
36.5502	13.0879	32.5947	10.5324	43.7788	6.9466	10.9575	24.4370
35.0770	13.4386	32.0678	10.8553	42.2302	7.2639		
34.1312	13.9794	29.1506	11.5405	40.6019	7.6593		
32.8241	14.2450	27.8870	12.1211	39.1487	8.1093		
31.7028	14.5477	27.3756	12.4586	37.4811	8.2817		
30.2208	15.3318	26.8674	12.7469	36.3467	8.5527		
28.3978	16.1937	25.6239	13.6923	35.3796	8.8117		
27.8386	16.4653	25.0401	14.0154	34.5481	9.0611		
27.2691	16.7319	24.4870	14.2415	33.5101	9.2900		
26.4884	17.4968	22.6722	15.0782	32.6664	9.4897		
25.4908	18.0547	21.8793	15.7214	31.5901	9.9985		
24.6919	18.7448	20.8241	16.4387	30.4569	10.5764		
23.7332	19.2341	19.6307	18.5430	29.6016	10.7434		
23.2839	19.4249	19.3357	18.5453	29.1003	10.9652		
22.6274	20.0168	17.0628	20.1884	28.2516	11.5057		
22.0293	20.5238	16.4335	20.6799	27.1456	11.7318		
21.3505	20.8697	15.6755	21.3473	26.5879	12.2269		
20.8101	21.3969	15.1071	21.9024	25.9404	12.5196		
20.4555	21.5852	14.7864	22.2729	25.1396	12.6329		
19.9875	22.1150	14.5126	22.7060	23.9538	12.9995		
19.4955	22.6714	14.1541	22.7205	23.0370	13.5410		
18.8630	22.9970	13.5237	23.4890	22.4053	13.8492		
18.3951	23.4678	13.0076	23.7844	21.7388	14.3094		
17.5490	24.1697	12.7396	24.0960	20.9602	14.7788		
17.1939	24.5979	12.1180	25.0286	20.3241	15.2128		
		11.7603	25.3532	19.5962	15.7613		
				18.4586	16.6578		
				17.7894	17.2612		
				17.2629	17.6150		